The Pennsylvania State University
The Graduate School
The Eberly College of Science

ROLE OF THE SPECTRIN BASED MEMBRANE SKELETON IN PLASMA MEMBRANE PROTEIN PRESENTATION: A PROTEOMIC APPROACH

A Dissertation in
Integrative Biosciences
by
Mansi R. Khanna

Submitted in Partial Fulfillment
of the Requirements
for the Degree of
Doctor of Philosophy

August 2011

The dissertation of Mansi R. Khanna was reviewed and approved* by the following:

Graham H. Thomas
Associate Professor of Biology and of Biochemistry and Molecular Biology
Dissertation Adviser
Chair of Committee

Hong Ma
Distinguished Professor of Biology

Richard Ordway
Associate Professor of Biology

Melissa Rolls
Assistant Professor of Biochemistry and Molecular Biology

Bruce A. Stanley
Director, Proteomics/Mass Spectrometry Facility
Penn State College of Medicine, Hershey
Special Member

Peter J. Hudson
Willaman Professor of Biology
Director, Huck Institutes of the Life Sciences

* Signatures are on file in the Graduate School.

ABSTRACT

The plasma membrane (PM) and its associated proteins play an important role in determining how a cell interacts with its neighbours as well as how it responds to the components of, and conditions in the extracellular environment. As a reflection of this, more than 50% of the current drug targets lie at the cell surface. The amount of a protein at the cell surface is determined by its rate of delivery, internalization, recycling and degradation. All these parameters are subject to change under normal physiological adjustments, development, varying environmental influences and pathological conditions.

The spectrin based membrane skeleton (SBMS) is a ubiquitous feature of all metazoan cells. This network of spectrin and associated proteins is attached directly or indirectly to plasma membrane proteins. Among the numerous functions of the SBMS, are roles in protein trafficking and turnover that determine levels of plasma membrane proteins. Regulated spectrin proteolysis, mediated by calpain, occurs under normal physiological conditions for various cellular processes, including establishment of synaptic contacts, long-term potentiation and platelet activation. Spectrin cleavage is also observed in age-related pathologies such as stroke and other ischemic events, Alzheimer's and Parkinson's diseases. However, little is known about the consequences of spectrin breakdown *per se* under these conditions.

The goal of this work is to establish the fruit fly, *Drosophila melanogaster* as model system for some aspects of ischemic stroke, of which spectrin breakdown is a hallmark. The hypothesis being tested in this work is that disruption of the SBMS will affect the levels of many proteins at the cell surface under pathological conditions. The significance of this with respect to an ischemic stroke is that changes in levels of cell surface proteins in the event of SBMS breakdown need to be compensated for in post-stroke drug therapies and rehabilitation.

In order to observe changes in the cell surface proteome under SBMS breakdown, one would first need to establish what it looks in normal conditions. Towards this, I developed a technique to isolate pure PM that employs a unique combination of density gradient centrifugation and aqueous two-phase affinity partitioning (2PAP). Density gradient centrifugation is an accepted method of fractionation on the basis of the buoyant

densities of biomolecules and organelles but results in an overlap in cellular compartments due to similarities in densities. 2PAP is an established method for PM isolation in vertebrate model systems and makes use of the glycosylation pattern of PM proteins to isolate them from those in other compartments. My work demonstrates that a novel combination of both the techniques results in a robust PM preparation, which neither technique can achieve on its own. Using the new technique, 432 proteins were identified from *Drosophila* heads by MudPIT, of which 22% were found to be known PM residents and 34% are currently unassigned to any compartment and represent candidate PM proteins.

The SBMS was disrupted in *Drosophila* with the help of a temperature sensitive α-spectrin allele (*α–spec*^{R22S}*, R22S*) that causes spectrin network disassembly at non-permissive temperature (29^{o}C) and has been previously characterized. The R22S allele was introduced as a transgene into wild-type flies as well as an α-spectrin null background. My data suggests that although there is no precedent for an effect of α-spectrin R22S (α(R22S) being expressed in a wild-type background, the mutant protein in my hands, shows a difference in distribution in the ovaries in comparison to its wild-type counterpart. α(R22S) is excluded from the spectrin network at the apical membrane of the ovarian follicle cells and is instead exclusively localized in the basal membrane in the presence of the wild-type α-spectrin. It is also unstable in the presence of the wild-type α-spectrin, while in an α-spectrin null background, it is stable and its distribution in the ovaries resembles that of the wild-type protein. These data suggest a faster turnover of α(R22S) in the presence of wild-type α-spectrin due its selective exclusion from the membrane bound spectrin network. The work presented also shows similarity in phenotypes in the ovaries when α(R22S) is present as the sole source of α–spectrin and when it is present in a background heterozygous for α–spectrin (heterozygous flies): at a frequency of about 8%, abnormal late stage egg chambers are observed, with gross morphological defects in the follicle cell layer, absence of nurse cells and necrosis. This effect seems to be independent of temperature and genotype. Also, flies with α(R22S) as the sole source of α-spectrin (rescued flies) don't produce any progeny.

Since the heterozygous flies show similar phenotypes as the rescued flies, I decided to record significant changes in the *Drosophila* plasma membrane proteome by

iTRAQ in these flies. iTRAQ analysis revealed a significant change in 18 proteins, of which 4 are PM proteins and have been established in literature to being affected by the SBMS.

The structural role of the SBMS has been long established. The results presented in this thesis point to a more dynamic role for the SBMS in maintaining intercellular communication and maintaining surface protein levels.

TABLE OF CONTENTS

LIST OF FIGURES

LIST OF TABLES

LIST OF ABBREVIATIONS

1D – 1 dimensional
2D – 2 dimensional
2PAP – Aqueous 2-phase partitioning
ALP – Alkaline phosphatase
CCR – Cytochrome c reductase
CI – Confidence interval
ConA – Concanavalin A
DIGE – Difference gel electrophoresis
DTT – Dithiothreitol
ER – Endoplasmic reticulum
FDR – False discovery rate
GSL – Glycosphingolipid
HB – Homogenization buffer
HRP – Horseradish peroxidase
iTRAQ – Isobaric tag for relative and absolute quantitation
LC – Liquid chromatography
MS – Mass spectrometry
MTFP – Membrnae targeted fluorescent protein
MudPIT – Multidimensional protein identification technology
Nrv – Nervana
PAGE – Polyacrylamide gel electrophoresis
PBS – Phosphate buffered saline
PC – Phosphatidylcholine
PE – Phosphatidylethanolamine
PEG – Polyethylene glycol
PI – Phosphatidylinositol
PM – Plasma membrane
PS – Phosphatidylserine
RP – Reversed phase
SBMS – Spectrin based membrane skeleton
SCX – Strong cation exchange
SDH – Succinate dehydrogenase
SM – Sphingomyelin
WGA – Wheatgerm agglutinin
αSP – alpha spectrin

ACKNOWLEDGEMENTS

The efforts involved in completing my dissertation haven't been mine alone and I take this opportunity to express my heartfelt thanks and gratitude to all those who have contributed to the success of this endeavor.

I thank my advisor Graham Thomas for being such a wonderful and considerate mentor and friend. The Thomas Lab has been my second home and I thank him for making it such a comfortable and open working environment. I have grown immensely in my years as a graduate student, both, as a person and as a scientist and he has contributed greatly to both. I will always remember my time at the Thomas Lab with fondness.

I thank my dissertation committee members Drs. Hong Ma, Bruce Stanley, Richard Ordway and Melissa Rolls for being so involved in my work and their thoughtful suggestions and ideas. I have sought their help multiple times over the years and I thank them for always being available with their time, efforts and reagents. I also thank my former committee members Drs. Kouacou Konan and Randen Patterson for taking the time to serve on my committee while they did.

Thanks are due to Dr. David Gilmour and his lab for being so generous with their instruments and reagents. I also thank the late Dr. John Sisson and Dr. Ophelia Papoulas, University of Texas, Austin for being such wonderful hosts during my visit to their lab and teaching me the density gradient technique. I thank Dr. Ronald Dubreuil, University of Illinois, Chicago for sharing the α-spectrin cDNA.

I have troubled Bob Boor and Anne Stanley (Proteomics and Mass Spectrometry Core Facility, Hershey) umpteen times for technical help ☺ and I thank them for their assistance and patience.

The memorable years I have spent in the Thomas Lab are also thanks to all lab members, past and present. I particularly thank my close friends- Seung-Kyu for being such a great friend and partner in crime ☺; Hyun for being so willing to offer advice and help; Monika for being considerate, especially during my crazy experiment days and Meagan for being such an understanding and sweet friend. You all made lab such a sunny place!

My first stint at living so far away from my family wouldn't have been the same without my housemates Harshini and Rucha. They have been my friends and family and I thank them for sharing all my joys and sorrows as if they were their own. You have been selfless with your friendship and I love you both!

My thanks are also due to my dear friends Bhavana and Juilee for always being there for me. I thank Bhavana for providing a sympathetic ear and for being such a kind and thoughtful friend. The endless nights in lab would have been most difficult to get through had Bhavana not stopped by with sustenance☺. Frear was a better place because of Bhavana. I thank Juilee for her care and concern. I have relied on her fortitude and experience in dealing with a lot of situations and I'm grateful for her friendship.

My friends Juhi, Eddie and Nikhil have been a constant presence in my life, even though they're spread out in different parts of the world and I thank them for making sure that our attachment remains unaffected in spite of the distances that separate us.

My years in graduate school would have been incomplete without my husband Deepak. I thank him with all my heart for being a terrific friend, boyfriend, fiancé and husband over my student years. I am grateful for his loyalty and for being by my side even when times were tough. Commitment to a grad student with crazy work hours was a challenge and I thank him for taking it in his stride, for supporting and encouraging my efforts and letting me do things my way.

Last but not the least; I credit the blessings and prayers of my grandparents Pitaji, Chaiji, Bade Papa and Badi Mama for all my accomplishments. I thank my parents and my sister Tina - Papa for being my strength and such a caring friend, Mama for being my inspiration and Tina for being my sounding board. They have always had faith in my abilities and have encouraged me to achieve my heart's desire. I am particularly thankful to Tina-her unwavering involvement in my life is invaluable. Words are insufficient to express my gratitude to my little sister. To my family, I remain indebted-for their sacrifices, strength, unconditional love, support and pride in my work and me.

Dedicated to

Pitaji, Chaiji, Bade Papa and Badi Mama-for their blessings

Papa and Mama-for all the time I spent away from them in pursuing my dreams

My darling little sister Tina-for being the "real" elder sister and for cheerfully shouldering my share of the responsibility towards our parents.

Deepak-for being brave enough to marry a scientist!

Chapter 1 Introduction

Preamble: *Drosophila* as a model system for human diseases

With the advent of genome sequencing, there is a burgeoning realization that the cells of the humble insect *Drosophila melanogaster* work in a fundamentally similar way to ours, and that by making use of its powerful genetic tools we can identify molecular pathways relevant to human pathologies. *Drosophila* is being modeled for numerous human diseases including Alzheimer's and Parkinson's diseases (Abedinpour and Jergil, 2003; Feany and Bender, 2000), type 2 diabetes (Lasko, 2002) and muscle degeneration (Shcherbata *et al*., 2007), to name a few. The genes and proteins implicated in these disorders in humans not only have homologues in *Drosophila*, they are found in the same molecular pathways that lead to the symptoms associated with these pathologies. I would like to contribute to this list by introducing *Drosophila* as an effective model system for some of the cellular impacts of stroke on neuronal tissue.

1.1 The Plasma Membrane: Composition and functions in Eukaryotes

The functioning and survival of a cell depends on the availability of nutrients, communication with its environment as well as other cells, and the protection of its internal components. The cellular organelle responsible for these functions is the plasma membrane. While the plasma membrane has structural roles, serving as a barrier that shields cellular components from the outside environment and as a scaffold for membrane associated proteins and signaling molecules, it also has an active role involving the engagement of its constituent lipids in signal transduction pathways.

Biological membranes are constituted of three main classes of lipids: diacylglycerol (DAG) derivatives, sphingosine derivatives and sterol lipids (Binder *et al*., 2003). DAG derivatives all have DAG as their hydrophobic portion and include phosphatidylcholines (PCs), phosphatidylethanolamines (PEs), phosphatidylserine (PS) and phosphatidylinositol (PI). Sphingolipids have ceramide as their hydrophobic backbone and include sphingomyelin (SM) and glycosphingolipids (GSLs). Sterol lipids

are derivatives of steroids and are mostly represented by cholesterol in animals and ergosterol in yeast (Binder *et al*., 2003; van Meer *et al*., 2008).

The animal plasma membrane consists mainly of PC, PE, SM and cholesterol; however the distribution of these lipids between the two membrane leaflets is asymmetrical- PC and SM predominate in the outer leaflet while the inner leaflet is mainly comprised of PS and PE (van Meer *et al*., 2008; Zachowski, 1993). In human erythrocytes, the most extensively studied membrane system, up to 80% of SM and 77% of PC and <4% of PS reside in the outer leaflet (Zachowski, 1993), whereas cholesterol is enriched in the inner leaflet (75% ± 5%) in erythrocytes (Schroeder *et al*., 1991). The inner leaflets of the plasma membranes of synapses in mice, fibroblasts and the Chinese hamster ovary cell line are all enriched in cholesterol (Wood *et al*., 2011).

Other organelles (except the endoplasmic reticulum, ER) also exhibit lipid asymmetry between the membrane leaflets. The Golgi and endosomal membranes are enriched in SM and GSLs in the outer leaflet (in contact with the cytoplasm) while the inner leaflet consists mainly of PS and PE (van Meer *et al*., 2008). Amongst these organelles, the ER has the least concentration of sphingolipids and cholesterol, the Golgi has an intermediate concentration and the PM has the highest (reviewed by Lippincott-Schwartz and Phair, 2010). Maintaining different lipid profiles in different organelles serves 2 functions: First, it imparts a distinct function to that organelle. For example, high concentrations of cholesterol and sphingolipids render thickness to the PM and make it impermeable. Second, the lipid profile helps sort integral membrane proteins, since the latter insert themselves into lipids that have a thickness that matches their integral membrane domain (reviewed by Lippincott-Schwartz and Phair, 2010). In fact, differing lipid profiles within the Golgi membranes may actually serve as a sorting mechanism for membrane proteins-proteins with different lengths of transmembrane domains never overlap during their localization in the Golgi and this association with different lipid domains acts as a sorting signal, which either send the protein to the plasma membrane or then back to the ER (Patterson *et al*., 2008). However, it's interesting to note that this concept of protein sorting dependent on intracellular lipid profiles hasn't been demonstrated in insects as yet (Rolls *et al*., 1997).

The asymmetric distribution of lipids between the membrane leaflets is functional, and alterations in these distributions are often associated with physiological events. For example, relatively large amounts of PS are seen in the outer leaflet of blood platelets upon activation, providing a platform for the assembly and activity of coagulation factors involved in blood clotting upon injury (reviewed by Zwaal and Schroit, 1997). In fact, in the case of a rare inherited bleeding disorder known as Scott syndrome, platelets show decreased levels of PS in the outer leaflet upon activation, leading to a reduced ability to assemble coagulation factors (reviewed by Zwaal and Schroit, 1997; Bevers *et al*., 1999). Sickle cells also exhibit increased amounts of PS in their outer leaflet, as do apoptotic and tumorigenic cells, making them targets of macrophage recognition and subsequent phagocytosis (reviewed by Zachowski, 1993; Zwaal and Schroit, 1997). Lipid asymmetry has also been implicated in the regulation of membrane curvature, particularly during the cellular processes of endocytosis and exocytosis; positive correlations have been found between augmented lipd translocation from the outer leaflet to the inner one and endocytosis in K562 cells (transformed cells derived from human erythroblasts; Devaux, 2000).

The lipids in the plasma membrane are also organized such that they form specialized microdomains within the lipid bilayer. The two most well studied microdomains are rafts and caveolae. Rafts are small (10-200 nm) cholesterol and sphingolipid enriched domains involved in a number of cellular processes such as endocytosis and signaling (Pike, 2006; Lajoie and Nabi, 2010), and are heterogeneous in their lipid and protein contents. Within rafts, there exist subdomains that have higher amounts of cholesterol (Ohno-Iwashita *et al*., 2010). Certain raft-associated proteins, such as Src family kinases and flotillins, have been found to prefer these high-cholesterol subdomains (Ohno-Iwashita *et al*., 2010).

Specific proteins are associated with rafts and the signals that normally target a protein to rafts involve lipid modifications such as glycophosphatidylinositol (GPI) anchors, palmitoylation (e.g. Hedgehog) and double acylation (e.g. Src-family kinases; Ohno-Iwashita *et al*., 2010; Chichili *et al*., 2010). The proteins that are attached to and part of the underlying cytoskeleton also interact with rafts. In fact, the role of the cytoskeleton in rafts extends to the formation and structuring of these lipid domains. For

example, the cytoskeletal protein actin has been implicated in the formation and maintenance of raft structure (reviewed by Chichili and Rodgers, 2009; Lajoie and Nabi, 2010). A study that used fluorescence resonance energy transfer (FRET) to investigate the effects of actin on the clustering of membrane-targeted fluorescent proteins (MTFPs) found that treating Jurkat cells with Latrunculin B disrupted the co-clustering of raft-associated MTFPs (Chichili and Rodgers, 2007). In the same way, the cytoskeleton has been shown to be essential for maintaining raft integrity at the immunological synapse, where a T cell adheres to an Antigen Presenting Cell (Chichili *et al*., 2010). Here, the T cell Receptor is associated with rafts and its activation is dependent upon raft and actin integrity (reviewed in Chichili *et al*., 2010).

Caveolae are a sub-set of rafts that are invaginations of the plasma membrane characterized by the presence of the Caveolin family proteins. Caveolae are involved in endocytosis, transcytosis and various signaling pathways, including calcium- signaling pathways engaging Annexin A6 (Grewal *et al*., 2010). The presence of caveolins is a prerequisite for the formation of caveolae (Lajoie and Nabi, 2010; Ohno-Iwashita *et al*., 2010). Caveolins are palmitoylated proteins that have high affinity for cholesterol and recent studies have found that another family of proteins named cavins also localize to caveolae. Cavin-1 has been shown to be required for maintaining the structure and number of caveolae primarily by structuring caveolins at the plasma membrane (reviewed by Hansen and Nichols, 2010).

Rafts have been implicated in a variety of disorders (Ohno-Iwashita *et al*., 2010), with anomalies in rafts and their associated molecules being linked to disorders such as Alzheimer's and Parkinson's diseases, diabetes, asthma, atherosclerosis and muscular dystrophy (Ohno-Iwashita *et al*., 2010). Raft associated molecules are also used by viruses to gain entry into host cells. For example, the human immunodeficiency virus (HIV) receptors (CD4, CXCR4 and CCR5) are all associated with rafts in T lymphocytes and reducing cholesterol increases infection efficiency (Manes *et al*., 2000). Rafts are also exploited in the internalization of bacterial toxins into host cells (Ohno-Iwashita *et al*., 2010).

In summary, while the plasma membrane has a vital structural role, it is clear that it is not just a static component of the cell. Its constituent lipids and proteins participate actively in a diversity of cellular pathways.

1.2 The Spectrin Based Membrane Skeleton and its Role in Cell Surface Protein Presentation

Spectrin is a peripheral membrane protein that is the defining component of the Spectrin Based Membrane Skeleton (SBMS) in metazoan cells. It is a heterotetrameric protein comprised of two α and two β subunits (Fig. 1.1A). α- and β-spectrins dimerize in an antiparallel fashion and the dimers then associate head-to-head to form tetramers. Individual spectrin subunits are primarily composed of a characteristic number of triple α-helical spectrin repeats. α-spectrin contains 22 segments, of which all but two (segment 10 and 22) are spectrin repeats. Segment 10 is an SH3 domain and segment 22, a calcium binding site, is related to calmodulin. β–spectrins contain an amino-terminal actin binding domain, 16 spectrin repeats and a C-terminal Pleckstrin Homology (PH) domain. Repeat 16 is a partial triple-helix (2 helices) that pairs with the first helical repeat (0 helix) at the N-terminus of α-spectrin to form a complete repeat and hence a spectrin tetramer. β_{Heavy}-spectrin, a more massive isoform of β–spectrin, contains 30 spectrin repeats and differs from conventional β–spectrin in lacking an ankyrin binding domain and the presence of an SH3 domain **(**Fig. 1.1A**).**

Spectrin tetramers are thought to form a cytoskeletal mesh on the cytosolic face of the plasma membrane by crosslinking actin. Spectrin interacts directly with the plasma membrane *via* the PH domain or indirectly through its interactions with adaptor or integral membrane proteins (Fig. 1.1 B). In red blood cells, the spectrin-actin network associates with the plasma membrane *via* the adaptor protein ankyrin, which is in turn bound to the integral membrane protein Band 3. Another protein, Protein 4.1 mediates the interaction of spectrin with glycophorin C, a transmembrane protein, thus linking the network to the plasma membrane (Bennett and Baines, 2001; Hansen *et al*., 1996; Winkelmann and Forget, 1993). Binding of Protein 4.1 as well as adaptor proteins called adducins, to spectrin also strengthens its interaction with actin (Baines, 2010). Although the erythrocyte membrane skeleton is well studied and spectrin and its associated proteins have been found in non-erythroid cells, the latter shows a larger diversity in the number of interacting partners (Bennett and Baines, 2001; De Matteis and Morrow, 2000). Also,

Figure 1.1 The Spectrin Based Membrane Skeleton

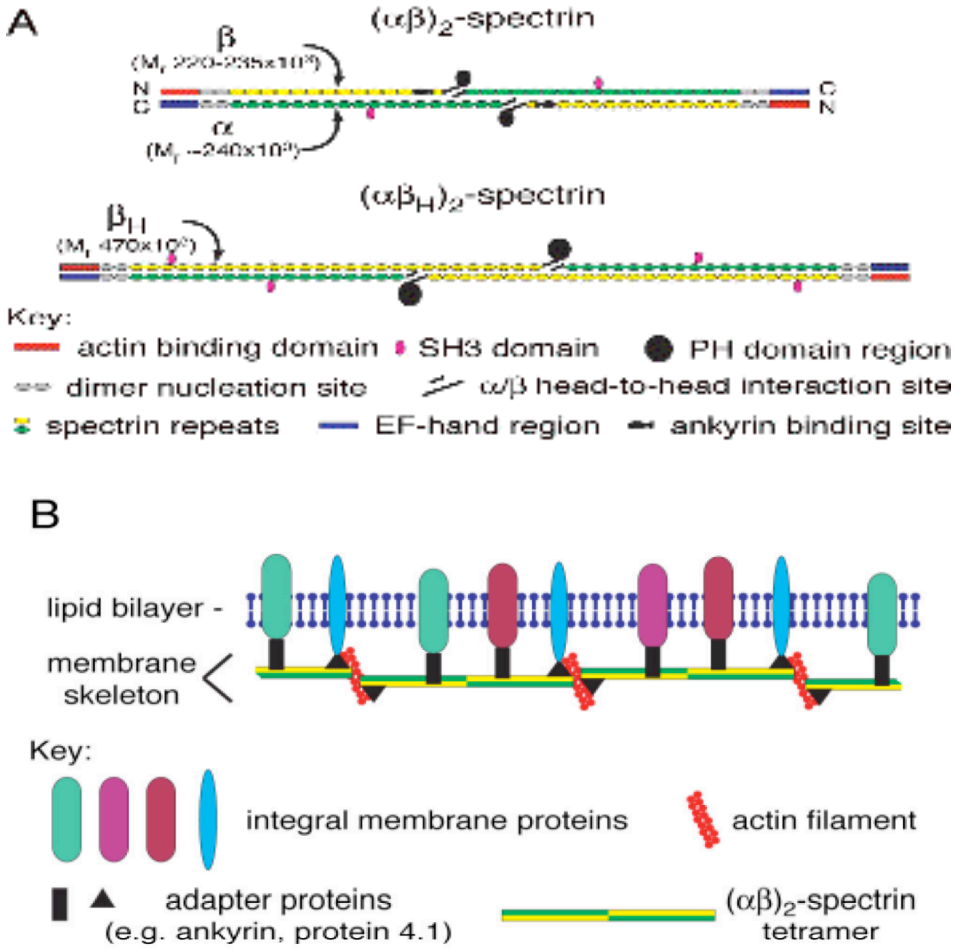

Fig 1.1 The Spectrin Based Membrane Skeleton A- *Drosophila* has 3 isoforms of spectrin- α, β and βH spectrins. **B**-Spectrin is cross-linked by actin and binds various integral membrane proteins. Figure adapted from Thomas (2001).

non-erythroid spectrin exhibits a higher affinity for actin than in RBCs (Bennett and Baines, 2001).

Spectrin was first discovered in erythrocytes (Marchesi and Steers, 1968), where it provides mechanical support to the membrane and maintains the survival of the cells during circulation (Bennett and Gilligan, 1993). The SBMS also has roles in organization of membrane domains, membrane trafficking, vesicle transport, protein sorting, morphogenesis and in protein presentation and maintenance at the cell surface (Bennett and Baines, 2001; De Matteis and Morrow, 2000).

Experiments have suggested that the close association of the SBMS with the plasma membrane and its proteins affects membrane and hence membrane protein turnover. The SBMS has the potential to regulate cell surface protein levels in the following ways-

a) *The "Anchor", "Fence" and "Picket" Hypotheses* suggest that the presence of the cortical cytoskeleton prevents the lateral diffusion of membrane proteins in a variety of ways and hence restrict them to certain membrane domains. Acting as an Anchor, the binding of the cytoplasmic domains of transmembrane proteins with the cytoskeleton confines such proteins to a certain membrane domain. For example, in MDCK cells, the retention of Na^+, K^+ ATPase was found to be greater in the basolateral domain versus the apical domain (Hammerton *et al*., 1991). This was found to be due to the absence of the SBMS complexes to which it is anchored *via* ankyrin in the apical domain of MDCK cells. The authors concluded that the association of the Na^+, K^+ ATPase with the membrane skeleton in the basolateral domain excluded it from endocytic vesicles. A more recent example of protein destabilisation was seen in spinocerebellar ataxia type 5 (SCA5) patients who have mutations in β-III spectrin and correlated loss of the glutamate transporter EAAT4 from the cell membrane (Ikeda *et al*., 2006). Cell culture studies on cells carrying the β-III spectrin mutation found in SCA5 patients using total internal reflection microscopy revealed that the lateral movement of EAAT4 was greater in the presence of the mutant versus wild type spectrin. Another recent example of anchoring is that of the mobility of CD45, a transmembrane phosphatase which becomes immobilized during T cell activation when either spectrin-ankyrin or spectrin-actin interactions were disrupted (Cairo *et al*., 2010). Another case in point is that of Lutheran (Lu) blood group

glycoproteins that lie on the surface of erythrocytes and function as receptors for laminins, that reside in the extracellular matrix. Lu proteins interact directly with spectrin and it has been found that upon weakening this interaction, there is increased cellular adhesion to laminin (An *et al*., 2008). This has been attributed to a presumed increase in clustering of Lu proteins upon release from the cytoskeleton, thus leading to greater adhesion. The cytoskeleton also functions as a "fence", that allows the movement of transmembrane proteins which are not directly bound to the SBMs only when enough space is formed between their cytoplasmic domain and the skeleton. For example, the ankyrin-free fraction of the transmembrane protein Band 3 exhibited greater lateral diffusion in the erythrocyte membrane when its cytoplasmic domain was cleaved (Tomishige *et al*., 1998; Tsuji and Ohnishi, 1986) and when spectrin was dissociated into dimers (Tsuji and Ohnishi, 1986). In a more recent study using 12 different hemolytic anemia samples that had structural defects in the cytoskeleton, the rate of diffusion of Band 3 was found to be greater in pathogenic erythrocytes than in healthy ones (Kodippili *et al*., 2009).

Another indirect way in which the membrane skeleton could restrict the movement of phospholipids and transmembrane proteins is *via* a "picket" mechanism wherein those membrane proteins that are associated with the SBMS restrict the lateral diffusion of those that are not (Kusumi *et al*., 2005; Nakada *et al*., 2003).

b) The barrier hypothesis suggests that the presence of the SBMS acts as a barrier to endocytosis and the assembly of endocytic coat protein structures. In erythrocytes, endocytosis occurs in zones that are devoid of spectrin (Hardy *et al*., 1979). In a more recent study performed in human fibroblasts, the Annexin A6 mediated removal of spectrin was suggested to be required for coated-pit budding (Kamal *et al*., 1998).

c) The scaffolding hypothesis suggests that the SBMS functions as a molecular scaffold to nucleate protein complexes that in turn regulate membrane protein turnover. The presence of a variety of protein interaction domains along its length gives spectrin the function of a multimolecular scaffold. It can bind numerous signaling complexes (De Matteis and Morrow, 2000; Odell *et al*., 2008), directly or *via* adaptor proteins and hence regulate signaling pathways that control membrane protein levels. For example, α-II spectrin has been shown to be necessary for the surface expression of human TRPC4

(hTRPC4) channels, a component of the EGF receptor-stimulated Ca^{2+} influx pathway. Studies in COS-7 cells have shown that hTRPC4 and α-II spectrin are constitutively associated just below the cell surface in the absence of EGF mediated stimulation. However, stimulation by EGF results in dissociation of the channel from spectrin and insertion of activated hTRPC4 channels into the plasma membrane. siRNA depletion of α-II spectrin in COS7 cells inhibited the membrane insertion of hTRPC4 channels and thus their normal plasma membrane levels. The authors concluded that association of the channel with spectrin was required to couple it with the translocation machinery. Since they also found other components of the hTRPC4 signaling complex associated with α-II spectrin by immunoprecipitation, they also suggested that α-II spectrin provided a "stabilizing platform" for the assembly of the hTRPC4 signaling complex at the plasma membrane (Odell *et al*., 2008). Spectrin can also directly associate with proteins that regulate membrane and protein trafficking such as Annexin and Dynamin (Williams *et al*., 2004, Tjota *et al* 2011 in press).

d) The tension hypothesis suggests that the cytoskeleton-plasma membrane attachment has also been shown to contribute to membrane tension, which provides resistance to membrane deformation. This cytoskeleton-membrane adhesive force has to be overcome in order to allow vesicle formation and hence endocytosis (Sheetz, 2001). Membrane tension is maintained by a balance between endocytosis and exocytosis: A decrease in tension results in endocytosis whereas exocytosis follows an increase in tension (Apodaca, 2002). This implies that the physical presence of the cytoskeleton plays a role in controlling the rate of membrane turnover and may thus indirectly maintain a certain protein profile at the cell surface.

e) The transport and recycling hypothesis suggests that Spectrin is involved in the secretory pathway through its direct association with the Golgi and other components of the endomembrane system (De Matteis and Morrow, 2000; Phillips and Thomas, 2006). Golgi spectrin in association with ankyrin has been shown to aid in the ER to Golgi transport of proteins being targeted to the cell surface (Devarajan *et al*., 1997; Stabach *et al*., 2008). The transport of Na^+, K^+ ATPase from the ER to the Golgi was found to be blocked in MDCK cells transfected with a β-spectrin construct lacking the ankyrin binding site. In these cells, there was a decrease in the detergent-insoluble pool of Na^+,

K^+ ATPase, implying the lack of association with the cytoskeleton. The authors suggested that Golgi-associated β-spectrin along with adaptor proteins are required for the vesicular transport of proteins destined for the plasma membrane. In another study with vesicles prepared from rat brains, β-III spectrin, a Golgi-specific isoform was found to interact with the Arp1 subunit of the dynactin complex, a multi-subunit complex that mediates the interaction between microtubules and the motor protein dynein (Holleran *et al*., 2001). A more recent report demonstrated that in mice, a mutation in β-III spectrin that disrupts its association with Arp1, prevents the trafficking of the membrane protein EAAT4 (which is known to interact with β-III spectrin and has been implicated in spinocerebellar ataxia type 5) to the plasma membrane (Clarkson *et al*., 2010). Even more recent is a report from Aayalon *et al*. showing that the interaction between Ankyrin B and β-II spectrin is required for the proper organization of costamere-associated microtubules in the mouse skeletal muscle (Ayalon *et al*., 2010). Costameres are protein assemblies at the plasma membranes of striated muscle such as the heart and protect it from contraction injury. An example of the role of spectrin/ankyrin in delivering proteins at the plasma membrane can be seen in lymphocytes. Lymphocytes are characterized by the presence of a spectrin-ankyrin rich cytoplasmic skeleton in the perinuclear region in addition to the membrane-associated cytoskeleton. This perinuclear complex gets recruited to the plasma membrane upon T cell activation. If the ankyrin-mediated link between the membrane protein CD45 and spectrin is disrupted, the expression of CD45 and CD3 at the cell surface is suppressed (Pradhan and Morrow, 2002). The authors presumed this was due to the role of the spectrin/ankyrin complex in tethering the cargo (membrane proteins) to microtubule - based motors. One more example is in mouse embryos where Ankyrin G and β-II spectrin are required for the accumulation of E-cadherin at the lateral membrane (Kizhatil *et al*., 2007). The authors show that E-cadherin binds directly to Ankyrin G and that this interaction is essential for the exit of E-cadherin from the trans-Golgi network and maintenance at the lateral membrane. Finally, the role of spectrin in the endomembrane system is also seen in *Drosophila* mutants of β_H-spectrin (*karst*). *karst* larvae show gut acidification defects, which have been attributed to the loss of the H^+ V-ATPase from the plasma membrane due to a defect in protein recycling (Phillips and Thomas, 2006).

In conclusion, Spectrin has numerous roles, as a structural support to the plasma membrane as well as more dynamic roles in protein trafficking. It is evident that spectrin is a ubiquitous presence in the endomembrane system and has widespread influence on protein movement and its proper localization. Its active role there, as well as its close association with the plasma membrane and its proteins render it an important factor in defining the cell surface proteome. The hypotheses presented build a case for the many changes that might be expected in cell surface proteins upon disruption of the spectrin network.

1.3 The SBMS in *Drosophila melanogaster*: Similarity to the Vertebrate System and Evidence for the Role in Cell Surface Protein Presentation

In *Drosophila*, spectrins are essential. α- and β-spectrin protein null mutants are larval lethal while β_{Heavy}-spectrin mutants are ≥ 90% larval lethal (Dubreuil *et al*., 1998; Dubreuil *et al*., 2000; Thomas *et al*., 1998). Spectrin mutants show a range of phenotypes: Loss of epithelial tissue integrity (Dubreuil *et al*., 1998; Thomas *et al*., 1998); defective cyst formation and oogenesis (de Cuevas *et al*., 1996; Deng *et al*., 1995) as well as loss of fertility (Deng *et al*., 1995; Thomas *et al*., 1998); defects in neurotransmitter release in the embryonic neuromuscular junction (Featherstone *et al*., 2001); defects in synapse size post embryonic development (Pielage *et al*., 2006) and embryonic axon patterning (Hulsmeier *et al*., 2007); and loss of polarized localization of certain membrane proteins (Dubreuil *et al*., 2000; Featherstone *et al*., 2001).

The *Drosophila* spectrin isoforms *(α,* β*,* and β_{Heavy}) are each encoded by a single different gene. This is in contrast to the 7 genes (encoding 2 α-spectrins and 5 β-spectrins) found in vertebrates and hence provides an advantage of this model system for genetic investigations. *Drosophila* spectrins are also differentially polarized in epithelia: αβ-spectrin is found in the basolateral domain while $\alpha\beta_{Heavy}$-spectrin is primarily apical (Dubreuil *et al*., 1998; Thomas *et al*., 1998), making the fly a good model system to study the role of the cytoskeleton in polarity. While the number of domains in each spectrin isoform is invariant between vertebrates and invertebrates, certain features differ- the 11^{th} domain in the vertebrate α-spectrin is extended by 35 residues and contains a calmodulin binding site. In *Drosophila*, a calmodulin binding site has been predicted to be in a different region viz. the 15^{th} domain (Dubreuil *et al*., 1989)**.** Also, β_H –spectrin (*karst*) in *Drosophila* has an SH3 domain inserted in the 5^{th} spectrin repeat.

The degree of homology between *Drosophila* and vertebrate spectrins along with similarity in their expression patterns (Bennett and Baines, 2001) makes *Drosophila* an ideal model organism for the proposed study. In addition, supporting data for the role of the SBMS in regulating plasma membrane area and protein presentation in the fly has emerged:

a) *β_H-spectrin and the transmembrane protein Crumbs regulate apical stalk membrane area in the photoreceptor:* Photoreceptor cells are an example of polarized epithelia, where the apical plasma membrane is divided into distinct domains. Crumbs is a transmembrane protein that is a determinant of apical polarity and recruits β_H-spectrin at the apical membrane (Wodarz *et al*., 1995; Medina *et al*., 2002). The stalk membrane contains Crumbs, which is also associated on its cytoplasmic face with β_H-spectrin. Crumbs interacts indirectly with β_H-spectrin *via* its FERM binding domain and together, these proteins regulate the surface area of the apical domain, indicating that they modulate trafficking to and/or from this region. The absence of Crumbs results in decreased stalk membrane size, an effect that is enhanced by *karst* (Pellikka *et al*., 2002), implicating spectrin in regulating membrane area in association the former.

b) *Overexpression of β_H-spectrin segment 33 results in membrane protrusions in the salivary gland and these protrusions sequester dynamin:* An overexpression of the C-terminal 33rd segment of β_H-spectrin resulted in extension of the plasma membrane in the salivary gland. These membrane extensions were shown to sequester Dynamin and Annexin B9, suggesting that the C-terminus of β_H-spectrin normally scaffolds endocytic components (Williams *et al*., 2004, Tjota *et al* 2011 in press).

c) *β_H-spectrin is required for maintaining surface H^+ V-ATPase levels and endosome recycling in the brushborder of the larval midgut:* Brush borders, a feature of absorptive epithelia, are characterized by apical microvilli, an endocytic/exocytic zone at the base of the microvilli and the terminal web in the apical cytoplasm which contains spectrin and myosin II, that cross-link actin protruding from the microvilli. The *Drosophila* middle midgut exhibits a well-developed brush border and cells in this region acidify the gut lumen. Acidification is dependent upon α-spectrin (Dubreuil *et al*., 1998) and the apical β_H-spectrin (Phillips and Thomas, 2006). This gut acidification defect is attributed to loss of the H^+ V-ATPase from the plasma membrane *via* a defect in pump endocytosis and recycling. This phenotype is associated with defects in the early endosome and probably arises due to abnormal recycling. Here, the brush border SBMS is thus implicated in maintenance of the surface level of H^+ V-ATPase *via* a role in early endosome recycling.

d) *β_H-spectrin is required to maintain surface levels of Roughest during eye development:* The *Drosophila* eye is characterized by photoreceptor cells (ommatidia) arranged in a regular lattice, interspersed with pigment and bristle cells. During pupal development, undifferentiated interommatidial cell (IOC) precursors vie for contact with differentiated pigment cells. This is a period of IOC rearrangements and apoptosis to set their final number. One of the proteins responsible for IOC morphogenesis and contact with pigment cells is the Ig-CAM protein Roughest. Roughest has been found to colocalize with β_H-spectrin during early pupal eye development. It is specifically pulled-down from embryonic extracts in an immune complex with β_H-spectrin. In *karst* eye discs, Roughest is observed in punctae in early stages of pupal development whereas the later stages display weaker and interrupted immunostaining for Roughest at the membrane. This is distinct from Roughest staining in wild type eye discs, where Roughest is observed in cytoplasmic punctae as well as at the membrane (Lee *et al*., 2010). Hence, an intact apical membrane spectrin skeleton is implicated in the appropriate localization of Roughest at the plasma membrane.

All these results support the central hypothesis of this thesis, that Spectrin has an important role in maintaining levels of cell surface proteins.

1.4 Effects of ischemia on the cytoskeleton

Stroke is the third leading cause of death in the United States (www.strokeassociation.org) and the leading cause of debilitation in the world (Rafii and Hillis, 2006). Based on their origin, strokes can be classified as ischemic, hemorrhagic or embolic. An ischemic stroke occurs when there is loss of flow in a blood vessel supplying the brain, thus depriving the tissue of oxygen and nutrients. In the case of a hemorrhagic stroke, a blood vessel supplying the brain bursts, causing bleeding in the brain. An embolic stroke occurs when brain ischemia results due to an embolus elsewhere in the body (Collins, 2007). 85% of strokes are ischemic in nature (Rafii and Hillis, 2006).

Ischemia can be further classified as global or focal. In global ischemia, there is loss of blood supply to the brain in general, following circulatory arrest and resuscitation. Global ischemia results in neuronal cell death in isolated regions (Lipton, 1999). Just a few minutes of global ischemia is sufficient to cause irreversible damage, which can be manifested over a time scale of days (Endres and Dirnagl, 2002). In contrast, focal ischemia results from a loss of blood supply to a particular region of the brain due to blockage in a vessel that supplies it (Endres and Dirnagl, 2002). The afflicted region is further divided into "core", "penumbra" and "extrapenumbral" on the basis of the residual blood supply it receives (more in the latter two than the former). Thus, a gradient is established in which major cellular damage, mostly resulting in cell death, occurs in the core, while there is limited cell death in the extrapenumbral region, the effects are less severe and on a longer time-scale (Lipton, 1999). In all models of ischemia studied to date, it has emerged that even in the "core" region of focal ischemia, there is a higher amount of blood flow than in global ischemia hence the attack can be endured for longer (Lipton, 1999).

Following cerebral ischemia, a series of events occur at the cellular level due to the loss of oxygen and vital nutrients. These events can be distinguished on the basis of their time of occurrence post-insult, although overlaps are likely (Endres and Dirnagl, 2002; Lipton, 1999):

a. *Excitotoxicity:* As a consequence of the drop in oxygen and glucose levels, energy-dependent ion channels are inactivated in a matter of minutes, leading to a loss of membrane potential. This in turn causes depolarization of neuronal and non-neuronal cells, the activation of voltage-dependent calcium channels and the release of excitatory amino acids into the synaptic cleft. Accumulation of these excitatory molecules in the synaptic cleft results in the activation of ligand-gated and metabotropic calcium channels. The massive influx of calcium that follows triggers a cascade of events leading to cellular disorder and death. Calcium can activate a number of enzymes, including calpain (causing proteolysis of the cytoskeleton such as spectrin, actin and microtubule-associated proteins), phospholipases (causing membrane degradation), cyclooxygenases (leading to the formation of free radicals) and neuronal nitric oxide synthase.

b. *Peri-infarct depolarization*: In the "core", the cells are irreversibly depolarized and eventually die. However, in the "penumbra", the cells may be able to repolarize. Since this requires energy, there may then follow a series of repolarizations-depolarizations, which are called "peri-infarct depolarizations". Such a phenomenon has only been observed in animal models of ischemia, not in humans.

c. *Inflammation*: Following cerebral ischemia, an inflammatory response may result in additional blockages in blood vessels due to an increase in the numbers of circulating leukocytes. Toxic enzymes may also be secreted by macrophages, which can cause further damage.

d. *Cell death*: Apoptosis is most prominent in focal ischemia, at the border of the core and penumbral regions. In the core, which is the region characterized by maximum infarct, cell death is predominantly by necrosis.

One of the hallmarks of cerebral ischemia is calpain-mediated degradation of the cytoskeletal protein spectrin (Vanderklish and Bahr, 2000; Chen *et al.*, 2007). Calpain is a calcium-dependent thiol protease that targets an array of proteins, from kinases to membrane receptors and cytoskeletal proteins (Kastrykina, 2000). Regulated α-spectrin cleavage by calpain is a feature of several normal cellular processes such as long-term potentiation, platelet and neutrophil activation, dendritic and postsynaptic density remodeling (Czogalla and Sikorski, 2005; Vanderklish and Bahr, 2000; Dosemeci and

Reese, 1995). On the other hand, calpain cleavage of α-spectrin also arises in various pathological conditions such as ischemia, hypoxia, Alzheimer's and Parkinson's diseases (Lipton, 1999; Kastrykina, 2000; Vanderklish and Bahr, 2000). In fact, α-spectrin has been shown to be the most calpain-sensitive component amongst the proteins that constitute the postsynaptic density, getting degraded even at low calpain:protein ratios when actin, tubulin and α-CaM kinase remain unaffected (Dosemeci and Reese, 1995). Calpain-mediated proteolysis of spectrin results in characteristic breakdown products (BDPs) of approximately equivalent electrophoretic mobilitites (BDP1 and BDP2) and these characteristic breakdown products of spectrin are widely used as markers for the progression of calpain activity in models of ischemia (Pike, 2003; Chen *et al*., 2007). The extent of spectrin breakdown has been shown to be advanced in the core whereas it is variable in the penumbra (Yao *et al*., 1995) and this might suggest a scope for recovery of cells in the extrapenumbral region and perhaps in the penumbra. This would be of particular importance in administering drugs to patients recuperating from an ischemic stroke as it would make sense to target those cells that lie in the penumbral region and beyond (Barone, 2009).

In light of the emerging role for spectrin in setting plasma membrane protein levels, we hypothesize that ischemic damage to the SBMS would be expected to have widespread effects on the levels of many many cell surface proteins in cells that survive such events. Since it is known that more than 50% of current drug targets lie on the cell surface (Overington *et al*., 2006), many of these targets are likely to change level. Thus, knowledge of the changes in the surface protein composition of the cells in the penumbra and extrapenumbral region of an ischemic stroke would help physicians to effectively target the surviving cells as well as to adjust any preexisting therapies that the patient might be on. The elderly are most at risk of stroke and are generally taking several drugs prior to being afflicted. In fact, hypertension is the most critical predisposing factor for a stroke (Armario and de la Sierra, 2009) and Clonidine (brand name Catapres), a common drug for hypertension treats this by targeting the α-adrenergic receptor in the brain. Another drug, Pramlintide (brand name Symlin), used in controlling Type II Diabetes, also binds to a cell surface protein called the Calcitonin receptor in the brain. After a stroke, the surface levels of these drug targets may well be affected due to spectrin

breakdown and this should be compensated for through adjustments in post-stroke drug therapies.

Several studies have implicated SBMS degradation in ischemic diseases (Lipton, 1999) and some studies have been done in vertebrate systems to identify changes in global protein levels upon ischemic insult (Maurer *et al*., 2003; Chen *et al*., 2007). Maurer *et al*. analyzed the brain microdialysate from 3 stroke patients by 2D gel electrophoresis and mass spectrometry. They identified 10 novel proteins (including Tubulin α–1 and Creatine Kinase B subunit, both of which are brain specific proteins) in these patients that may serve as potential biomarkers for stroke progression. In contrast, Chen *et al*. tried to establish the protein profile in a rat model of stroke. Proteins that showed more than 3-fold change were identified- dihydropyrimidinase-related protein 2, spectrin alpha II chain, heat shock cognate 70 pseudogene 1 and tropomodulin 2. It was interesting that their study found that the molecular weight of the spots corresponding to spectrin on their gel was actually consistent with the molecular weight of a breakdown product. Early gene expression changes following ischemic insult have also been observed (Indraswari *et al*., 2009) and has been suggested as a neuroprotective mechanism. Upregulation of α spectrin II in the penumbra region of a rat stroke brain (but not in the core) has been proposed as a protective mechanism for neuronal survival since α–spectrin is a component of the neuronal cytoskeleton that contributes to neuronal membrane integrity (Indraswari *et al*., 2009). These studies were all whole tissue investigations and a documentation of specific plasma membrane proteins that change in level hasn't been attempted in a systematic fashion.

1.5 Modeling a key aspect of ischemic stroke, spectrin degradation, in *Drosophila melanogaster* using the temperature sensitive *α-spectrin*^{R22S} allele

Calpain-mediated degradation of spectrin is a key event in cerebral ischemia (Vanderklish and Bahr, 2000; Chen *et al*., 2007). *In vitro* studies (Glantz *et al*., 2007; Harris and Morrow, 1990) as well as those in cultured rat hippocampi (Glantz *et al*., 2007) have shown that calpain cleavage of α- and β-spectrin is a sequential event: α–spectrin is cleaved first, followed by β-spectrin, which requires the binding of calmodulin. Calpain cleaves α–spectrin in its 11th segment, first between Y_{1176} * G_{1177} and then G_{1230} * S_{1231} (Glantz *et al*., 2007). Phosphorylation of Y_{1176} renders spectrin insensitive to calpain (Nicolas *et al*., 2002). Following α–spectrin cleavage, the binding of calmodulin results in dissociation of spectrin tetramers to dimers and a decrease in actin binding. Persistence of calcium and calmodulin increases the susceptibility of β-spectrin to the action of calpain and β-spectrin cleavage results in an irreversible loss of actin binding as well as the ability to form tetramers (Harris and Morrow, 1990).

To date, four calpain genes (*Calpain A-D*) have been identified in *Drosophila melanogaster* (Friedrich *et al*., 2004). Of the four encoded proteins Calpains A and B are "typical" calpains that most closely resemble the mammalian calpains (Spadoni *et al*., 2003). Calpain A expression is restricted to a few neurons of the posterior protocerebrum and the anterior tritocerebrum, the ventral ganglion of the thorax, the midgut, and hemocytes (Theopold *et al*., 1995). Calpain B is found in trachea and larynx of late embryos, third instar salivary gland and in the follicle and border cells of the oocyte (Farkas *et al*., 2004). Calpain C, although structurally similar to other calpains, is an inactive calpain that has three mutated residues in its catalytic site (Spadoni *et al*., 2003). Calpain C RNA is expressed solely in the third instar salivary gland (Spadoni *et al*., 2003); (Friedrich *et al*., 2004). Calpain D (originally SOL, small optic lobe) is an "atypical" calpain in which the domain with the active site residues has been conserved while all other domains are different from those of the calpain superfamily (Friedrich *et al*., 2004).

While *Drosophila* Calpains A and B are functionally similar to their mammalian counterparts in their dependence on calcium ions for activation (Pinter and Friedrich, 1988; Farkas *et al*., 2004; Bozoky *et al*., 2009), whether their substrates are identical has yet to be determined. The action of *Drosophila* calpain on the cytoskeleton was merely suggested by an early study done to determine the localization of calpain during embryogenesis (Emori and Saigo, 1994). The authors found that calpain colocalized with the actin cytoskeleton in the developing embryo in the stages prior to cellularization and proposed that even in *Drosophila*, calpain might be involved in reorganization of the cytoskeleton. However, in a more recent attempt to develop a technique to identify substrates of calpain in *Drosophila* Schneider S2 cells (Bozoky *et al*., 2009), no components of the SBMS were identified as calpain substrates.

Besides spectrin, Calpain has many other cellular targets including receptors and channel proteins (e.g. inositol 1,4,5 triphosphate receptor), signaling enzymes (e.g. calcium/calmodulin dependent protein kinase), apoptotic proteins (e.g. caspases) and transcription and translation factors (e.g. c-jun and eukaryotic initiation factor eIF4G; Saatman *et al*., 2010). Hence, the use of a strategy that would involve induction of calpain action didn't seem feasible since it would be difficult to isolate the effects of spectrin degradation alone. Therefore, in order to model what might be the fate of cell surface proteins in the penumbra after an ischemic insult as a consequence of calpain-mediated spectrin degradation specifically, I decided to disrupt the SBMS with the help of a temperature sensitive mutation in α-spectrin (*α-spec*^{R22S}*; R22S*) that causes spectrin network disassembly at non-permissive temperature (29^{o}C; Deng *et al*., 1995). The R22S mutation was created to mimic the mutation in human erythroid α-spectrin codon 28 (Arg 22 in *Drosophila* α-spectrin) that leads to defective spectrin tetramerization. While the R22S mutation doesn't mimic the activity of calpain on α-spectrin, specific effects of SBMS disruption can be studied, without proteolytic effects on the other cellular targets of calpain.

Chapter 2 Developing a novel method for the isolation of pure plasma membrane from *Drosophila* tissues

(The Results from this chapter have been published: Khanna, 2010)

2.1 Introduction

The plasma membrane (PM) and its associated proteins play an important role in determining how a cell interacts with its neighbours as well as how it responds to components and conditions of its extracellular environment. As a reflection of this, more than 50% of the current drug targets lie at the cell surface (Overington *et al*., 2006). The amount of a protein at the cell surface is determined by its rate of delivery, internalization, recycling and degradation. All these parameters are subject to change during normal physiological adjustments, development, varying environmental influences and pathological conditions (Josic *et al*., 2008). Obviously, to monitor such changes *via* total protein level, when the surface pool is the active population, would mask key regulatory changes that arise from movement to and from other sub-cellular compartments. Thus, it is essential to develop techniques that permit the effective study of the surface pool specifically.

The challenge for isolation of the PM is its low abundance – 10% or less of the cellular membrane, depending on the tissue type – that is easily overwhelmed by high abundance compartments such as the endoplasmic reticulum (ER). Various techniques to isolate plasma membranes exist, and each has its strengths and weaknesses. Density gradient centrifugation separates biomolecules and organelles on the basis of their buoyant densities. Although this results in fractionation, similarities in membrane density inevitably lead to an overlap between cellular compartments (reviewed by Josic and Clifton, 2007). Immunoaffinity purification using antibodies against cell surface proteins has been used to isolate plasma membranes from rat liver (Lawson *et al*., 2006) and mouse livers with relatively low contamination from other compartments (Pierce *et al*., 2008). However, this method depends on the availability of a good antibody to a single protein and is thus likely to be tissue specific and potentially biased towards a specific

membrane domain if the source cells are polarized. Global surface labeling with biotin and then isolation of biotinylated surface proteins with the use of streptavidin has been used before (reviewed by Schindler *et al*., 2006). However, this is not a practical technique for plasma membrane isolation from a whole organ or organism. Recently, aqueous two-phase affinity partitioning (2PAP) has emerged as a useful technique to isolate plasma membranes from several sources (Abedinpour and Jergil, 2003; Ekblad and Jergil, 2001; Persson and Jergil, 1992; Persson *et al*., 1991; Schindler *et al*., 2006). In this method, plasma membrane is first partitioned into the polyethylene glycol (PEG) layer of a two-phase PEG/Dextran system, and then selectively pulled into the dextran phase by the use of the lectin wheat germ agglutinin (WGA) coupled to the dextran to select for membrane containing glycosylated proteins.

It is a desirable goal to combine 2PAP with a genetic approach to facilitate regulatory studies of global cell surface protein population. However, the currently established method for this depends upon the use of the lectin wheat germ agglutinin (WGA), which has specificity for N-acetylhexosamines or sialic acid in certain linkages (Iskratsch *et al*., 2009). This limits the utility of this phase separation for the isolation of plasma membrane from invertebrate genetic models, such as *Drosophila,* where glycoyslation patterns are much simpler, and have a high mannose content (Koles *et al*., 2007; Rendić *et al*., 2008). Simply changing the lectin to Conconavalin A (ConA), which has a high affinity for mannose, creates a new problem as this will now efficiently isolate endoplasmic reticulum and Golgi resident proteins because oligomannosidic proteins are extensively present in the ER. Here, we present a novel combination of density gradient centrifugation and affinity purification using 2PAP to isolate plasma membranes from *Drosophila melanogaster*. We show that 2PAP alone, is not sufficient to eliminate contaminating membranes, and that prior enrichment of plasma membranes is required. The addition of an initial gradient fractionation permits the efficient removal of the ER and Golgi membranes.

2.2 Materials and methods

2.2.1 Extract Preparation

The wild-type *Drosophila* line Oregon R was used for all extractions. *Embryos*: 1.5-3.0 g of embryos (*Oregon R*; 0-15 hours old) were dechorionated in 50% bleach, thoroughly rinsed, and carefully homogenized in 10 volumes of homogenization buffer I (**HB-I**; 0.22 M sucrose, 0.12 M mannitol, 1 mM EDTA and 10 mM tricine, pH 7.2) (Beziat *et al*., 1997) containing 1X protease inhibitor cocktail (10 μM benzamidine, 1 μg/ml phenanthroline and 10 μg/ml each of aprotinin, leupeptin and pepstatin A) (Papoulas *et al*., 2005) by 15 strokes of Pestle A in a Kontes homogenizer on ice. *Heads*: Heads were isolated from 15-20 g of 4-5 day old flies using a modification of the standard freezing protocol (Ashburner, 1989): Flies were frozen at -80 ^{o}C for a minimum of one hour in a 200 ml centrifuge bottle, shaking briskly to decapitate and passing through a stack of frozen metal sieves of decreasing pore size (850 μm, 600 μm and 355 μm) to eliminate other body parts and to capture the heads. The heads were then homogenized in 5 ml of **HB-I** by 3 strokes in a 2 ml Kontes homogenizer (in 3 batches) and motor driven ground glass pestle, followed by 10 strokes of Pestle A in a 40 ml Kontes homogenizer on ice in a total volume of 20 ml. All subsequent steps were carried out at 4^{o}C. Use of liquid N_2 for head isolation (Ashburner, 1989) is to be avoided as this leads to a catastrophic mixing of membrane compartments. The initial homogenate was centrifuged: at 3,000 x *g* for 10 min at 4^{o}C to pellet nuclei; at 10,000 x *g* for 30 min at 4^{o}C to pellet mitochondria; and at 100,000 x *g* for 1 hr to obtain a microsome pellet.

To proceed directly with 2PAP, the pellet was washed once by resuspending and repelleting in **HB-II** (0.25 M sucrose, 15 mM Tris, pH 7.4; Schindler *et al*., 2006) containing 0.1X protease inhibitor cocktail. The pellet thus obtained was then resuspended in 400 μl of **HB-II** and used for affinity partitioning. To proceed with density gradient centrifugation, the microsome pellet was resuspended in 5 ml **HB-I**.

Protein estimations were performed using the Advanced Protein Assay Reagent (Cytoskeleton Inc., Denver CO) according to the manufacturer's instructions.

2.2.2 Preparation of ConA-Dextran

ConA was coupled to tresyl-dextran as previously described for coupling of WGA to dextran (Persson and Jergil, 1992). All solvents used to activate dextran were dried using silica gel (0.02 g/ml). All glassware to be used for activation was dried overnight at 65^{o}C. The tresyl-dextran should be used as soon as possible after preparation for coupling to avoid loss of capacity.

2.2.3 Aqueous two-phase affinity partitioning

Aqueous two-phase affinity partitioning was done essentially as previously described (Schindler *et al*., 2006; Fig. 1). In brief, 100 µl of the microsomes in **HB-II** (~3 mg protein) were added to 0.9 g of a two-phase system (6.3% or 5.7% (w/w) dextran plus 6.3% or 5.7% (w/w) PEG, respectively, in 15mM Tris/H_2SO_4, pH 7.8) to complete a 1-g system. This was mixed by 20 inversions, vortexing for 10 sec, followed by another 20 inversions. Phase separation was assisted by centrifugation at 150 x *g* for 5 min, to give a top phase (P1) and a bottom phase (D1). The bottom phase (D1) was re-extracted with an equal volume of fresh top phase (P2) from a pre-equilibrated 1-g two-phase system and combined with (P1). P1 and P2 were combined and layered onto a fresh bottom phase (D2) that had been pre-equilibrated against PEG. After extraction, the resulting top layer was extracted once again with a fresh bottom phase (D3) as before. The top phase was then subjected to affinity purification with the bottom phase of a 2-g two-phase system (6.3% or 5.7% (w/w) dextran, 6.3% or 5.7% (w/w) PEG, 200 µg of ConA as ConA-dextran, 2 mM $LiSO_4$, 15 mM Tris borate, pH 7.8). The top phase (P1+P2) was kept aside and the bottom phase was re-extracted with the same volume of a fresh top phase (P3) from a new 2-g two-phase system (6.3% or 5.7% (w/w) dextran, 6.3% or 5.7% (w/w) PEG, 2 mM $LiSO_4$, 15 mM Tris borate, pH 7.8). The resulting bottom phase (ConA) was diluted with 10 volumes of **elution buffer** (0.1 M mannose, 0.25 M sucrose). All other phases (D1, D2, D3, P1+P2 and P3) were diluted 10-fold in **HB-II**. All samples were centrifuged at 100,000 x *g* for 1.5 h at 4^{o}C to pellet membranes. The pellets thus obtained were resuspended in 200 µl of HB-II prior to further analysis.

2.2.4 Density gradient centrifugation

Density gradient centrifugation was done essentially as previously described (Papoulas *et al*., 2005). Briefly, the resuspended 100,000 x *g* microsome pellet (see above) was mixed with OptiPrep (Accurate Chemical and Scientific Corp., Westbury, NY) such that a 10-30% gradient was created with a total protein content of 12-15 mg per gradient. Centrifugation was at 286,675 x *g* (60,000 rpm, rotor Vti80) for 3.6 h. 0.25 ml fractions were collected from the bottom of the tube for further analysis.

2.2.5 Combined density gradient centrifugation and aqueous two-phase separation

The uppermost fractions (15-20) from the density gradient contains the bulk of the plasma membrane and were pooled, diluted in 5 volumes **HB-II** and pelleted by centrifugation at 100,000 x *g* for 1.5 h at 4^{o}C. The pellet was resuspended in **HB-II** (= 'Pool') and subjected to 2PAP (see above). Gel loading (see section 2.2.6) with the gradient and 2PAP fractions were with 50 μg of proteins or then equal volumes if protein amount was less than 50 μg.

2.2.5 Antibodies

The following primary antibodies were used for immunoblotting: mouse anti-α-Spectrin (1:75,000; ascites #N3 from Dr. D. Branton, Harvard University, Cambridge, MA); rat anti-BiP (1:20,000; Babraham Institute, Cambridge, UK); mouse anti-ATP synthase (1:100,000; MitoSciences, Eugene, OR), mouse anti-Nervana (1:10,000; Developmental Studies Hybridoma Bank, Iowa City, IA), rabbit anti-HRP (1:2000; a gift from Dr. Richard Ordway, Penn State, PA), rabbit anti-Lava lamp (1:50,000 gift from Dr.John Sisson, University of Texas, Austin, TX). HRP-conjugated anti-mouse, anti-rat and anti-rabbit secondary antibodies (1:2500) were all purchased from Jackson Immunoresearch (West Grove, PA).

2.2.6 SDS-PAGE and Immunoblotting

Proteins were separated on SDS-polyacrylamide gels according to standard (12 % for Nervana, ATP synthase, BiP and HRP; (Laemmli, 1970) or high molecular weight

(7.5% for α-Spectrin, ATP synthase and BiP and 6% for Lava lamp; Fritz *et al*., 1989) protocols. For direct visualization of proteins, gels were stained with Colloidal Coomassie Blue (Invitrogen, Carlsbad, CA). For immunoblotting, proteins were transferred to Hybond ECL nitrocellulose membrane (Amersham Biosciences, Piscataway, NJ) and probed using standard protocols with final detection by 'normal sensitivity' chemiluminescence (~ 10 pg detection limit; ECL, Amersham Biosciences, Piscataway, NJ) or 'high sensitivity' chemiluminescence (low fg detection limit; SuperSignal West Femto, Pierce Biotechnology, Rockford, IL) using Pierce CL-Xposure Film (Thermo Scientific, Rockford, IL).

2.2.7 Enzyme Assays

The following marker enzyme assays were used to detect specific subcellular compartments: Alkaline phosphatase for the plasma membrane (Akcakaya *et al*., 2007), Succinate dehydrogenase for mitochondria (Munujos *et al*., 1993) and Cytochrome c reductase (NADPH) for the endoplasmic reticulum (Cytochrome c Reductase (NADPH) Assay Kit, Sigma-Aldrich, St.Louis, MO).

2.3 Results

2.3.1 Aqueous two-phase affinity partitioning I (6.3%PEG/Dextran)

Aqueous two-phase affinity partitioning (2PAP) separates membranes through their differing affinities for the polyethylene glycol and dextran phases coupled with the affinity of glycosylated surface proteins for lectins, and represents a quick and easy method to isolate plasma membrane (PM) proteins. We first attempted to isolate plasma membrane from *Drosophila melanogaster* using the 2PAP method previously used to enrich for PM from rat brains (Schindler *et al*., 2006). To adapt the protocol for fly tissue, we made two changes to this previously described protocol: First, we changed the lectin used from WGA to ConA. This was an essential change because the pattern of *Drosophila* protein glycosylation is simpler than that in vertebrates, containing a high proportion of mannose (Montreuil *et al*., 1995; Rendić *et al*., 2008). WGA has specificity for N-acetylhexosamines or sialic acid in certain linkages, and while there is some tissue reactivity with WGA (Koles *et al*., 2007), this lectin is primarily used as a nuclear stain in fly embryos and does not react with the PM (e.g. Vaccari *et al*., 2009). In adapting this methodology to other model systems similar consideration of species-specific glycosylation patterns should be made. Second, we used a slightly different isolation buffer to try to maintain the integrity of the mitochondria during the initial stages of the preparation (Beziat *et al*., 1997). The basic procedure is laid out in Figure 2.1.

Evaluating PM purity is not straightforward, because few PM proteins are completely absent from any internal compartment due to continuous biosynthesis and turnover from the cell surface. Previous studies using 2PAP have reported plasma membrane enrichment and removal of contaminating compartments with the help of marker enzyme activities (Persson *et al*., 1991; Abedinpour and Jergil, 2003; Schindler *et al*., 2006). However, the PM marker Alkaline Phosphatase (ALP) also has a significant internal pool (Rustin *et al*., 1979), and only ~5% is recovered in the PM fraction (Schindler *et al*., 2006). Clearly, yield and enrichment calculations become less dependable when they are based on a tiny fraction of the marker activity. Moreover, enzyme activity must survive the preparation to be fully accurate, and in our preparations the additional complication of significant levels of ConA in the final pellets (see Fig. 3.1A) leads to false estimates of total protein and therefore final specific activities.

Figure 2.1 Aqueous two-phase affinity partitioning

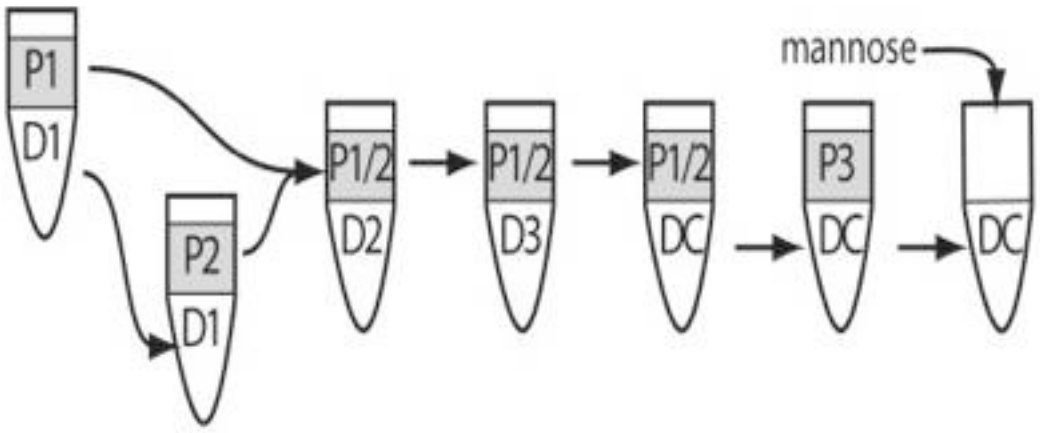

Fig 2.1 **Schematic representation of the two-phase affinity purification technique**. See Methods section for procedure. P1-3 - PEG phases; D1-3 - Dextran phases; DC - Conconavalin A-coupled dextran; mannose - sugar used for elution from ConA.

Immunoblotting is an obvious alternative but has similar problems (see discussion in Schindler *et al*., 2006; results presented below). We performed both evaluations with our initial samples but eventually selected immunoblotting, and define our optimal PM fraction to have the maximum yield of a known PM marker with the simultaneous absence of the ER marker BiP.

We chose two tissue sources for our experiments: Embryos, which are easy to produce in large amounts, but are heterogeneous in tissue content, and heads, which are relatively homogeneous (~85% neuronal - brain plus optic lobe) and thus provide a tissue type that is readily isolated en masse (see Methods). Typically, heads from ~5 g of flies yielded ~7.5 mg of protein, of which ~2 mg of protein was used for a single 1-g phase separation system, that was set up as previously described (Schindler *et al*., 2006). ~1.5 g of embryos yielded ~15 mg of protein, of which ~3.5 mg of protein was used for a single 1-g phase separation system. To track the isolation of different membrane compartments we performed immunoblot analyses. As plasma membrane markers we eventually settled on Nervana (Nrv; the brain-specific isoform of the β subunit of the Na^+/K^+ ATPase; Sun and Salvaterra, 1995) for head extracts, and α-Spectrin in embryo extracts (Papoulas *et al*., 2005). In addition, we used the chaperone BiP and the α subunit of ATP synthase for both tissue sources as markers for the endoplasmic reticulum (ER) and mitochondrial membrane, respectively. We also characterized our preparations from embryos using enzyme assays for Alkaline phosphatase (PM) and Succinate dehydrogenase (SDH; mitochondria) as previously suggested (Schindler *et al*., 2006) and Cytochrome c reductase (CCR; ER), all of which have homologues in the fly. However, these results are expressed as yields rather than relative specific activities (Persson *et al*., 1991; Schindler *et al*., 2006) because the protein concentration cannot be accurately estimated in our final eluates due to significant leaching of ConA from the dextran. This release arises because not all subunits of the ConA tetramers are cross-linked to the dextran and some disassembly occurs at the elution step.

This basic 2PAP procedure removes a large amount of the ER and mitochondrial membrane through partitioning into the dextran phases (Fig. 2.2; lanes D1, D2 and D3). However, the PM fraction (Fig. 2.2; ConA) still contains detectable levels of ER and

Figure 2.2 Immunoblot analysis of samples fractionated by two phase affinity partitioning using 6.3%PEG/Dextran

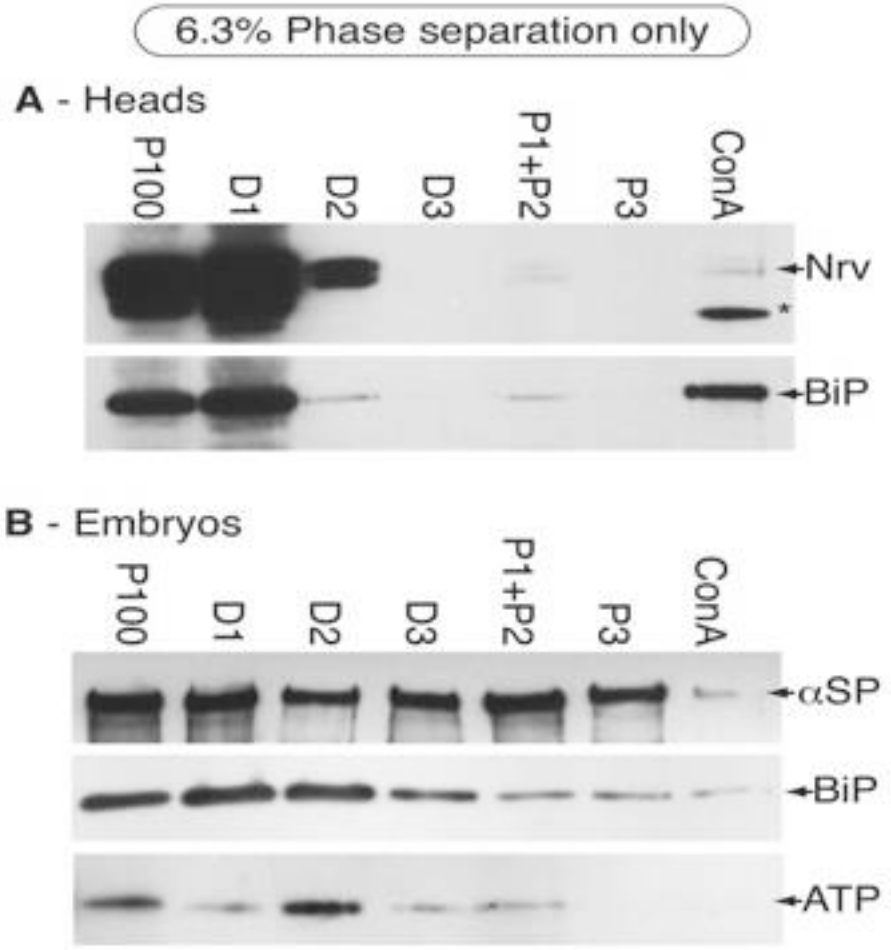

Fig 2.2 Immunoblot analysis of samples fractionated by two phase affinity partitioning using 6.3%PEG/Dextran. **A -** Fractionation of microsomes prepared from heads. Only small amounts of Nervana are recovered in the ConA fraction, and these contain significant amounts of the ER marker BiP. *Labeling*: P100 - input microsomes from the 100,000 × g pellet; D1-3 - Dextran fractions D1-3 in figure 1; P1+P2, P3 - PEG fractions P1-3 in figure 1; ConA - eluate released from the ConA-dextran fraction DC in figure 2.1. All samples represent remaining protein after each fractionation step. Asterisk - non-specific antibody binding to a large amount of ConA that coelutes from the dextran. Nrv - Nervana; BiP - ER chaperon BiP; ATP - α subunit of the mitochondrial F_1F_0 ATPase; αSp - α-Spectrin. *Loading:* All samples have equivalent loading, except P100, which was $1/5^{th}$ of the others. *Detection:* normal sensitivity chemiluminescence (see Methods). **B -** Fractionation of microsomes prepared from 0-15 hr embryos. Only small amounts of α-Spectrin are recovered in the ConA fraction. This fraction also contains readily detectable amounts of the ER marker BiP and small amounts of ATP synthase from mitochondria. Labels, loadings and detection are the same as A.

mitochondria. In preparations from both, heads and embryos, a significant amount of PM markers partition into the dextran phases perhaps representing an endomembrane pool of these proteins. The overall result is a relatively low yield in the final ConA fraction. To quantify these results the eluted ConA fraction was assessed using the marker enzyme assays, with the microsomal fraction for reference (Table 2.1). The results indicate a slight selectivity for the plasma membrane in the ConA phase: 0.55% of the ALP activity was recovered, compared to 0.37% for both the SDH and CCR activities (Table 2.1). Given the disproportionate ratio of ER to PM in a typical cell, this represents a significant level of contamination, and suggests that the 2PAP protocol alone is not sufficient to reduce contamination by these other fractions to the same extent as with vertebrate samples. This probably reflects the use of ConA, since mannose is extensively present in the ER.

2.3.2 Density gradient centrifugation

The persistence of contaminating sub cellular compartments using 2PAP alone prompted us to first try to enrich for plasma membrane using density gradient centrifugation on the P100 microsomal fraction (Papoulas *et al*., 2005). We began by characterizing the efficacy of Optiprep density centrifugation in isolation. Immunoblot analysis of the gradient fractions shows that different sub cellular compartments lie in different parts of the gradients as previously documented (Fig 2.3A, B; Papoulas *et al*., 2005). In gradient fractions with heads as the starting tissue (Fig 2.3A), the ER is predominantly found in fractions 8-14, while residual mitochondrial membrane lies mostly in fractions 6-12. Nrv is seen from fractions 8-20 overlapping with the ER. Based on the extent of this overlap and prior characterization of these gradients (Papoulas *et al*., 2005) we operationally define the PM pool in these gradients to be in fractions 15-20. In gradient fractions using embryos as the starting material (Fig 2.3B) similar results are obtained: The ER is predominantly found in fractions 6-13 while mitochondrial membrane lies in fractions 5-10. In both preparations, Golgi is typically in fractions 4-10 (Fig. 2.4A, and (Papoulas *et al*., 2005), while post Golgi compartments detected by anti-HRP staining extend from the Golgi region through to the PM fractions (Fig. 2.4B). α-Spectrin can be seen throughout the gradient, although it shows a peak in the Golgi and PM fractions as previously described (4-8 and 15-20 respectively; Papoulas *et al*., 2005).

Table T2.1

Method	Enzyme	Microsomes	PM Pool	ConA
Affinity	ALP	100		0.55±0.44
	SDH	100		0.37±0.15
	CCR	100		0.37±0.26
Combination	ALP	100	0.7±0.14	0.4±0.17
	SDH	100	0.8±0.07	0.25±0.04
	CCR	100	1.1±0.52	0.1±0.02
Gradient+2PAP (6.3%)	ALP		100	54.0±23.4
	SDH		100	30.0±5.31
	CCR		100	12.9±1.7

Table T2.1. Relative yields of membrane compartments determined from marker enzymes. Embryos were used as the starting material. Yields of Alkaline phosphatase (ALP; EC 3.1.3.1; PM marker), Succinate dehydrogenase (SDH; EC 1.3.5.1; mitochondrial marker) and Cytochrome c reductase (NADPH) (CCR; EC 1.6.2.4; ER marker). Because significant amounts of ConA elute in the final fraction, specific activities cannot be presented and these figures are raw activity yields, normalized to the activity present in the microsome pellets. Results represent mean ±1 standard deviation of values obtained from three experiments after adjustment for differences in protein concentration in the microsomal input fraction. The addition of the pre-fractionation by density gradient centrifugation preferentially reduces the amount of contaminating ER in the ConA fraction.

Immunoblot analysis of the pooled fractions 15-20 shows that contaminating BiP and ATP synthase are still present in low amounts (Pool, Figure 2.5A, B). Enzyme assays indicate that the yields of ALP, SDH and CCR in the pool are 0.7%, 0.8% and 1.1% respectively (Table 2.1). As expected, the persistence of the ER and mitochondrial membrane in plasma membrane fractions indicates that density gradient centrifugation alone is not the best method to obtain pure plasma membranes. However, the level of these compartments in the PM region is substantially reduced as seen by immunoblot analyses, suggesting that this might be a good preliminary enrichment for 2PAP.

2.3.3 Combined density gradient centrifugation and aqueous two-phase affinity partitioning I (6.3% PEG/Dextran)

Since neither of these methods alone produced a satisfactory enrichment for PM, we decided to combine density gradient centrifugation and 2PAP. Thus the PM pool of fractions 15-20 from the gradient was subjected to 2PAP, and analyzed as before except that we switched to high sensitivity chemiluminescence substrates with 100-1000 times the sensitivity of the previous analyses to assess ER and mitochondrial contamination (Fig 2.5A, B). The level of BiP in the ConA eluate for both heads and embryos is now below the level of detection, suggesting that the combined preparation has significantly increased PM purity. Low levels of mitochondrial membrane persisted in head preparations but not embryos, perhaps reflecting slightly greater compartment mixing due to the head isolation protocol (ConA, Fig 2.5A, B). The enzyme yields corroborate these results with 50% of the PM (ALP activity) in the input pool being recovered in the ConA eluate, whereas the majority of the residual mitochondrial and ER membrane are eliminated (70% of the SDH and 87% of the CCR respectively; Table 2.1). Overall, we recover 0.4% of the ALP yield in the ConA pellet after combining the two methods, which is comparable to that obtained when 2PAP is used alone (0.55%); however, we observe a reduction in the yield of CCR. We conclude that pre-enrichment for PM by density gradient fractionation results in a significant increase in PM purity after 2PAP. However, significant amounts of both Nrv and α-Spectrin are still lost through partitioning into the dextran phases.

Figure 2.3 Immunoblot analysis of samples fractionated on 10-30% Optiprep density gradients

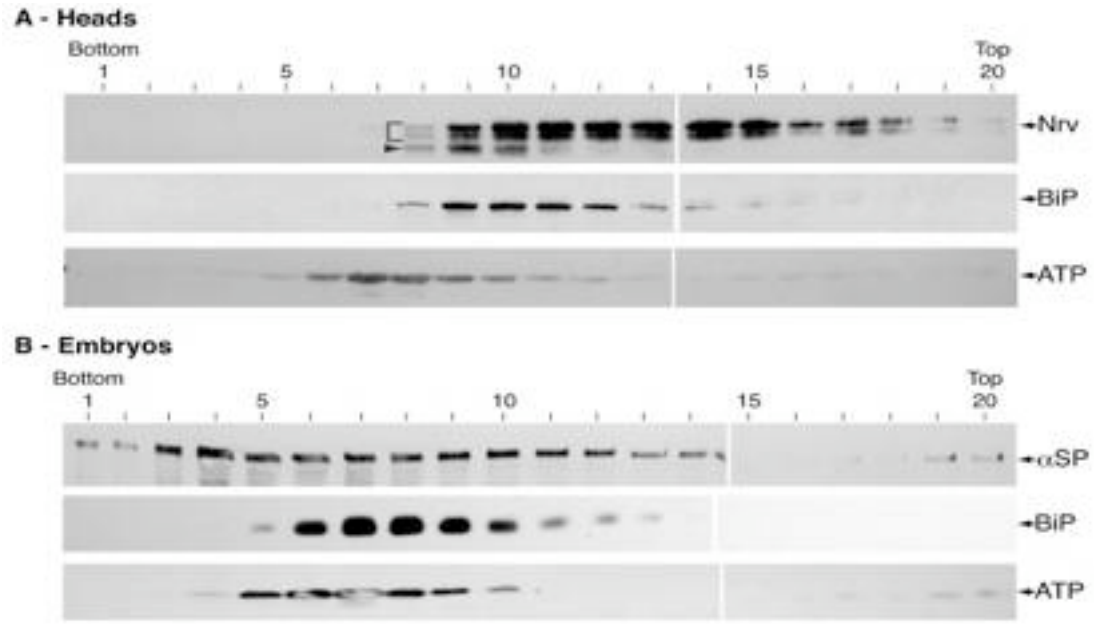

Fig 2.3 Immunoblot analysis of samples fractionated on 10-30% Optiprep density gradients. **A -** Fractionation of microsomes prepared from heads. BiP, marking the ER, peaks in the center of the gradient in fractions 9-11. ATP synthase shows that residual mitochondrial membrane is slightly heavier than the ER with a peak in fraction 7, but also shows a small presence in higher fractions at the top of the gradient. Nervana is seen as three prominent bands. The lowest (arrowhead) represents minimally processed protein and is restricted to the ER. The mature glycosylated forms (bracket) represent post-Golgi compartments and the plasma membrane. **B -** Fractionation of microsomes prepared from 0-15 hr embryos. BiP, marking the ER, peaks slightly lower than the ER from head gradients in fractions 7-9. ATP synthase again peaks in fraction 7, and again has a small presence in higher fractions at the top of the gradient. α-Spectrin has a peak in the Golgi region (fractions 3-4), extends through the ER and shows a distinct peak at the top of the gradient. *Labeling:* 1-20 - fraction number from bottom to top of tube; all other labels are as in figure 2. *Loading:* An equal volume of all fractions were loaded, except the peak protein fractions (4-6) where 50 μg of protein was loaded to prevent overloading.

Figure 2.4 Golgi and post-Golgi proteins in head microsomes fractionated by density gradient centrifugation followed by two phase affinity partitioning at 5.7% PEG/Dextran.

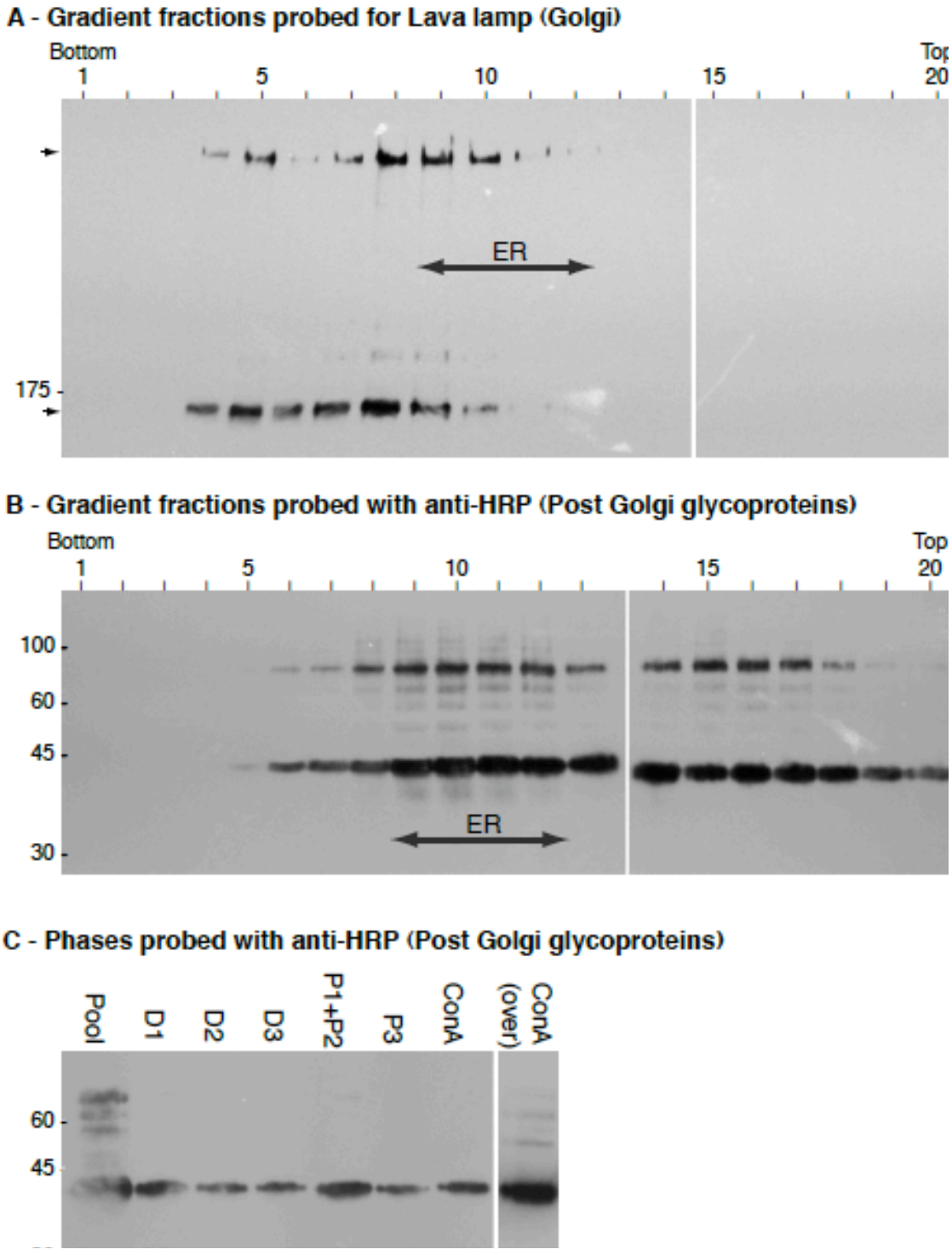

Fig 2.4 Golgi and post-Golgi proteins in head microsomes fractionated by density gradient centrifugation followed by two phase affinity partitioning at 5.7% PEG/Dextran. **A -** Fractionated microsomes prepared from heads and probed for the Golgi protein Lava lamp. Two isoforms of Lava lamp are detected (arrows) at ~170 kDa and ~315 kDa. On average Golgi membrane is heavier than the peak ER fractions as expected (double headed arrow; see Figure 2.3), but some overlap is seen especially with the larger isoform which has a bimodal distribution. **B -** Fractionated microsomes prepared from heads and probed with anti-Horseradish Peroxidase (HRP). The epitopes recognized by anti-HRP depend on the presence of *N*-glycan core α1,3-linked fucose and thus detects proteins in trans-Golgi and post-Golgi compartments. The prominent epitope at 42 kDa is thought to be our PM marker Nervana. Trans- and post-Golgi proteins detected by anti-HRP extend from the Golgi fractions through to the lightest region of the gradient as seen with the fully glycosylated Nervana isoforms (see Figure 2.3A). **C** - Fractionation by two phase affinity partitioning following an initial density gradient fractionation and probed with anti-HRP. The most prominent band behaves the same way as Nervana (see Figure 2.7B) and probably *is* Nervana. An overexposure of the final ConA eluate (ConA over) is included to show that other anti-HRP detectable proteins are also present in the PM fraction. *Labeling*: same as figure 2.3 for A and B and figure 2.5 for C. *Loading*: Equivalent amounts of all fractions were loaded.

Figure 2.5 Immunoblot analysis of samples fractionated by density gradient centrifugation followed by two phase affinity partitioning using 6.3%PEG/Dextran

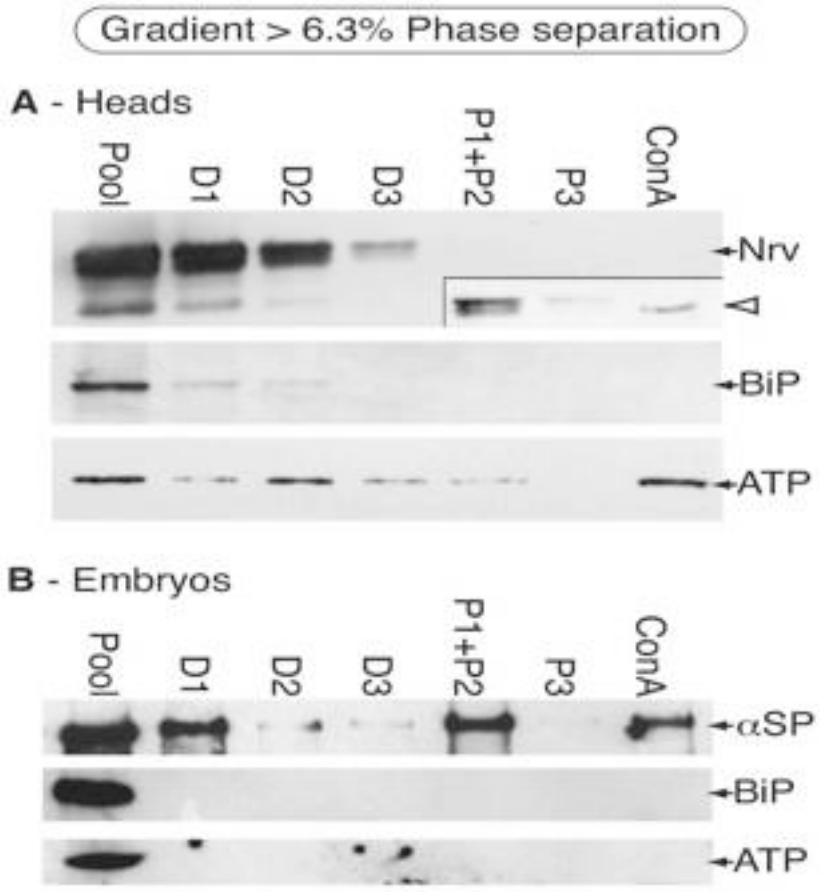

Fig 2.5 Immunoblot analysis of samples fractionated by density gradient centrifugation followed by two phase affinity partitioning using 6.3%PEG/Dextran. **A -** Fractionation of microsomes prepared from heads. Most Nervana is left behind in the dextran fractions, although a 60× exposure shows that a low yield of Nervana is found in the eluted ConA fraction (arrowhead in inset). BiP is no longer detectable in this combined preparation, demonstrating the utility of pre-fractionation on an Optiprep gradient. Residual ATP synthase is detected in the eluted fraction. *Labels*: Pool - pooled fractions 15-20 from the initial Optiprep gradient. Other labels are as described in figure 2A. *Loading*: Equivalent amounts of all fractions were loaded. *Detection*: normal sensitivity chemiluminescence (Nrv), high sensitivity chemiluminescence (BiP, ATP synthase). **B -** Fractionation of microsomes prepared from 0-15 hr embryos. Some α-Spectrin is recovered in the eluted fraction although some seems to have partitioned into dextran phase D1 and some has been excluded from the ConA as seen in the PEG phase (P1+P2). Neither BiP, nor ATP synthase is detectable in the eluted ConA fraction. *Labels*: same as A. *Loading*: Equivalent amounts of all fractions were loaded. *Detection:* high sensitivity chemiluminescence (α-Spectrin, BiP and ATP synthase). N.B. 'high' sensitivity detection reagents are 100-1000× more sensitive than the 'normal' sensitivity substrates and were used to detect even low-level residual contamination.

2.3.4 Optimization of PEG/Dextran concentration for aqueous two-phase affinity partitioning

Despite successfully eliminating the ER, substantial loss of PM markers by non-specific partitioning into the dextran phases during equilibration clearly reduced the yield in the final ConA fraction. In order to increase our PM yield, we decided to test the effect of various PEG/Dextran concentrations on the partitioning of the marker proteins for the PM and ER (Fig. 2.6). Since the spectrum of membrane lipids in vertebrates and invertebrates are significantly different (Rietveld *et al*., 1999; Stark *et al*., 1993; Zachowski, 1993), the optimal concentrations of PEG and Dextran for 2PAP derived for vertebrate analyses may well be inappropriate for invertebrates. Moreover, because we are pre-enriching for PM through the use of a density gradient we need be less concerned about differential partitioning of PM from endomembane based upon their relative solubility in the PEG and dextran phases. Thus our goal need only be to maximize the fractionation of membrane into the PEG phase from which the ConA-Dextran could effect the final purification.

To optimize the yield of PM in the PEG phase, we performed an experiment on unfractionated P100 microsomes from heads, using a range of PEG/Dextran concentrations from 5.4-6.9%. To standardize the input a single P100 preparation was evenly split into individual 1-g systems made up with the indicated PEG/Dextran concentrations (Fig. 2.6). Immunoblot analyses on the upper PEG phases and lower Dextran phases for each concentration used shows that at PEG/Dextran concentrations of 6.3% and above Nrv partitions exclusively into the dextran phase, whereas from 6.0% and below a prominent fraction is found in the PEG fraction (Fig. 2.6A). Interestingly, at around 5.7% the majority of Nrv is always found in the PEG fraction. It is striking that the partitioning of the ER (BiP) mimics that of Nrv at all PEG/Dextran concentrations suggesting that the PEG/Dextran mixture does not significantly enrich for PM on its own as it does with vertebrate sources. To further investigate this transition we performed experiments interpolating values between 5.7% and 6.0%. There is always a transition between these two values, but the nominal percentage at which this occurs may vary between 5.8% and 6.0% (Fig. 2.6B). This variability may arise from very slight

Figure 2.6 Optimization of PEG/Dextran concentrations to be used for two phase affinity partitioning

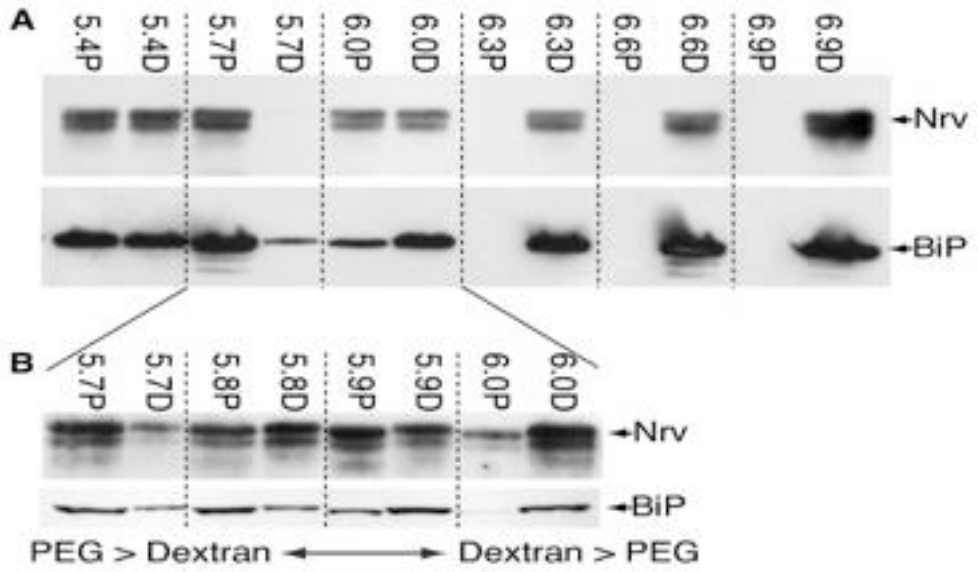

Fig 2.6 Optimization of PEG/Dextran concentrations to be used for two phase affinity partitioning. **A**. Immunoblot analysis of partitioning of Nervana and BiP into PEG (P) and Dextran (D) at different concentrations of PEG/Dextran (from 5.4% PEG/Dextran to 6.9% PEG/Dextran). At concentrations above 6.0-6.3% Nervana partitions into the dextran phase preferentially while at 6.0% and below Nervana is found in both phases. BiP behaves identically. The significant drop in microsome partitioning into dextran seen between 5.7% and 6.3% is seen in all preparations but can be variable in extent, as illustrated in B. **B**. The same experiment performed for a range of percentages from 5.7-6.0% PEG/Dextran reveals a fairly abrupt transition between 5.8% and 5.9%. While a majority of both markers is seen in the PEG fraction at 5.7% and in the Dextran phase at ≥ 6.3%, the precise fractionation behaviour in the transition zone is somewhat variable. The Nrv and BiP blots shown in this panel are from different preparations to illustrate this phenomenon (see text for further discussion).

differences in the actual percentage that can easily arise during weighing to make up each system, or perhaps from slight variation in protein content in each microsomal preparation. To maximize our final yield of PM in the PEG fraction, and to ensure maximum reproducibility we decided to use a 5.7% PEG/Dextran mixture.

2.3.5 Aqueous two-phase affinity partitioning II (5.7% PEG/Dextran)

We next applied the optimized 5.7% PEG/Dextran percentage to a 2PAP - only protocol. This results in a significant increase in Nrv yield in the ConA fraction (Fig. 2.7A; compare with Fig 2.5A); however, a readily detectable amount of BiP is still seen in this same fraction. Based upon these results, we decided to combine density gradient centrifugation with 2PAP, this time with 5.7% PEG/Dextran phase separation systems.

2.3.6 Combined density gradient centrifugation and aqueous two-phase affinity partitioning II (5.7% PEG/Dextran)

To apply the optimized combined protocol, head microsomes were subjected to density gradient fractionation as before, and the pool of PM fractions (15-20) from the gradient was subjected to 2PAP with 5.7%PEG/Dextran (Fig 2.7B). With the optimized concentration the yield of Nrv is still satisfactory, while BiP is reduced to undetectable levels in the final ConA fraction. Probing phases with anti-HRP further corroborates the presence of post-Golgi glycosylation patterns in the final preparation (Fig. 2.4C). Thus the overall yield and purity of the PM is considerably improved in comparison to that after performing 2PAP with 6.3%PEG/Dextran. Residual ATP synthase is still detected; however, we believe that this represents low levels of membrane mixing (see Discussion).

Figure 2.7 Immunoblot analysis of head microsomes fractionated by two phase affinity partitioning alone or by density gradient centrifugation followed by two phase affinity partitioning at 5.7% PEG/Dextran

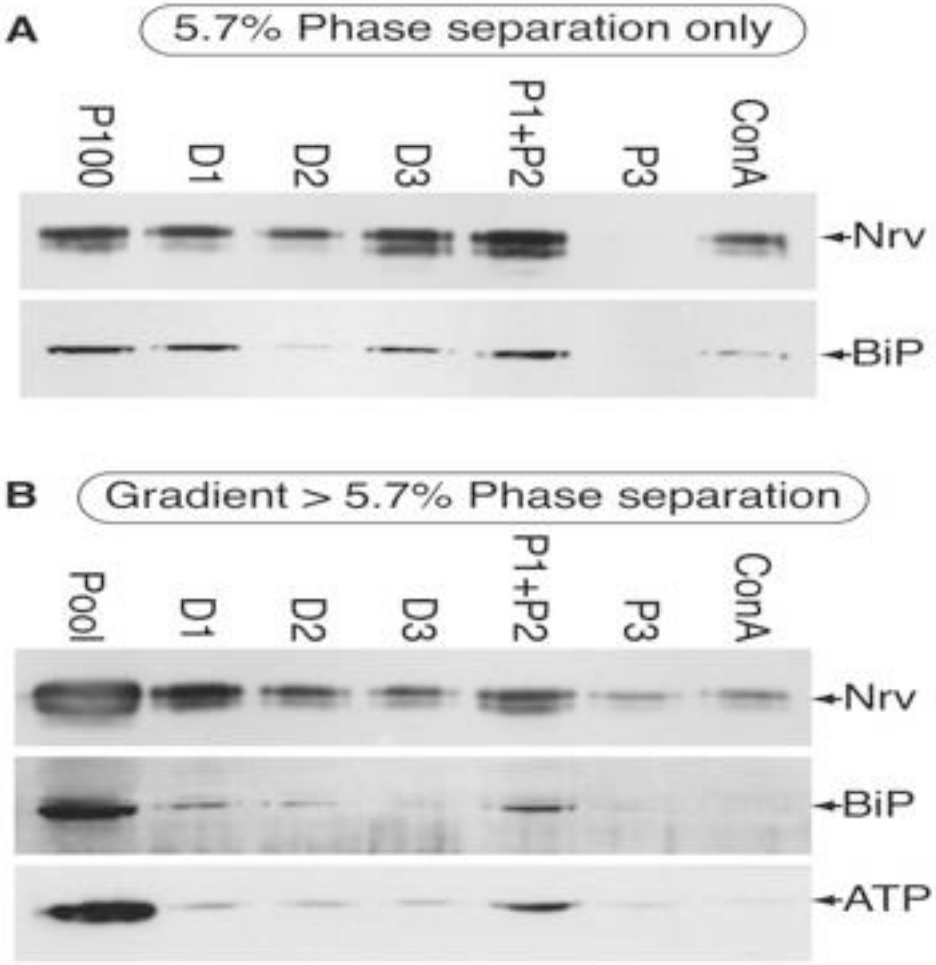

Fig 2.7 Immunoblot analysis of head microsomes fractionated by two phase affinity partitioning alone or by density gradient centrifugation followed by two phase affinity partitioning at 5.7% PEG/Dextran. **A** - Fractionation by two-phase affinity partitioning alone. The yield of Nervana is significantly improved (compare to Figure 2.5A.) However, BiP is still present in the ConA fraction indicating that 2PAP alone at the 5.7% concentration is still insufficient to produce high purity PM. *Labeling*: same as figure 1.2. *Loading*: All samples have equivalent loading, except P100, which was $1/5^{th}$ of the others. **B** - Fractionation by two phase affinity partitioning following an initial density gradient fractionation. The Nervana is still found in the ConA sample, but this fraction no longer contains detectable BiP. Small amounts of residual ATP synthase are still present. *Labeling*: same as figure 4. *Loading*: Equivalent amounts of all fractions were loaded.

2.4 Discussion

The success of aqueous two-phase affinity purification (2PAP) to isolate high purity plasma membranes from rat livers, lungs and brain (Abedinpour and Jergil, 2003; Ekblad and Jergil, 2001; Persson and Jergil, 1992; Persson *et al*., 1991; Schindler *et al*., 2006) suggested that this would be an excellent technique to combine with the sophisticated genetic approaches possible with the invertebrate *Drosophila melanogaster*. To date, plasma membrane isolation from *Drosophila* tissues has been based on density gradient centrifugation (Rao *et al*., 2007; Eroglu *et al*., 2003; Jiang *et al*., 1986), and to the best of our knowledge the use of 2PAP has not yet been reported for this model. Here we adapt 2PAP to the fly model. In contrast to reports using 2PAP with vertebrate tissue sources, we found that the initial PEG/Dextran partitioning steps in the 2PAP technique are not effective in differentially partitioning PM from ER membranes. In addition, a necessary substitution with respect to most recent 2PAP protocols (Schindler *et al*., 2006) is the use of the lectin Concanavalin A (ConA) for wheat germ agglutinin (WGA) to select for glycoprotein-containing microsomes. This is because protein glycosylation patterns in insects are simple and rich in mannose (Rendić *et al*., 2008). However, this lectin is less specific for post-ER proteins. To overcome these two problems we extend the 2PAP technique through the use of a pre-enrichment density gradient centrifugation step to produce PM of high purity.

2PAP is reported to enrich for PM in part by preferential enrichment in the PEG fraction (Schindler *et al*., 2006); however, this was not our experience with *Drosophila* membranes. A key difference in partitioning behavior may arise from differences in lipid composition between vertebrates and insects and as well as differences in the way lipids are segregated between organelles. In mammals the plasma membrane is rich in phospholipids (sphingomyelin, phosphatidylcholine, phosphatidylethanolamine, phosphatidylserine and phosphatidylinositol) along with large amounts of cholesterol (van Meer *et al*., 2008). In contrast, intracellular compartments have a higher percentage of phosphatidylcholine and phosphatidylethanolamine, much-reduced sphingomyelin and phosphatidylserine, and much lower cholesterol levels (*ibid*). Whereas, plasma membranes from *Drosophila* contain similar head groups to vertebrate sources, they have shorter fatty acid chains (Rietveld *et al*., 1999; Stark *et al*., 1993), and the major sterol is

ergosterol (Rietveld *et al*., 1999). We have found no reports comparing the lipid profile of PM and intracellular membranes in *Drosophila*; however, a study on mosquito *Aedes aegypti* (also of order *Diptera*), suggests that sphingosine containing lipids are not significantly enriched in the PM, nor are phosphatidylcholine and phosphatidylethanolamine enriched on internal compartments (Butters and Hughes, 1981). If this lack of distinction between the types of bulk lipids in different compartments holds for *Drosophila* as well, this might explain the lowered efficiency of PM enrichment in PEG/Dextran system compared to mammalian tissue sources. This problem, coupled with the lower discrimination by ConA, fully explains our initial results and the continued presence of ER in the final affinity selected fraction. To solve this problem we used density gradient centrifugation to separate the plasma membrane from intracellular membranes. Since this is based on density and not on differential solubility of the microsomes, this effectively removes the vast majority of ER. The small amount that does carry through with the PM fractions on the gradient is then removed with the help of the affinity step in 2PAP. Because differential lipid solubility in the PEG/Dextran system is not an essential enrichment step in our implementation of 2PAP we further adjusted our method to increase the fraction of PM in the PEG phase (by changing from 6.3% to 5.7% PEG/Dextran mixtures), boosting our overall yield of PM. This is probably an important optimization step in adaptation to other models. In vertebrates, the use of PEG/Dextran concentrations above 5.7% can result in a slight enrichment of PM over ER in the PEG phase during the equilibration steps (Schindler *et al*., 2006); however, in our hands this reduces the PM yield by about 50%. Combining more fractions from the density gradient could offset this, but only at the cost of PM purity. Thus we favour our current strategy.

Although our method eliminates almost all ER, low-level contamination with mitochondrial proteins remains (Fig. 2.7B). In the hope of keeping most of the mitochondria intact we adjusted our extraction conditions buffer to one that should optimize *Drosophila* mitochondrial integrity (Beziat *et al*., 1997). Intact mitochondria should be removed by early low speed spins, and the major peak of residual mitochondrial membrane in the Optiprep gradients is well below our PM pool (see Fig. 2.3). Thus, the presence of low levels of mitochondrial membranes in the lighter PM

fractions is probably due to organelle fragmentation and mixing with PM during initial homogenization. However, we note that this is not the only possibility: ConA has been reported to have affinity for some mitochondrial membrane proteins (Chandra *et al*., 1998, Lopez *et al*., 2000 and Distler *et al*., 2008), and some mitochondrial proteins have been reported to also reside at the plasma membrane (seen in rat livers (Bae *et al*., 2004). Thus, we conclude that such contamination may be unavoidable or possibly of functional significance.

Finally, in extending this method to whole flies and to other stages in the life cycle, additional lectins should perhaps be considered. While glycosylation in adult brains is mostly mannosidic or paucimannosidic (Koles *et al*., 2007) ~ 40% of N-glycans in adult flies are α-1,6 fucosylated (Fabini *et al*., 2001). *Aleuria aurantia* lectin for example has affinity for α 1-2, -3, -4 and α 1-6 fucosylated glycans (Iskratsch *et al*., 2009; Tateno *et al*., 2009), and might be of some utility, perhaps in combination with ConA. However, we note that Nervana and Fasciclin 1, which are both known to be core fucosylated, are present in our preparation suggesting that other groups on such proteins still allow their purification by our method.

Chapter 3 Defining the plasma membrane proteome of the *Drosophila* head

(Some results from this chapter have been published, Khanna, 2010).

3.1 Introduction

A search for the key word "proteomics" in PubMed (www.ncbi.nlm.nih.gov/pubmed/) yields approximately 30,000 results, the earliest of which dates back to just 1998. This is a relatively young field, dedicated to the study of proteins in a given organism, organ or tissue under a given set of conditions. Progress in the field has been largely dependent on advances in mass spectrometry (MS)-based methods that have enabled the creation of proteome databases for various model organisms and the identification of protein modifications and interactions. The future of proteomics is a bright one, which promises to shed light on cellular mechanisms, molecular pathways and potentially novel disease biomarkers (Gstaiger and Aebersold, 2009).

The success of MS-based proteomics for the identification of proteins relies on a well-annotated genome, making *Drosophila* an ideal candidate for proteomic studies. In a recent pioneering study (Brunner *et al*., 2007) performed to catalog the *Drosophila* proteome, 63% (updated to 65% in 2009) of the predicted proteome was cataloged. 9124 proteins were detected at a false discovery rate of 1.37%. Other studies on global protein expression have been on whole embryos and heads (Taraszka *et al*., 2005b; Taraszka *et al*., 2005a) or have focused on comparing protein profiles in whole flies under different conditions, such as age (Fleming *et al*., 1986; Xun *et al*., 2007), presence of a conditional lethal mutation (Pedersen *et al*., 2010), a *parkin* null mutation (Xun *et al*., 2009) and presence or absence of sex peptide during mating (Domanitskaya *et al*., 2007). Various subcellular proteomes have also been studied and documented, including those of the mitochondria (Alonso *et al*., 2005), ribosome (Alonso and Santaren, 2006), lipid droplets (Beller *et al*., 2006), nuclear matrix (Kallappagoudar *et al*., 2010) and the centrosome (Muller *et al*., 2010).

Originally, the analysis of proteomes required the proteins to first be separated and then digested. Separation of the proteins was usually gel-based and in one or two dimensions. Proteins can be separated on the basis of their size alone on a 1D-SDS PAGE and the gel slices can then be digested with trypsin or other proteases. The resulting peptides are further separated by liquid chromatography (LC) and analyzed by tandem mass spectrometry (MS/MS). One advantage of using a 1D gel is its ability to separate proteins in a wide molecular mass range. Secondly, relative abundance of proteins in a sample can be determined by staining and these low-abundance bands can be digested and analyzed separately so that their identification isn't masked by proteins present in larger amounts (Stasyk and Huber, 2004). However, recovery of hydrophobic peptides from in-gel digestion continues to be a problem (Lu *et al*., 2008). Proteins can also be separated in two dimensions, first on the basis of their isoelectric points using immobilized pH gradients (IPGs) and then on the basis of size in the second dimension by PAGE. The spots on the gel can then be cut out, digested and peptides separated and analyzed by LC-MS/MS. Separation of proteins in two dimensions allows for greater resolution and IPGs are capable of taking high protein loads (up to 5 milligrams), permitting the visualization of low-abundance proteins as well (Molloy, 2000). One of the problems that have long plagued protein separation by 2D PAGE has been its limited capacity to resolve membrane proteins. This was found to be mostly due to their poor solubilization during sample preparation and successful attempts to overcome this shortcoming have involved the addition of chaotropes (urea, thiourea) and certain surfactants (ASB-14) to solubilization reagents (Molloy, 2000). While advances in protein resolution by 2D PAGE continue, this technique hasn't as yet allowed a comprehensive view of a membrane proteome.

A seminal study reported in 2001 surpassed the capability of 2D PAGE in identifying an unparalleled number of proteins from *Saccharomyces cerevisiae* in comparison to any proteome up until that time (Washburn *et al*., 2001). The technology used was termed Multidimensional Protein Identification Technology (MudPIT). It involves digestion of an unresolved protein mixture into peptides and their subsequent separation in multiple dimensions, each dimension exploiting a different molecular property of the peptides being separated. The most common approach is the use of strong

cation-exchange (SCX) in the first dimension, followed by reversed phase (RP) chromatography in the second dimension and finally MS analysis. SCX separates peptides on the basis of charge: acidified peptides are loaded onto a column containing SCX resin. The positively charged peptides adhere to the negatively charged column and are eluted with increasing salt concentrations. The fractions thus obtained are then separated in the second dimension on the basis of their hydrophobicity *via* RP chromatography. In this method, the SCX-eluted peptides are loaded onto a hydrophobic solid support and are eluted with increasing concentrations of organic solvents (reviewed by Stasyk and Huber, 2004; Lu *et al*., 2008; Yates *et al*., 2009). MudPIT has revolutionized the field of proteomics. It is a method that has overcome the bias of traditional proteomic methods towards abundant and soluble proteins. Proteins that have extreme pIs or molecular weights or which are hydrophobic have been well represented by this method (Washburn *et al*., 2001).

Having developed and optimized the technique to isolate plasma membrane proteins from *Drosophila*, we sought to identify the proteins isolated from heads using this technique. Knowing that the sample would be predominantly comprised of membrane proteins, we chose MudPIT for protein identification. The goal was twofold: First, it would confirm the specific enrichment and isolation of plasma membrane proteins versus residents of the ER and the Golgi as demonstrated *via* immunoblots in Chapter 3. Second, it would provide an initial profile of the *Drosophila* head plasma membrane proteome. We identified 432 *Drosophila* head proteins by MudPIT analysis, 22-56% of which are likely to be PM proteins. Our results provide an initial PM proteome for this largely neuronal tissue source. To the best of our knowledge, this sub-proteome has been undefined in *Drosophila* to date.

3.2 Materials and Methods

3.2.1 Preparation of samples for Mass Spectrometry

The ConA pellet was subjected to in-solution proteolysis as previously described (Zhao *et al*., 2008). Eluted membrane pellets were resuspended and reduced (2.5 mM DTT, 50 mM ammonium bicarbonate, pH 8) at 50^{o}C for 30 min with sonication. This was followed by alkylation (10 mM iodoacetamide, 50 mM ammonium bicarbonate, pH 8) in the dark for 30 min at 37^{o}C and quenching with 11 mM DTT at 37^{o}C for 30 min. The reduced and alkylated proteins were then digested with 1 μg of Promega Gold Trypsin (Promega Corp., Madison, WI) in 200 μl 50 mM ammonium bicarbonate and 37% acetonitrile at 48^{o}C for 3 h, followed by 37^{o}C for 16 h. Following digestion, the reaction was dried to remove solvents and buffers, and resuspended in 200 μl of distilled water. Drying and resuspension were done two more times, and the pellet was finally resuspended in 10 μl of 0.1% trifluoroacetic acid.

3.2.2 Mass Spectrometry and data interpretation

Mass spectrometry and data acquisition was done at The Mass Spectrometry Core Research Facility at Penn State, Hershey as described (Zhao *et al*., 2008). Peptides were separated using LC-MALDI techniques through two sequential columns: strong cation exchange (SCX) and C18 nanoflow chromatography. The samples were dried down, loaded in SCX loading buffer and SCX separations were carried out on a passivated Waters 600E HPLC system, using a 4.6 X 250 mm PolySulfoethyl Aspartamide column (PolyLC, Columbia, MD) at a flow rate of 1 ml/min. Buffers used were Buffer A (10 mM ammonium formate, pH 3.6, in 20% acetonitrile/80% water) and Buffer B (666 mM ammonium formate, pH 3.6, in 20% acetonitrile/80% water). The gradient was Buffer A at 100% (0- 30 minutes following sample injection), 0%→35% Buffer B (30-48 min), 35%→100% Buffer B (48-49 min), 100% Buffer B (49-56 min), then at 56 min reverted to 100% A to re-equilibrate for the next injection. The first 28 ml of eluant (containing all flow-through fractions) were combined into one fraction, then 14 additional 2-ml fractions were collected. All 15 of these SCX fractions were dried down completely to reduce volume and to remove the volatile ammonium formate salts, resuspended in 15 μl

of 2% (v/v) acetonitrile, 0.1% (v/v) trifluoroacetic acid and filtered before reverse phase C18 nanoflow-LC separation. For reverse phase nanoflow-LC, each SCX fraction was autoinjected onto a Chromolith CapRod column (150 X 0.1 mm; EMD Chemicals Inc., Gibbstown, NJ) using a 5 µl injector loop on a Tempo LC MALDI Spotting system (ABI-MDS/Sciex). Buffers used were Buffer C (2% acetonitrile, 0.1% trifluoroacetic acid) and Buffer D (98% acetonitrile, 0.1% trifluoroacetic acid). The elution gradient was {95% C/ 5% D (0-8 min)}), ®40% D (8.1-40 min), ®80% D (41-44 min), ®5% D (44-49 min) (initial conditions). Flow rate was 2.5 µl/min, and an equal flow of MALDI matrix solution was added post-column (7 mg/ml recrystallized CHCA (α-cyano-hydroxycinnamic acid), 2 mg/ml ammonium phosphate, 0.1% trifluoroacetic acid, 80% acetonitrile). The combined eluant was automatically spotted onto a stainless steel MALDI target plate every 6 seconds (0.6 µl per spot), for a total of 370 spots per original SCX fraction. The resulting 5500 MALDI spots were analyzed and MS and MS/MS spectra were obtained using an ABI 4800 MALDI TOF-TOF analyzer. Peptide and protein identification was performed with the Paragon "Sequence Temperature Value" algorithm (Shilov *et al*., 2007) contained in Protein Pilot software version 2.01 (Applied Biosystems/MDS Sciex), and the ProGroup algorithmfor protein inference and grouping from tandem mass spectrometry (MS/MS) spectral/peptide data. Search criteria were trypsin-cleaved peptides; iodoacetamide-modified cysteines; ID Focus = Biological Modifications; Thorough Search setting; and Detected Protein Threshold = 0.05 (10.0%). Protein Pilot automatically searches for a series of potential biological and sample preparation-induced modifications once a suitable sequence tag of 3-4 amino acids has been found within an MS/MS spectrum.

MS/MS data from 2D LC MALDI MudPIT experiments were analyzed using both Mascot and Protein Pilot software version 2.0. For both algorithms, protein identification acceptance criteria were C.I ≥ 98% (equal to a Protein Pilot Unused Score of 1.7) for proteins identified with multiple peptides, and C.I ≥ 99.9% for proteins detected from a single peptide, plus acceptable false discovery rates (FDRs). In the Protein Pilot analyses, proteins identified through MudPIT were accepted only if they met our C.I. criterion and also had an estimated FDR <0.05. The decisions about how to arrive at the minimal protein list which accounts for all the observed spectral evidence are

calculated by the ProFound algorithm also contained in the Protein Pilot software. All identified proteins had an Unused Score of 1.7 or higher, which corresponds to a confidence of 98% or higher. A second requirement was that all identified proteins have an estimated local FDR of 5% or less, based on the number of IDs at any cutoff Unused Score from a "normal" database (database searched was the NCBInr *Drosophila* Protein Sequences as of 11/26/2008, containing 89,592 protein sequences) compared to the number of IDs from a concatenated forward and decoy database plus a list of known (ConA) or common potential contaminants such as keratins, common laboratory reagents such as BSA, and trypsin autolysis peaks. The decoy database was a randomized version of the same NCBI nr database, where amino acid frequencies in the database were kept the same as in the normal database. The FDR used as a cutoff for accepting Protein Pilot identified proteins was a local (sometimes called "instantaneous") FDR of 5% or lower, meaning that the protein with the lowest accepted score still had an estimated probability of less than 5% of being a false positive, based on the rate of increase in the accumulation of decoy database hits at that particular cutoff score. This local FDR was calculated using the Proteomics System Performance Evaluation Pipeline (PSPEP) tool (Tang *et al.*, 2008). Proteins appearing in databases under different names and accession numbers is taken care of by the ProGroup algorithm embedded in ProteinPilot software, which groups all homologous proteins with different names in the database under one Protein Family, selecting only one of these equivalent protein IDs for inclusion on the list of 432 proteins.

3.3 Results

3.3.1 Protein identification of affinity purified proteins from *Drosophila* heads

In our initial (pre-optimisation) analyses, apparently satisfactory protein concentrations in the final ConA fraction failed to result in reliable protein identifications. Analysis of such preparation by SDS polyacrylamide gel electrophoresis (PAGE) and staining with colloidal coomasie blue revealed that ConA was the only band on the gel (not shown). This indicates that during elution a significant amount of ConA is released from the column. This probably results from the tetrameric structure of this lectin and that coupling to the dextran for each tetramer is *via* less than four subunits: Crosslinked subunits can therefore dissociate and be released. However, when we analyzed a ConA fraction from an optimized combined preparation by SDS PAGE, a robust protein ladder was seen in addition to the ConA band (Fig. 3.1A).

Proteins from an optimized ConA fraction were trypsin digested and identified by MudPit. 432 protein identifications were accepted with >95% confidence and a <5% false discovery rate (see Methods; Table 3.1). To evaluate this sub-proteome we performed two analyses. Since, integral membrane proteins can be hard to identify by MS due to poor peptide solubility we subjected the primary sequence of all identified proteins to hydropathy analysis by the method of Kyte and Doolittle (Kyte and Doolittle, 1982) to estimate the total number of integral membrane proteins identified in our preparation. For this analysis we used the Protean tool in DNASTAR using a stringent 19 residue window, and only accepted results with at least one region scoring >1.6 that was not at the N-terminus as recommended by Kyte and Doolittle (Kyte and Doolittle, 1982); annotations are listed in Table 3.1 with cross reference to the hydropathy plots in Supplementary Table 4 (refer to file uploaded for BMC Genomics www.biomedcentral.com/1471-2164/11/302). 159 out of the 432 proteins identified (37%) were positive in this assay indicating that our digestion and identification protocol is more than satisfactory for the identification of these challenging proteins. However, there are alternatives to the Kyte and Doolittle method (e.g. TMHMM method at www.cbs.dtu.dk/services/TMHMM/), which can also be used.

Figure 3.1 Protein identification from head PM preparation

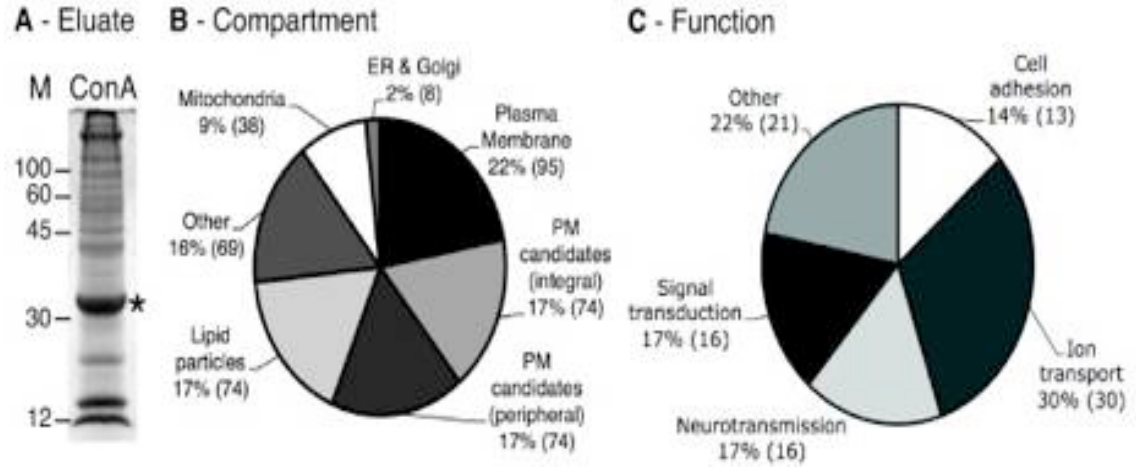

Fig 3.1 Protein identification from head PM preparation. **A -** SDS PAGE analysis of proteins eluted from the ConA in a head PM preparation from ~20 g of flies. Gel is stained with colloidal coomasie blue. Asterisk - prominent ConA band that coelutes from the dextran, probably due to tetramer disassembly. The presence of this band prevents us from an accurate protein determination from our preparation; however we estimate there to be 50-100 µg protein on this gel. Three such preparations were combined for our MudPIT analysis. **B -** Pie chart showing the breakdown of protein types and compartments identified with high reliability in our MudPIT analysis. Compartment assignments were taken from annotations at Flybase.org in conjunction with our hydropathy analsysis (see text and Table 2). Plasma Membrane -integral or peripheral plasma membrane proteins; PM candidates (integral) - integral membrane proteins with no current assignment to any compartment (see text); PM candidates (peripheral) - have no predicted transmembrane domain and no currently assigned compartment (see text); Other - ribosome, cytoskeleton, synaptic vesicle, cytoplasmic; Mitochondria - mitochondrial; ER & Golgi - endoplasmic reticulum and Golgi apparatus; Lipid particles - lipid particles. Some of these may also be present in mitochondria and/or ER (see text for discussion). **C -** Pie chart showing the functional annotation of proteins identified in the plasma membrane fraction in B. 78% are associated with cell surface activities (Cell adhesion, Ion transport, Neurotransmission, Signal Transduction). See Table 3.3 for the specific assignment of each protein.

Second, proteins were assigned to sub-cellular compartments based on their existing annotation in Flybase (Flybase.org) or in conjunction with our hydropathy analysis. These assignments are broken down in Table 3.2 and are illustrated in Figure 3.1B. Satisfyingly, the largest single category of proteins at 22% is annotated in Flybase as 'Plasma membrane', of which a majority are predicted to be integral membrane proteins. Two of the next largest groups we have designated as 'Candidate Plasma Membrane Residents'. This group does not have a currently assigned compartment, but given the high frequency with which we have recovered *bona fide* PM proteins we feel that a majority of these may well reside at the PM. Obviously this will require future experimental verification, and we expect that some will eventually prove to reside elsewhere. In fact, if one were to exclude these proteins from the categorization, then the new distributions would be: Plasma membrane (33%), ER+Golgi (3%), Mitochondria (14%), Lipid particles (26%) and Other (24%). Thus, a more conservative prediction of the compartments that the unassigned proteins may fall in would result in dividing this group in the same proportions as the newly assigned protein fractions. However, we have chosen to break this down into those that are predicted to be integral membrane proteins (17%) and those with no evidence of a transmembrane domain in our assay (17%). Together with the *bona fide* PM proteins this provides an upper limit of 56% (22+17+17) for the number of proteins in the PM compartment that we have identified. The remaining proteins have non-PM assignments in Flybase (Table 3.2; Fig. 3.1): 17% were from lipid particles; 16% were from 'Other' compartments; Only 9% are mitochondrial; and just 2% are ER or Golgi resident. A few of the proteins that are assigned to "lipid particles" by Flybase (Flybase.org; Beller *et al*., 2006) are also residents of the ER and mitochondria. This reflects the possibility that lipid droplets may originate from either the ER (Thiele and Spandl, 2008) or mitochondria (Caetano *et al*., 2002). If we were to reassign these proteins to the ER and mitochondrial categories the percentages of these two compartments would not change dramatically (3% and 16% respectively).

We further classified the definitive PM proteins on the basis of their cellular function (FlyBase; Fig 3.1C). The categories are: Cell adhesion, Neurotransmission (includes proteins involved in neurotransmitter transport and secretion), Signal

Table 3.2. Membrane and compartment assignments for identified proteins

Category	Compartment	Flybase annotation	Percent integral[1]	Number of proteins in category	Percentage of all proteins
Plasma Membrane	Plasma membrane	Plasma membrane	60% (57/95)	95	22%
Candidate Plasma Membrane Residents (Integral)	Not assigned	Membrane	50% (10/21)	74	17%
		Integral to membrane	100% (21/21)		
		None but we predict ≥1 transmembrane domain	100% (43/43)		
Candidate Plasma Membrane Residents (Peripheral)	Not assigned	Membrane	NA[2] 11 proteins	74	17%
		None with no predicted transmembrane domains	NA[2] 63 proteins		
Lipid particles	Lipid particles	Lipid particles	22% (16/74)	74	17%
Other	Cytoplasm and Nucleus	Cytoplasm Cytoskeleton Nucleus Ribosomes	6% (4/69)	69	16%
Mitochondrial	Mitochondrial	Mitochondrial	18% (5/38)	38	9%
Endoplasmic reticulum and Golgi	Endoplasmic reticulum and Golgi	Endoplasmic reticulum and Golgi	38% (3/8)	8	2%
All compartments			37% (159/432)	432	100%

[1]Proteins predicted by hydropathy analysis to have ≥ 1 transmembrane domain
[2]Not Applicable - neither category has any predicted integral membrane proteins.
The table shows the number of proteins assigned to compartments based on their Flybase annotation in conjunction with our hydropathy analysis. The biggest single category has been annotated in Flybase as 'Plasma membrane'. The next two categories we predict will also contain a substantial fraction, which are in the PM compartment; however, this will obviously require experimental verification by interested investigators (see text for discussion).

transduction, Ion transport, and Other (includes proteins that are structural, involved in cell polarity, ion/protein binding, have roles in axogenesis and central nervous system development). The largest category of proteins are involved in ion transport (30%) and include the likes of excitatory amino acid transporter 1 and Na^+/K^+ ATPase (α subunit). 17% each were involved in signal transduction and neurotransmission, and 13% in cell adhesion. Proteins involved in signal transduction include G-proteins as well as proteins in the InaD-signaling complex. Among those in the category "neurotransmission" are Syntaxin 1 as well as Neurexin 1 and 4. Cell adhesion proteins include Fasciclin 1 and 3, N-cadherin and Contactin. Most of these proteins were also found in the rat-brain plasma membrane preparation by Schindler *et al.* (2006). A complete list of the plasma membrane proteins along with their functional categories is provided (Table 3.3).

3.4 Discussion

The original 2PAP technique gave a preparation containing 34-42% PM proteins from rat brains (Schindler *et al*., 2006). In comparison, 22% of our proteins are annotated in Flybase as 'Plasma membrane'. If we add to this the 34% of proteins in our preparation that have not yet been assigned to a compartment by other techniques this suggests that we may have as many as 56% PM proteins in our preparation and conclude that that our likely yield for the PM proteome as a whole is in the 22-56% range. This is very comparable to these previous efforts.

Few prior attempts have been made to define the *Drosophila* head proteome (Taraszka *et al*., 2005a; Taraszka *et al*., 2005b; Matsumoto *et al*., 2007). Matsumoto *et al*. tried to define the total *Drosophila* brain and eye proteome through 2D PAGE analysis on dissected tissues and in comparison to our PM sub-proteome, they only identified ~15% of the definitive plasma membrane proteins identified in our preparation were found in the brain/eye lists. Taraszka *et al*. (2005b) mapped the whole head proteome of *Drosophila melanogaster* using the same MudPIT approach employed by us (SCX/RPLC). A total of 780 proteins were identified, of which the largest fraction (111 out of 780) of known proteins belonged to the mitochondria. A mere 38 proteins were found to be residents of the plasma membrane and only 38 proteins were membrane proteins (inclusive of those integral and extrinsic to the membrane; Taraszka *et al*., 2005b). Taraszka *et al*, in spite of having used a greater amount of total head protein (2.8 milligrams) compared to our ≤ 1 milligram of protein (a significant proportion of which was the contaminant ConA) for MudPIT were barely able to identify 76 membrane proteins (inclusive of the plasma membrane). Two other important distinctions exist between the method of sample preparation followed by Taraszka *et al*. and us. We carried out trypsin-digestion of the proteins in the presence of 37% acetonitrile (ACN; organic solvent) and at an initial temperature of 48^{o}C for 3 hours, followed by overnight at 37^{o}C. Taraszka *et al*. didn't use an organic solvent during digestion and carried it out for 24 hours solely at 37^{o}C. The use of an organic solvent most likely augmented the digestion and extraction of hydrophobic proteins and peptides respectively in our method. Also, the action of trypsin is said to be optimum at 48^{o}C (Bruce Stanley, personal communication).

Besides the fact that we enriched for plasma membrane, these other factors may have accounted for our high yield of membrane proteins. While our initial definition of the head PM proteome is by no means exhaustive, comparison with these other studies cited emphasizes the value of enriching for the study of the PM.

Finally, some improvements have been suggested to the current MudPIT strategy as applicable to membrane proteins (reviewed by Lu *et al*., 2008). The use of high pH and proteinase K in place of trypsin has been suggested – high pH is often used as a strategy to remove soluble proteins from membranes and proteinase K is quite stable at these pH values, unlike trypsin (Wu *et al*., 2003). The use of a combination of high pH, proteinase K and cyanogen bromide (CNBr) has also been tried, to allow better digestion and identification of hydrophobic peptides (Speers *et al*., 2007). Also, importance has been given to the optimization of the chromatography step in identification of integral membrane proteins. Application of heat during micro-LC of enriched transmembrane peptides resulted in a 500% increase in peptide identification in contrast to micro-LC at room temperature (Speers *et al*., 2007).

In conclusion, we have provided an initial definition of the *Drosophila* head PM proteome. It will be exciting to see more proteins added to this list in the future as current MudPIT strategies improve and other MS-based methods for membrane protein identification develop.

Chapter 4 Reestablishment of the temperature sensitive α-spectrin^{R22S} fly line

4.1 Introduction

Spectrin tetramers are formed when two αβ dimers associate head-to-head such that the N-terminus of α-spectrin (Nα) in one dimer interacts with the C-terminus of the β-spectrin (Cβ) in the opposite one. The Nα and Cβ regions each comprise partial triple helices of a 106-amino acid spectrin repeat, such that their interaction results in a complete triple α-helical bundle (Tse *et al*., 1990, Speicher *et al*., 1993). Numerous studies on human erythrocyte spectrin have revealed that tetramer formation involves residues 1-158 of α-spectrin (Kotula *et al*., 1993; Speicher *et al*., 1993). More specifically, residues 12-51 are involved in binding with β-spectrin and this is due to helical bundling in the region between residues 20-51 (Cherry *et al*., 1999). It has been demonstrated that amino acid residues 22-51 encode the partial triple helix in Nα, the residues 1-21 are a nonhomologous sequence and that the first spectrin domain begins with the 52nd residue (Lusitani *et al*., 1994). However, the involvement of residues distal to residue 52, that lie within the first spectrin domain hasn't been ruled out in formation of the tetramer (Cherry *et al*., 1999).

The disorders associated with defective spectrin tetramerization underscore the physiological importance of an intact spectrin network: The inability to form spectrin tetramers in erythrocytes results in hereditary elliptocytosis (HE; red blood cells are oval shaped instead of the biconcave disc shape of healthy cells) and hereditary pyropoikilocytosis (HPP; characterized by abnormally shaped erythrocytes that also show thermal instability; Tse and Lux, 1999). In patients with HE or HPP, the proportion of αβ dimers in erythrocytes can be as high as 60-70% in comparison to <5% in normal individuals (Tse and Lux, 1999). These disorders can be due to mutations in either, α– or β-spectrin (Tse and Lux, 1999; Zhang *et al*., 2001). β-spectrin mutations that lead to defective tetramerization can be point mutations in the C-terminal partial triple helix region (reviewed by Zhang *et al*., 2001), deletion, insertion, splice site, nonsense and missense mutations and may result in frameshifts, truncations or missense changes that

disrupt the triple α helical structure (Tse and Lux, 1999). In contrast, most mutations in α-spectrin that result in defective tetramerization are point mutations gathered around the first few spectrin repeats (Tse and Lux, 1999). Codon 28 of erythrocye spectrin (αI-spectrin) is one of the most common sites for point mutations. It encodes an arginine (R), which when mutated to histidine (H), cysteine (C), leucine (L) or Serine (S) results in impaired tetramer formation. The R→L and R→S mutations are the most severe, resulting in hemolysis that requires blood transfusion therapy (Zhang *et al*., 2001). Molecular modeling of the R→S mutation revealed its inability to form tetramers was because of a disruption in the 2 hydrogen bonds that form between R28 and residues 2018 and 2022 of βI-spectrin (Zhang *et al*., 2001). This phenotype has been found even in the presence of a mutation in residue 2018 of βI-spectrin (Zhang *et al*., 2001).

Unlike in the erythroid spectrins (αI- and βI –spectrins), the physiological effects of mutations in non-erythroid spectrins that lead to defective tetramerization haven't been extensively characterized. In fact, no pathology has as yet been attributed to mutations in the tetramerization domain of non-erythroid spectrins, probably because these mutations are lethal. A relatively recent attempt made to determine the effects of mutations in this region of human non-erythroid spectrin by yeast two-hybrid identified various single, double and triple mutations in αII-spectrin (in the partial triple helical region predominantly) that lead to defective tetramer formation (Sumandea and Fung, 2005). Interestingly, two mutations (E10D and R37P) lie outside the partial helix region and the authors presumed that this might imply a slightly longer partial helix (hence the effect of R37P) and a role for the non-homologous region upstream of the partial helix in tetramer formation in non-erythroid aII-spectrin (hence the effect of E10D). However, most important was the finding that the double mutation R19L/K30N resulted in the failure to form tetramers since residue R19 corresponds to residue R28 of αI-spectrin. In an endeavor to further characterize the tetramerization domain in non-erythroid αII-spectrin, proteins other than βII-spectrin that might interact with it were identified (Oh and Fung, 2007). 14 proteins were identified, of which 7 were unknown and 4 of the known ones had predetermined roles in the nucleus, reinforcing the idea that spectrin also has a role in the nucleus. 3 of the known proteins (Duo, TBP associated factor 1 and Lysyl-tRNA synthetase) lost their interaction with α-spectrin in the presence of a mutation (V22D)

that results in a failure to form tetramers, implying that there might be other proteins that aren't part of the conventional cytoskeleton, but may compete with one of its canonical components for reasons as yet unknown.

Defective tetramerization has also been modeled in *Drosophila* in a unique study. Deng *et al*. (1995) made two α-spectrin germ-line transformant lines, one bearing a construct carrying a deletion in the first 45 residues (*p[w$^+$UM-3,d1-45]*) and another bearing a construct that carried the arginine to serine mutation in codon 22 (erythroid spectrin Codon 28 ; *p[w$^+$UM-3,R22S], α(R22S)* and tried to rescue the α-spectrin null mutant *l(3)dre3rg^{41}/Df(3L)R-R2* with these transformants. Both the constructs were under the control of the ubiquitin promoter and carried an N-terminal myc tag. Neither mutant construct was reported to have any dominant effects and the flies were found to be normal. However, germ-line transformants carrying p[w$^+$UM-3,*d1-45*] failed to rescue the first instar lethality of α–spectrin mutations while the ones carrying p[w$^+$UM-3,*R22S*] rescued in a temperature-dependent fashion. α(*R22S*) was able to rescue the null mutant at 19^{o}C and 25^{o}C and the rescued flies displayed normal morphology although they seemed lethargic, had lowered fecundity and didn't fly. At 29^{o}C, the rescued females failed to lay viable eggs. It was found that α(R22S) didn't bind to the 18th segment of β-spectrin *in vitro* and hence the role of the R→S mutation in disrupting tetramerization in *Drosophila* was confirmed. The reduced fecundity was attributed to a reduction in the plasma membrane localization of α-spectrinR22S in the follicle cells and cystocytes in egg chambers of rescued females held at 29^{o}C.

The existence of a fly line in which the spectrin tetramer could be disrupted by merely shifting the flies to a different (restrictive) temperature seemed like an excellent tool to model the effects of the disruption of the SBMS that is characteristic of cerebral ischemia. Unfortunately, this fly line was lost- molecular and segregation analyses of both the original R22S line and the *w/w;R22S/R22S;Df(3L)R-R2/Tm6* stock by G. H. Thomas and myself in 2008 revealed: (a) that the original R22S line contained multiple P-elements distributed between both chromosomes II and III (b) that all of the chromosome II copies from the original R22S stock that were incorporated into the deficiency stock now had deletions and/or rearrangements that resulted in the loss of the 5' end of the P-element, the promoter and 5' end of the α-spectrin gene. One P-element

with an intact α-spectrin 5' end and promoter existed on chromosome III. However, this P-element probably contains rearrangements in sequences that were not analyzed. (c) that no detectable myc-tagged α-spectrin was produced by the original R22S line. Clearly rearrangements have arisen since this line was created in most of the inserts. We speculate that these were selected for because of the detrimental effects of continuous α-spectrin overexpression (mediated by the ubiquitin promoter) over the 16+ years the line was maintained.

Having lost the tool I was planning to use in order to study the effects of SBMS disruption, I chose to remake the fly line. The advantage of having a conditional mutant is the amount of control it confers on the experimental approach. Just changing the temperature to the restrictive one leads to the desired effect and bringing it back to permissive temperature would allow one to observe recovery, if any. Also, *Drosophila* is the only model system so far that has a conditional mutant for α-spectrin. Hence, we decided it was worth investing in the effort to remake the R22S line and the methods and results reported in this chapter describe how the mutant construct was remade, the fly line reestablished and confirmation of its temperature-sensitive nature.

4.2 Materials and Methods

4.2.1 Mutagenesis of α-spectrin cDNA to create α-spectrinR22S and its cloning into *P[w+UM-2]*

Plasmid *P[w+UPS]* which contains the α-spectrin cDNA under the control of the ubiquitin promoter was a gift from Dr. Ronald R. Dubrueil (University of Illinois, Chicago, IL). It was created by ligation of the α–spectrin cDNA to the *Drosophila* ubiquitin promoter using the NcoI restriction site and this product was inserted into the pW8 transformation vector, which carried the *white*$^{+}$ gene as a marker as well as 2 P element repeats (Lee *et al*., 1993; Fig 4.1). We decided that it would be best to exactly replicate their cloning scheme. So, a point mutation (c354a) was introduced in codon 22 to convert the arginine (CGT) to serine (AGT) using Stratagene's QuikChange® II XL mutagenesis kit to give α-spectrinR22S. The primers were designed using the QuikChange® Primer Design Program (www.genomics.agilent.com) and are listed in Table 4.1. In order to clone α-spectrinR22S into plasmid *P[w+UM-2]*, the NcoI restriction site (CCATGG) which included the ATG start codon in the α-spectrinR22S in *P[w+UPS]*, was mutated to a KpnI restriction site (GGTACC) using Stratagene's QuikChange® II XL mutagenesis kit. The primers were designed using the QuikChange® Primer Design Program (www.genomics.agilent.com) and are listed in Table 4.1. This step was necessary because plasmid *P[w+UM-2]* was created from the pW8 transformation vector by the introduction of the sequence encoding the first 12 amino acids of the protein myc contiguous with the ubiquitin promoter using the NcoI and EcoRI retriction sites, the former already part of the Ubiquitin promoter sequence (Heck *et al*., 1993). Between the myc sequence and the EcoRI sequence is the KpnI site, which I used to clone the α-spectrinR22S cDNA from *P[w+UPS]* into *P[w+UM-2].* This allowed me to recreate the exact construct *p[w+UM-3, R22S]* as done by Deng *et al*., (1995) under the control of the ubiquitin promoter and carrying the myc tag. The entire cloning scheme is depicted in Fig. 4.1.

Table 4.1 Mutagenesis Primer Sequences

Point mutation	Primer Sequence
c354α(R22S)	**Sense**: 5'-gacatccaggagcgaagtgagcaggttctgt-3'
	Antisense: 5'-ctgtaggtcctcgcttcactcgtccaagaca-5'
a288g	**Sense**: 5'-tgcccgcagaataatccgccatggagaactttaca-3'
	Antisense: 5'-tgtaaagttctccatggcggattattctgcgggca-3'
c289g	**Sense**: 5'-gcccgcagaataatccggcatggagaactttacac-3'
	Antisense: 5'-gtgtaaagttctccatgccggattattctgcgggc-5'
c290t	**Sense**: 5'-cccgcagaataatccggtatggagaactttacacc-3'
	Antisense: 5'-ggtgtaaagttctccataccggattattctgcggg-3'
t292c	**Sense**: 5'-ccgcagaataatccggtacggagaactttacaccc-3'
	Antisense: 5'-gggtgtaaagttctccgtaccggattattctgcgg-3'
g293c	**Sense**: 5'-gcagaataatccggtaccgagaactttacacccaa-3'
	Antisense: 5'-ttgggtgtaaagttctcggtaccggattattctgc-3'

Figure 4.1 Cloning scheme for the insertion of α(R22S) in *P[w+UM-2]*.

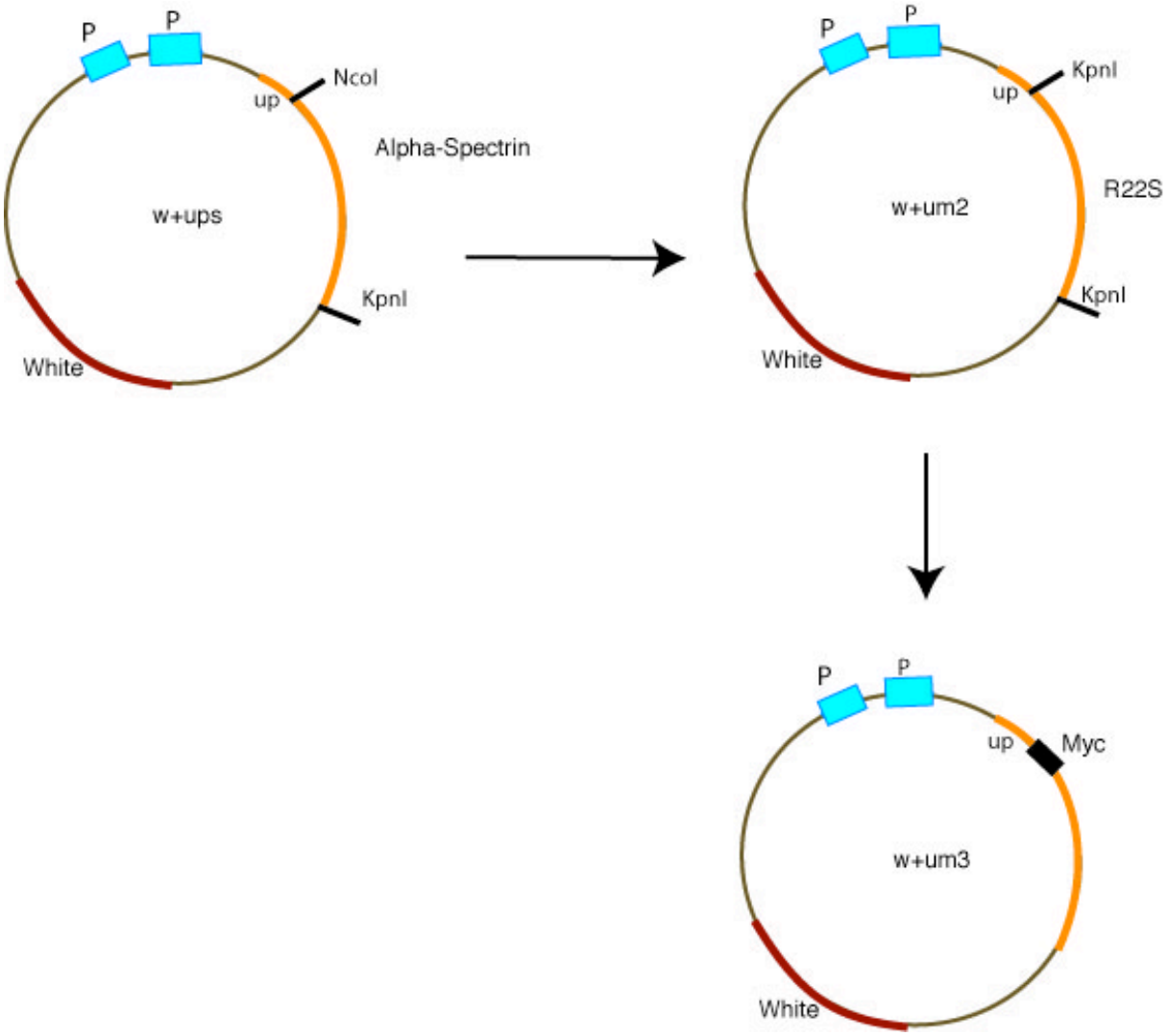

Figure 4.1 Cloning scheme for the insertion of α(R22S) in *P[w+UM-2]*. Schematic showing the creation by mutagenesis and insertion of α(R22S) into the vector *P[w+UM-2],* which was then used to create transformants. UP is the Ubiquitin promoter, P is P-element

4.2.2 Establishment of the α–spectrinR22S (R22S) fly line in an α-spectrin wild-type background

100 μg of *p[w+UM-3, R22S]* was sent to Rainbow Transgenic Flies, Inc (Newbury Park, CA) to be injected into *yellow white* (*yw)* embryos to create germline transformants. Three lines were established after two transformation attempts. In order to establish balanced fly stocks and to map the inserts, each transformant male and female (carrying the *white*$^+$ gene) was crossed to an *Apterous (Ap)/CyHu* female and male respectively. The resulting progeny, which carried the *white*$^+$, *Cy* and *Hu* markers from each cross were crossed inter se in order to establish a stock. To map which chromosome carried the insert, the male progeny carrying the *white*$^+$, *Cy* and *Hu* markers which were being used to establish stocks were also crossed to *yw* females and segregation analysis was carried out on the resulting progeny.

4.2.3 Antibodies

The following primary antibodies were used for immunoblotting / immunostaining: mouse anti-α-Spectrin (1:100,000 /1:10,000; ascites #N3 from Dr. D. Branton, Harvard University, Cambridge, MA), mouse anti-c-myc 9E10 (1:100 / 1:10; Calbiochem, San Diego, CA), mouse anti-actin #C4 (1:25,000 for immunoblot; Millipore, Billerica, MA), mouse anti-Hts 1B1 (1:25 for immunostaining; Zaccai and Lipshitz, 1996) and mouse anti-Dlg (1:50 for immunostaining; Developmental Studies Hybridoma Bank, Iowa City, IA). HRP-conjugated anti-mouse secondary antibodies (1:2500) for immunoblots were purchased from Jackson Immunoresearch (West Grove, PA). Alexafluor labeled secondary antibodies (1:250) for immunostaining, used after preadsorption against fixed embryos were purchased from Invitrogen (Carlsbad, CA).

4.2.4 SDS-PAGE and Immunoblotting

Single flies were homogenized in 60 μl of 1X Loading Buffer (Fritz *et al*.,1989). The extract was boiled for 10 minutes followed by centrifugation in a table-top microfuge at 14,000 rpm for 2 minutes. 45 μl of the supernatant was loaded onto a SDS-polyacrylamide gel (8% low-bis, ie 99:1 acrylamide:bisacrylamide ; Fritz *et al*.,1989).

The separated proteins were transferred to Hybond ECL nitrocellulose membrane (Amersham Biosciences, Piscataway, NJ) and probed using standard protocols with final detection by chemiluminescence (ECL, Amersham Biosciences, Piscataway, NJ) using CL-X Posure Film (Thermo Scientific, Rockford, IL).

4.2.5 Immunofluorescent staining of ovaries

2-4 days old females were fed with abundant yeast paste at either 21^{o}C (permissive temperature) or 29^{o}C (restrictive temperature) for 3-5 days. Dissected ovaries were teased apart into individual ovarioles in Phosphate Buffered Saline (PBS; 130mM NaCl, 7mM Na_2HPO_4, 3mM NaH_2PO_4, pH 7) and held in PBS on ice. They were then fixed (4% paraformaldehyde in 1X PBS) for 10 minutes at room temperature. Following four 10-minute washes with PBS, the samples were blocked in 10% normal goat serum (NGS) in PBS + 0.1% Tween-80 (PBT) for 1 hour at room temperature. They were then incubated with primary antibody (prepared in incubation solution - PBT containing 5% NGS) overnight at 4^{o}C. The next day, the sample was washed 4 times with incubation solution, 10 minutes each at room temperature and then incubated with secondary antibody (in incubation solution) overnight in the dark at 4^{o}C. The next day, the sample was washed in PBT four times for 10 minutes each. DAPI (at a final concentration of 1μg/ml to stain nuclei) or Alexa488-phalloidin (1:100 to detect F-actin) was added in the final wash. The samples were then mounted in mounting medium (80% glycerol, 0.1M Tris pH 8).

4.2.6 α-spectrin (R22S) rescues of α-spectrin null mutants

l(3)dre3^{rg41}/TM3 has been previously described (Lee *et al*., 1993). *l(3)dre3^{rg41}* was created by γ-ray mutagenesis and contains a 20-bp deletion that creates a premature stop codon near the 5' end of the transcript, resulting in a truncated protein product (segment 0 and 3 helices of segment 1). *l(3)dre3^{1151}/TM6* hasn't been described as yet. The aim was to rescue the larval lethality of *l(3)dre3^{rg41}* / *l(3)dre3^{1151}* with *α(R22S)*. Since the insert in one of our transformant lines that exhibited temperature sensitivity mapped to Chromosome III, the recombinant stock *l(3)dre3^{rg41}-R22S/TM6* was created (scheme shown in Fig. 4.2). Rescue of the α-spectrin null mutant was then carried out by crossing

Figure 4.2 Creating *l(3)dre3*^{rg41}*R22S/TM6* stock

Figure 4.3 Rescue of α-spectrin null mutant with α(R22S)

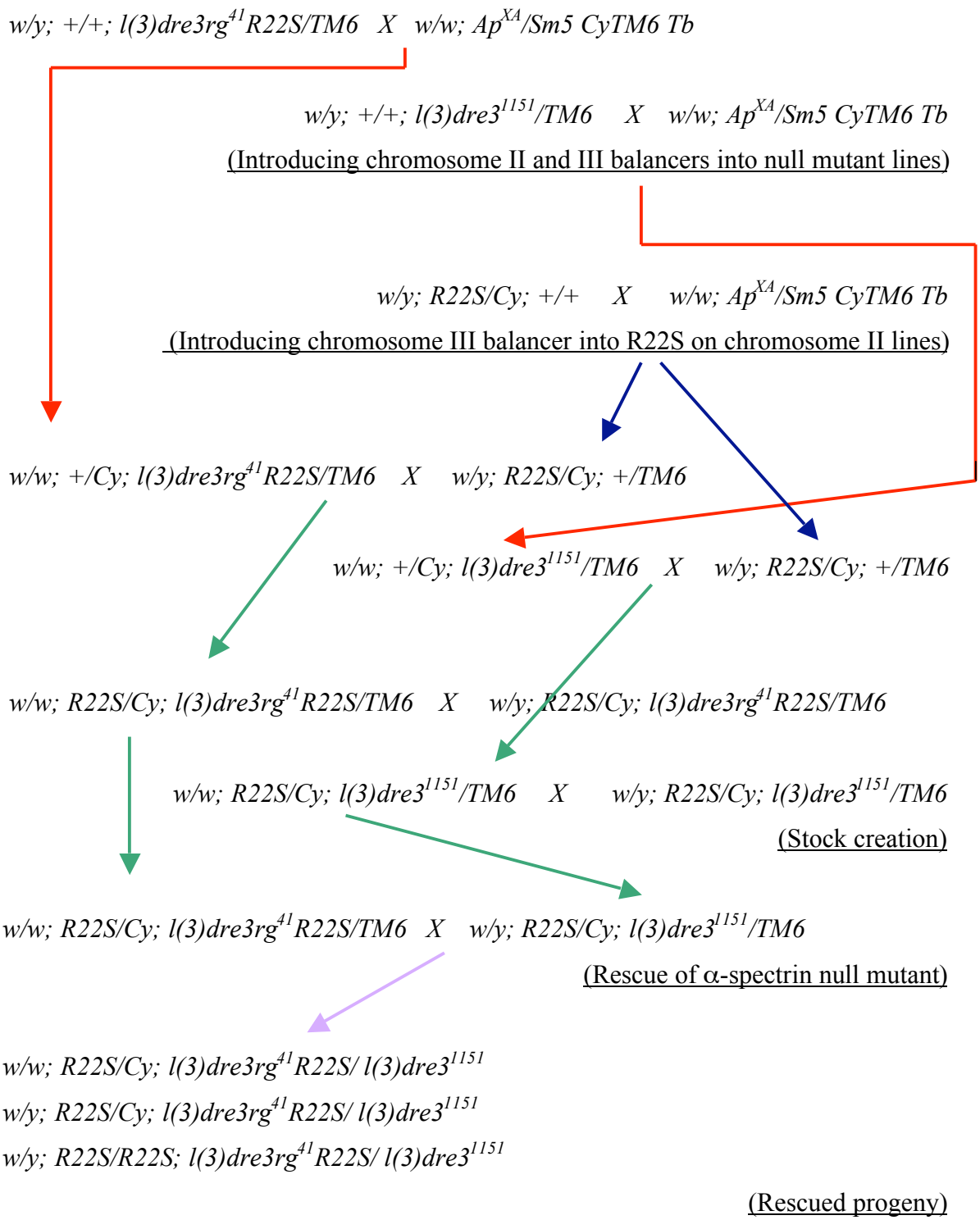

w/w; +/+; l(3)dre3^{rg41}*R22S/TM6* to *w/Y; +/+; l(3)dre3*^{1151}*/TM6.* In order to increase the amount of α(R22S) protein for rescue, two more stocks were created with a transformant line that had the insert on Chromosome II (line 2.2 R22S)- *R22S/Cy; l(3)dre3*^{rg41}*R22S/TM6* and *R22S/Cy; l(3)dre3*^{1151}*/TM6* (scheme shown in Fig. 4.3). Rescue was attempted by crossing *w/w; R22S/Cy; l(3)dre3*^{rg41}*R22S/TM6* to *w/Y; R22S/Cy; l(3)dre3*^{1151}*/TM6* (Fig. 4.3).

4.3 Results

4.3.1 Re-creation of α(R22S) mutant construct and confirmation of expression of its protein product in germ-line transformants

The sequence of the α-spectrin cDNA fragment in *P[w+UPS]* was compared to the α-spectrin cDNA sequence in FlyBase (www.flybase.org) using the SeqMan tool in the DNAStar software package. 21 single nucleotide polymorphisms were found in the sequence in *P[w+UPS]* compared to that given on FlyBase. None of them resulted in amino acid changes. The 22nd arginine of *α-spectrin* was found to be intact. After all rounds of mutagenesis had been carried out, the R22S point mutation as well as conversion of the NcoI restriction site to a KpnI restriction site in *P[w+UPS]* was also confirmed by sequence comparison to the unmutated *P[w+UPS]* sequence. After cloning into *P[w+UM-2]*, the entire spectrin coding region was once again sequenced to confirm that only the desired changes were introduced during cloning.

Once the α(R22S) fly stocks were established, the inserts were mapped to Chromosomes II and III. The expression of the myc-tagged protein product was confirmed by an immunoblot (Fig. 4.4).

4.3.2 Dominant effects of α(R22S)

Even though there was no precedent for a dominant effect of the α(R22S) as reported by Deng *et al*. (1995), I tested the behaviour and fecundity of the initial stock (*w; +; R22S/TM6*) at the permissive (22^{o}C) and restrictive (29^{o}C) temperatures. *ORR* and *yw* flies served as controls. The R22S stock established itself at permissive temperature and flies appeared healthy and active. After being held at restrictive temperature for 24 hours, compared to the wild-type controls, the R22S flies seemed less active. While the ORR and yw flies move rapidly around the vials at 29^{o}C, the R22S flies are relatively sedentary, although they did jump when the vial was tapped. After being held at restrictive temperature for 5 days, by which time the wild type control stocks were able to produce a good number of embryos and larvae (upto 2nd instar), the vial with the R22S stock had only a few eggs and only a few (<10) first instar larvae were observed.

Figure 4.4 Expression of myc-tagged product in α(R22S) fly lines

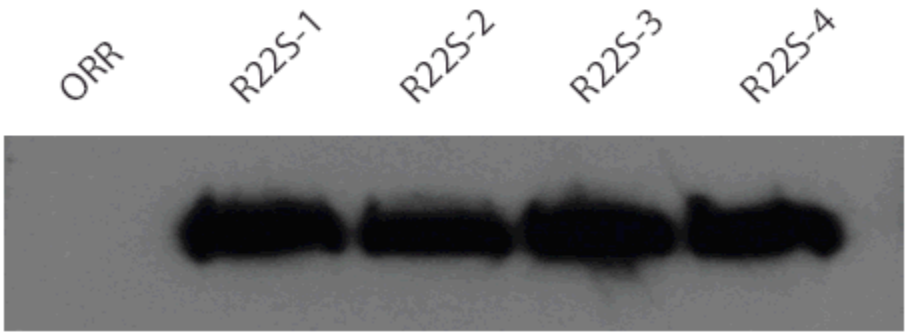

Fig 4.4 Expression of myc-tagged protein product in α(R22S) fly lines
Immunoblot analysis of flies from α(R22S) lines and ORR control for presence of myc-tagged protein. Each lane represents extract from a single fly. R22S-1-4 depict replicates, 4 homozygous flies from the same fly stock of α(R22S) on

The lowered fecundity in the R22S stock prompted a look at the ovary. Each ovary consists of about 16 ovarioles, each of which can be considered an independent egg-producing entity. At the tip of each ovariole lies the germarium, in which the germline stem cell divides asymmetrically to give rise to a stem cell and one cystoblast. The cystoblast undergoes four rounds of division with incomplete cytokinesis, giving rise to a germline cyst containing 16 interconnected cystocytes. 15 of these cells differentiate into nurse cells (NC) while the remaining one is destined to become the oocyte. Developing cysts contain a structure known as the fusome (and its supposed precursor, a spherical structure known as the spectrosome), which is comprised of membrane skeletal proteins such as spectrin, the motor protein dynein, and tubulovesicular membranous structures. The developing cyst then becomes enveloped in a layer of somatic follicle cells, thus giving rise to an egg chamber, which buds off from the germarium. Each egg chamber then progresses through more stages of development (14 in total), such that the older chambers are further away from the germarium in the ovariole than the younger ones (de Cuevas *et al*., 1997; Deng and Lin, 1997; Fig. 4.5).

The localization of α-spectrin (wild-type and mutant) was observed by immunostaining ovarioles from control and R22S females held at permissive and restrictive temperatures. In ovarioles from wild-type females, at both, permissive and restrictive temperatures, α-spectrin localizes at the apical and lateral plasma membrane domains of the follicle cells. α-spectrin localization in the lateral membrane seems to be concentrated towards the apical end of each cell (Fig. 4.5 A, B; Fig. 4.6 A). The follicle cells are arranged in a monolayer and their cuboidal shape is maintained. The structures of the spectrosome and fusome are also normal at both temperatures - α-spectrin is found to be localized in both (Fig. 4.5 A, C; Fig. 4.6 B,C). The structure of the spectrosome and fusome were also observed by staining for Hts (*Drosophila* adducin, known as *hu-li tai shao*). Hts is a spectrin-binding protein and is known to be part of the fusome (Lin *et al*., 1994; Lighthouse *et al*., 2008), and was observed to be part of the spectrosome and fusome at permissive temperature (Fig. 4.5D). In ovarioles from R22S females, at permissive and restrictive temperatures, while the localization of α-spectrin is maintained at the plasma membrane of the follicle cells, it now extends for the entire length of the

Figure 4.5 Wild-type distribution of α-spectrin in ovarioles at permissive temperature

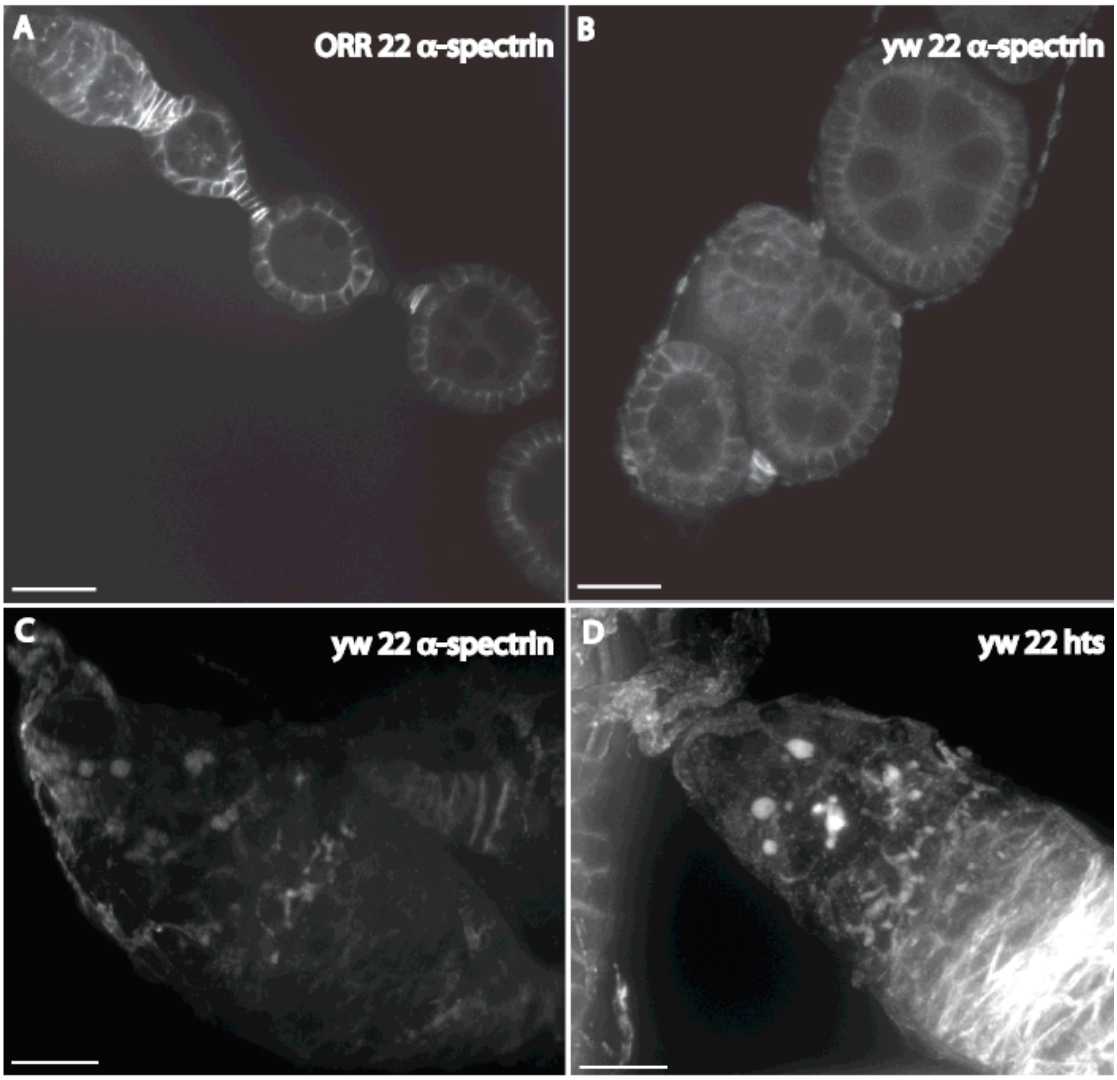

Fig 4.5 Wild-type distributed of α-spectrin in ovarioles at permissive temperature A-C Ovarioles from ORR and yw females held at permissive temperature are stained for α-spectrin ; **D** Ovarioles from yw female stained for hts. α-spectrin is localized at the apical membrane as well as the fusome.

Figure 4.6 Wild-type distribution of α–spectrin in ovarioles held at restrictive temperature

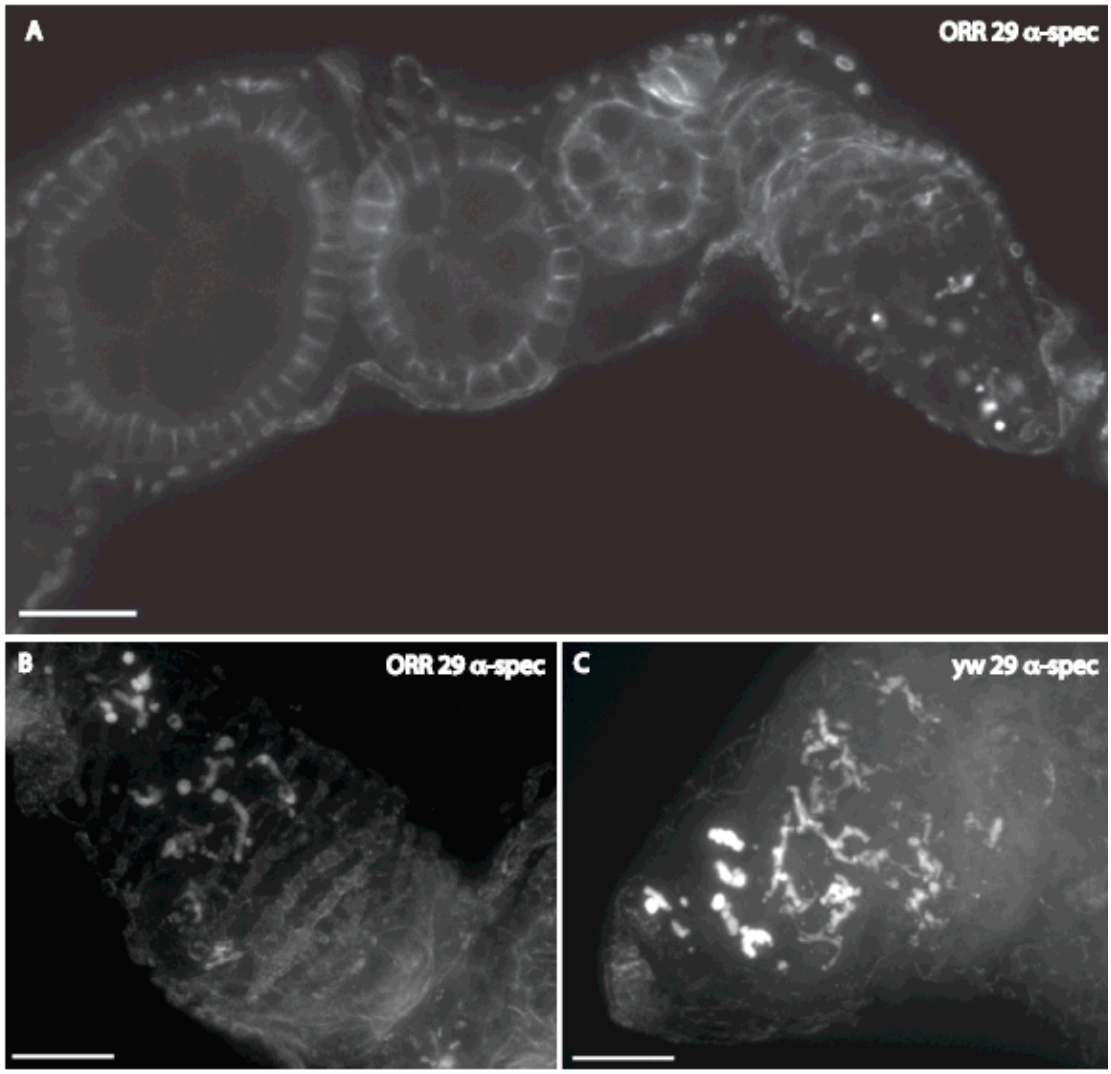

Fig 4.6 Wild-type distribution of α–spectrin in ovarioles held at restrictive temperature A Ovarioles from ORR females held at restrictive temperature stained for α–spectrin. **B** Germarium of ORR females stained for α–spectrin **C** Germatium from yw female stained for α–spectrin. Even at restrictive temperature, the localization of α–spectrin is as expected and the fusome integrity is intact.

Figure 4.7 Distribution of α-spectrin and α(R22S) in ovarioles from R22S flies at permissive temperature

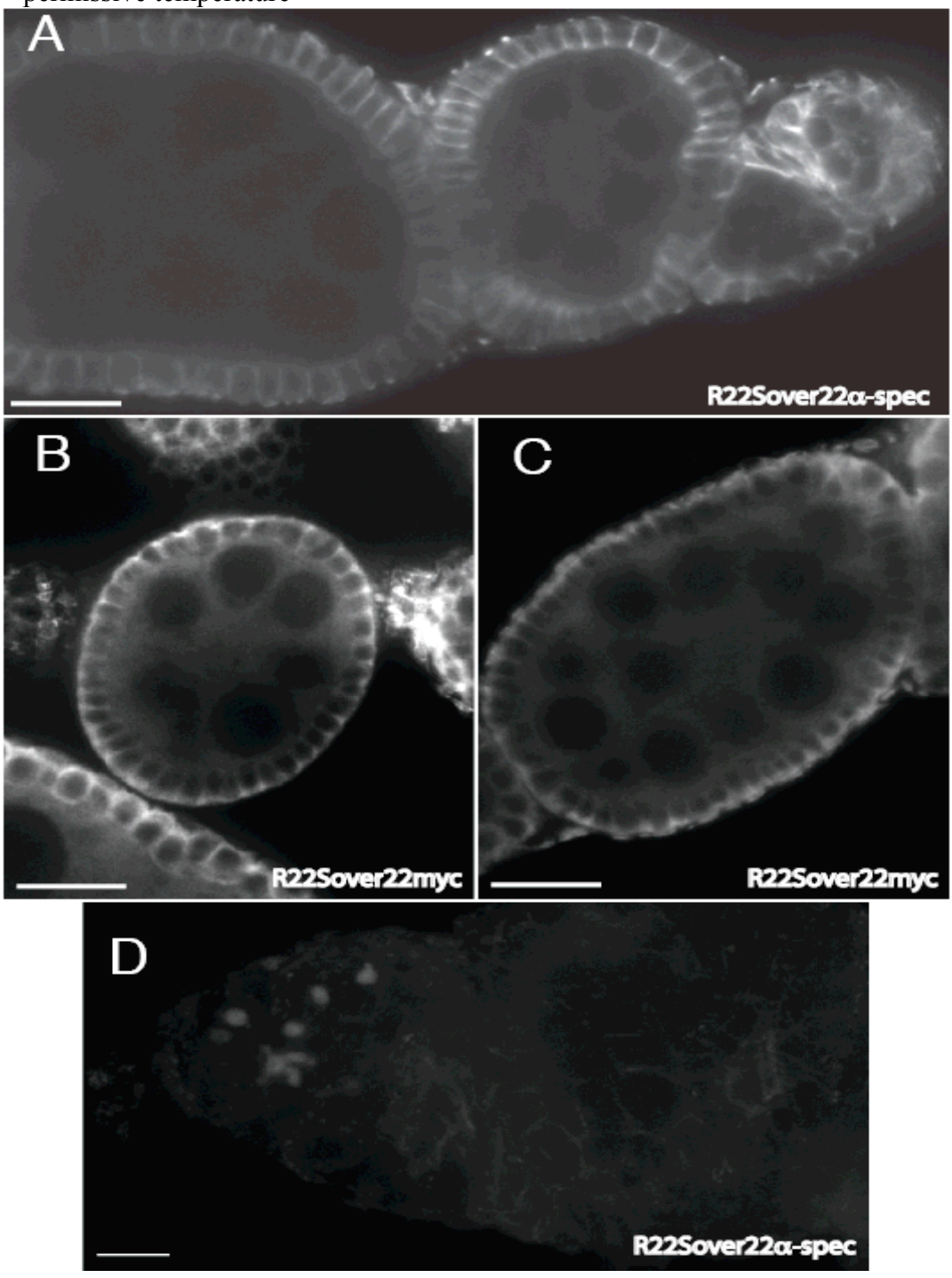

Fig 4.7 Distribution of α-spectrin and α(R22S) in ovarioles from R22S flies at permissive temperature A Ovariole from R22S female stained for α-spectrin. The protein distributes itself over the entire length of the lateral membrane **B,C** Egg chambers from R22S females stained for myc-tagged protein a(R22S). The mutant protein is excluded from the apical spectrin network into the basal domain **D** Germarium stained for α-spectrin. The fusomes are barely discernable. R22Sover = R22S overexpressed in the presence of two wild type copies of the α-spectrin gene.

Figure 4.8 Distribution of α-spectrin and α(R22S) in ovarioles from R22S flies at permissive temperature

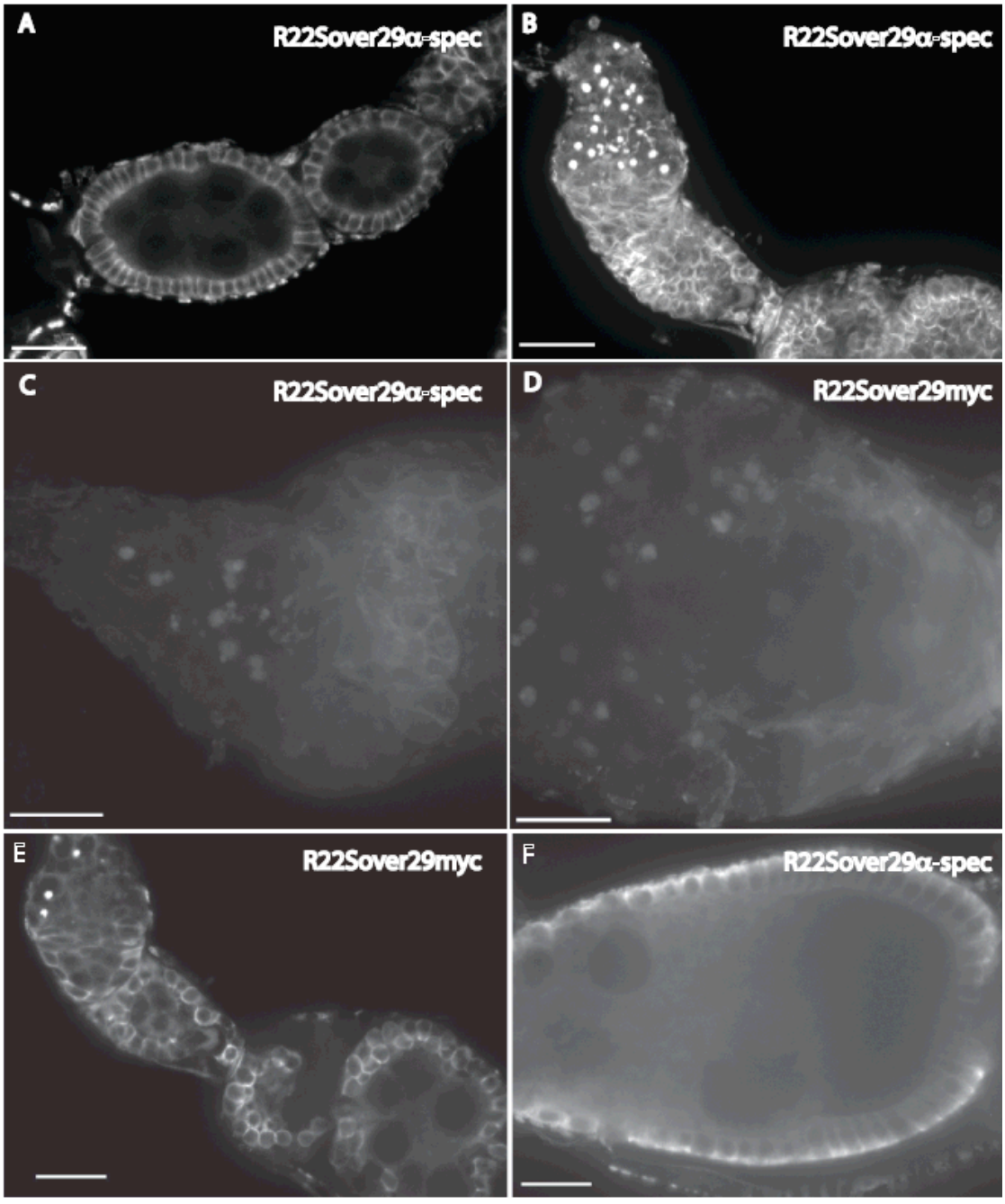

Fig 4.8 Distribution of α-spectrin and α(R22S) in ovarioles from R22S flies held at restrictive temperature A Ovariole stained for α-spectrin, which can be seen over the entire length of the lateral membrane. **B,C** Germaria stained for α-spectrin at 40X(B) and 100X(C) magnifications. A few branched fusomes can be seen, although most of the protein seems to be unable to form a fusome and is seen in aggregates. **D** Germarium stained for myc. α(R22S) is seen in aggregates, no tubulovesicular fusomes observed. **E** Occasionally, a disorganized follicle cell layer can be seen, with cells piling up on each other. **F** Egg chamber stained for α-spectrin shows how most of the protein is excluded from the apical network. R22Sover = R22S overexpressed in the presence of two wild type copies of the α-spectrin gene.

lateral membrane (Fig. 4.7 A, 4.8 A, contrast with concentration at the apical end of wild-type ovaries). In order to distinguish between wild-type and mutant α-spectrin, I also probed for myc (since the mutant protein is myc-tagged). Strikingly, α(R22S) was excluded from the apical regions and tended to concentrate at the basal end of the plasma membrane of the follicle cells, a phenomenon that seems to be independent of temperature (Fig. 4.7 B,C; Fig. 4.8 F). Another surprising finding was the absence of a properly branched fusome in the mutants – while the spectrosome could be observed at both temperatures (Fig. 4.7 D; Fig. 4.8 B, C, E), the fusome was barely discernable at 22°C by staining for α-spectrin, while its intricate filamentous structure was lost at 29°C (Fig. 4.7 D; Fig. 4.8 B, C). At the restrictive temperature, the fusome looked spherical, resembling the spectrosome. Staining for myc revealed that α(R22S) could be found at this unusually spherical fusome (Fig. 4.8 D). This suggests that perhaps a normal fusome structure requires an intact spectrin network. Also seen occasionally at 29°C was a disorganized follicle cell layer – the cells are spherical instead of cuboidal and piled upon one another (Fig. 4.8 E).

4.3.3 α(R22S) rescues the α-spectrin null mutant

Following the crossing scheme outlined in Fig. 4.3, it was determined that α(R22S) could rescue the α-spectrin null mutant at permissive temperature, though more than one copy was required to get more rescue. However, none of the rescued females ever carried more than 2 copies of the α(R22S). The rescued progeny have rough eyes, are relatively sluggish and don't fly as much as their control siblings. They also seem to attempt to set be lagging behind their control siblings in development by at least 48 hours or so. An attempt to set up a stock by mating rescued males and females failed even at permissive temperature, although mating didn't seem to be affected. Thus, in order to determine whether the male or the female rescued flies were responsible, each was out crossed to *yw* flies. While mating rescued males to yw females resulted in progeny, the cross set up between rescued females and *yw* males didn't take, implying defective oogenesis or then the presence of a sperm-hostile environment in the female reproductive tract. Since there was a precedent for the role of an intact spectrin network in oogensis

(Deng *et al*., 1995) and my own results showed disruption of the fusome in R22S flies (see section 4.3.2), I decided once again to look at the ovaries of these rescued females.

While looking at the ovaries of rescued females, I used the *w/w; R22S/Cy; l(3)dre3^{rg41}R22S/TM6* flies as controls. Egg chambers from control females at both, permissive and restrictive temperatures, largely looked healthy and the follicle cell monolayers were intact (Fig. 4.9 A-D). Even at restrictive temperature, α-spectrin was localized to the apical and lateral membrane of the follicle cells, the spectrosome and fusome were present and the tubular structure of the fusome could be seen by staining for α-spectrin (Fig. 4.9 B, D). However, occasionally, at both temperatures, degenerating late stage egg chambers could be seen, with gross disruptions in epithelial integrity, piling up of follicle cells, absence of nurse cells or an oocyte and highly condensed nuclei (Fig. 4.9 E, F), reminiscent of dying cells. This was similar to what was observed in egg chambers from rescued females. While they were mostly normal at both temperatures (Fig. 4.10 A, C), occasional degenerating egg chambers could be seen (at a frequency of about 8%; Fig. 4.10 B-D). One consistent feature however was that only Stage 8 or later egg chambers displayed this phenotype. This seems to be indicative of a nutritional checkpoint-the ovaries are extremely sensitive to the availability of nutrients and in case of a deficiency, the egg chambers (which progress only till Stage 7 till eclosion) may delay or not progress beyond this stage (see discussion; Spradling, 1993).

4.3.4 Level of α(R22S) protein product in rescued progeny and various heterozygous stocks

While the male rescued flies can carry up to 3 copies of the mutant construct, the rescued females carrying more than 2 copies are not recovered (see crossing scheme in Fig. 4.3). Also, although α(R22S) rescues the null mutant to adulthood, the rescued females don't lay eggs. Thus, I decided to determine the levels of α-spectrin protein expression in the rescued progeny and compare them to that in their parents as well in wild-type flies. An immunoblot probing for α-spectrin showed that rescued males and females had lower levels of protein in comparison to yw males and females (Fig. 4.11). Between the rescued progeny, the amount of α-spectrin seems to vary, seemingly equal on some blots and reduced in females on others. However, rescued females never seem to

Figure 4.9 Ovarioles from *w/w; R22S/Cy; l(3)dre3*^{rg41}*-R22S/TM6* femlaes held at permissive and restrictive temperatures

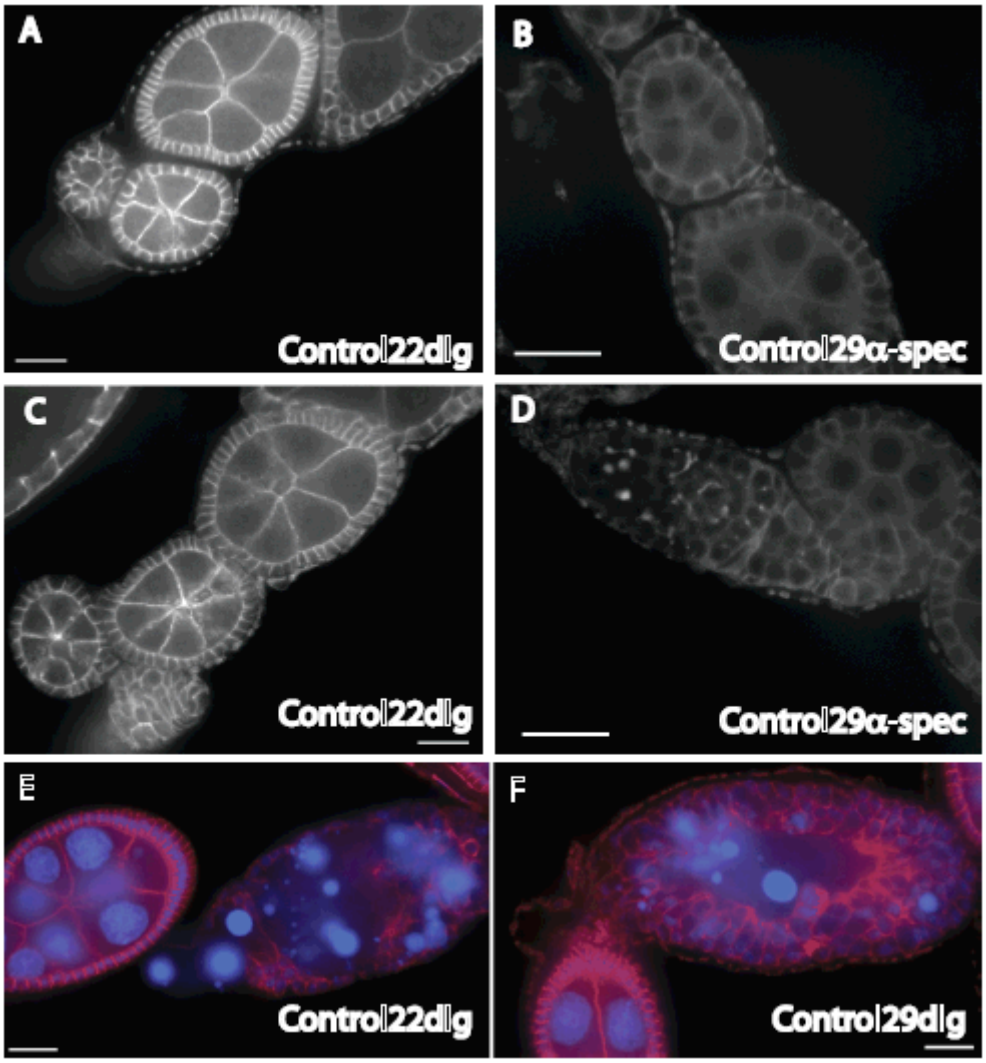

Fig 4.9 Ovarioles from *w/w; R22S/Cy; l(3)dre3*^{rg41}*-R22S/TM6* femlaes held at permissive and restrictive temperatures A, C, E show egg chambers at permissive temperature, stained for the membrane protein Dlg ; **B, D, F** show egg chambers at restrictive temperature, stained for Dlg. At both temperatures, normal looking egg chambers are observed **(A-D)** as well as degenerating ones (Blue-DAPI staining of nuclei). 29- 29^{o}C for 5 days; 22- 22^{o}C for 5 days.

Figure 4.10 Ovarioles from rescued females held at permissive and restrictive temperatures

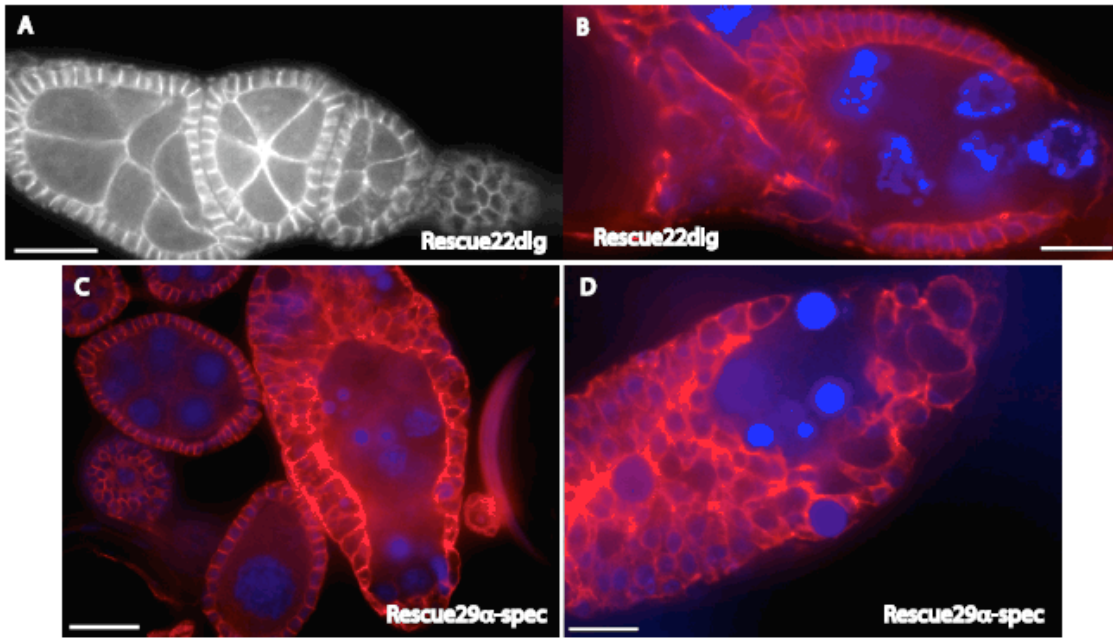

Fig 4.10 Ovarioles from rescued females held at permissive and restrictive temperatures A-B show egg chambers from rescued females at permissive temperature, stained for the membrane protein Dlg. **C-D** show egg chambers from rescued females at restrictive temperature, stained for α-spectrin. At both temperatures, normal looking egg chambers are observed as well as those with gross epithelial morphological defects. In defective egg chambers, nurse cells are absent. Nuclear stainng with DAPI reveals necrotic cells. 29- 29°C for 5 days; 22- 22°C for 5 days.

have more α-spectrin than their male counterparts. Flies from stocks that had one copy of wild-type α-spectrin on the balancer chromosome (*l(3)dre3^{rg41}/TM6 and l(3)dre3^{1151}/TM6*) had less protein than wild-type and rescued flies, as expected (Fig. 4.12 Lanes 5&8). The recombinant line *l(3)dre3^{rg41}-R22S/TM6* expressed more protein than *l(3)dre3^{rg41}/TM6* and surprisingly, introducing another copy of R22S into this stock (*R22S/Cy; l(3)dre3^{rg41}-R22S/TM6*) actually showed a decrease in the amount of α-spectrin (Fig. 4.13 Lanes 6&7). Introducing a copy of R22S into the *l(3)dre3^{1151}/TM6* stock (*R22S/Cy; l(3)dre3^{1151}/TM6*) didn't alter protein amounts, although the amount of loading control seemed less. Finally, the amount of α-spectrin in the stock containing R22S in the wild-type background (R22S/TM6) seemed comparable to that in the *R22S/Cy; l(3)dre3^{rg41}-R22S/TM6* stock (Fig. 4.12 Lanes 7&10). To distinguish between wild-type α–spectrin and α(R22S), I also probed for myc. Surprisingly, α(R22S) was barely expressed in the α-spectrin heterozygous stocks, while a high level of expression was observed in the rescued progeny (slightly less in females than in males; Fig. 4.12). These data indicate that α(R22S) is unstable in the presence of wild-type α-spectrin.

Fig 4.11 Levels of α-spectrin in rescued flies and various heterozygous stocks

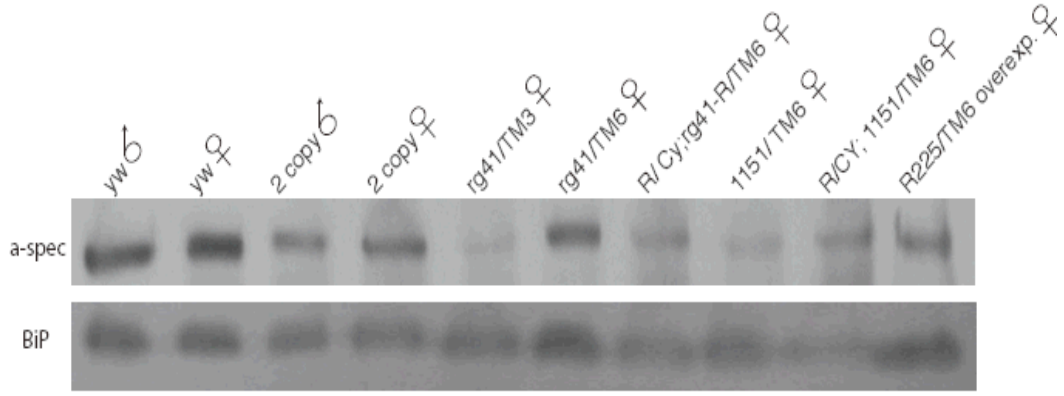

Fig 4.11 Levels of α-spectrin in rescued flies and various heterozygous stocks yw flies serve as a control. The rescued flies are denoted by "2 copy", implying they are of the genotype *R22S/Cy; l(3)dre3^{rg41}-R22S/l(3)dre3^{1151}*. BiP serves as a loading control. The levels of α-spectrin in the recued flies are less than those in the control flies of the same gender. *Loading* Single fly per lane.

Figure 4.12 Levels of α(R22S) in rescued flies and various heterozygous stocks

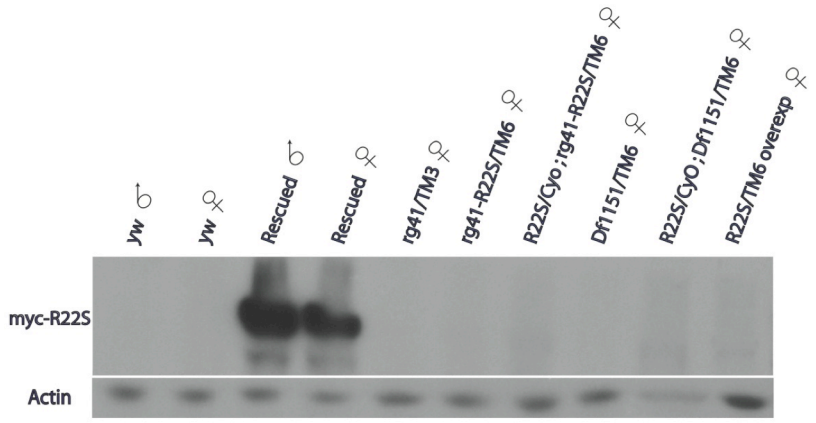

Fig 4.12 Levels of α(R22S) in rescued flies and various heterozygous stocks yw flies serve as a control. The rescued flies are denoted by "2 copy", implying they are of the genotype *R22S/Cy; l(3)dre3*^{rg41}*-R22S/l(3)dre3*^{1151}. Actin serves as a loading control. α(R22S) is expressed only in the rescued flies. *Loading* Single fly per lane.

4.4 Discussion

In an effort to model spectrin degradation characteristic of an ischemic event in *Drosophila*, I decided to use a fly line that carries α-spectrin with a temperature sensitive point mutation in its tetramerization domain (R22S). The integrity of the spectrin network in these flies is compromised at the non-permissive temperature of 29°C, while there is no effect at the permissive temperature of 21°C (Deng *et al*., 1995). Since the stock last used by Deng *et al*. (1995) was lost over the years, I decided to remake the fly line with the exact same construct that was originally used. This was done by using the same vector, which would drive the myc-tagged construct under the control of the ubiquitin promoter (Deng *et al*., 1995). This was particularly important because of the possibility that the tag, which is near the R→S mutation, is necessary to confer temperature sensitivity. In addition, spectrin expression is widespread and the ubiquitin promoter had already been demonstrated to be appropriate for rescue to viability by Deng *et al*. (1995).

Our rescue experiment results differed from Deng's in a number of ways. First, Deng *et al*. reported no effects of the mutant construct when expressed in the wild-type background. On the other hand, my R22S fly stock exhibits lowered fecundity at the restrictive temperature and the mutant protein seems to be excluded from the apical spectrin network (it is predominantly localized in the basal domain) and the structure of the fusome is disrupted. Both of these effects are independent of temperature. These observations might in part explain the breakdown of the original R22S stocks, suggesting that Deng's line might indeed have had a dominant phenotype that provided a selective environment for these deletions.

The fusome is a cytoplasmic organelle that connects the individual cystocytes in a germ line cyst through ring canals. The way it does this is by aligning itself with one of the spindle poles in a cystoblast during the first mitotic cycle. This way, at cytokinesis, it remains with only one daughter cell. After the cleavage furrow arrests and microtubules decrease, new fusome material accumulates at the spindle equator and the original fusome material now fuses with the new one. This happens for each of the 4 mitotic cycles and results in a highly branched fusome in the older cysts. After cyst formation, the fusomes begin to break down, there is transport of material through the ring canals

and the nurse cells begin to differentiate from the oocyte (reviewed by de Cuevas *et al*., 1997). The fusome plays a role in oocyte determination and this depends on the presence of α-spectrin in germ line cells (de Cuevas *et al*., 1996). De Cuevas *et al*. found that in ovarioles that were *α-spectrin* mutant in the germ line cells, cyst formation was severely disrupted, egg chambers contained fewer than 16 cells and lacked an oocyte if the total number of cells was less than 8. However, in ovarioles with weak *hts* alleles, cysts with even 6 cells were produced and nearly all cysts that had 8 cells had an oocyte (de Cuevas *et al*., 1996). In a more recent study to identify additional fusome components, some proteins such as tropomodulin, Scribble and Ferritin 1 heavy chain homolog were also found to be dispensable for the fusome as well as cyst production, while Rab11 was found to be required for maintenance of fusome structure, cyst production and germ line stem cells (Lighthouse *et al*., 2008). This might explain why my R22S stock has lowered fecundity at 29^{o}C. As found by Lighthouse *et al*., cysts that lack Rab11 also show spherical accumulations of fusome material, similar to the phenotype seen in the ovarioles from R22S females held at restrictive temperature (Fig. 4.9). Since the entire structure of the fusome isn't disrupted in these ovarioles from R22S females, it is possible that the presence of a mixed network (of wild-type α-spectrin and α(R22S)) is more susceptible to breakdown and results in an alteration in signaling events in the fusome as well as disrupts association with components of the fusome. This might account for a reduction in cyst production and hence lowered fecundity and suggest a normal role for spectrin in building or maintaining the structure and integrity of the fusome.

Another key difference between the results observed by Deng *et al*. and mine is the inability of the rescued progeny to establish a stock in my hands. My results once again point towards a defect in oogenesis, similar to that observed by Deng *et al*., although the effects I saw were independent of temperature. I also saw them in the control flies that are of the genotype *w/w; R22S/Cy; l(3)dre3^{rg41}R22S/TM6,* i.e. they have wild-type α-spectrin being expressed from the balancer chromosome. Deng *et al.* fail to mention at what frequency defects were observed in egg chambers from rescued females (I observe them at a low frequency of about 8%). They also mention that rescued females held at the restrictive temperature for up to 7 days contained comparable amounts of α-

spectrin as wild-type, in contrast to my observations (Fig. 4.12). While one might argue that reducing the total amount of α-spectrin in the rescued females (as compared to wild-type) might account for the inability to lay eggs, the levels of α-spectrin in the females from the *l(3)dre3*^{rg41}*/TM6* and *l(3)dre3*^{1151}*/TM6* stocks are actually slightly less than those in the rescued progeny and yet these are healthy stocks. However, we can't rule out the possibility that an intact spectrin network might be required at a certain threshold for sustaining life as well as reproductive success. In a study done to analyse the synthesis, assembly and turnover of eythroid and nonerythroid spectrins in rat hippocampal neurons (Sangerman *et al*., 1999), it was found that the half-life of nonerythroid spectrins is shorter when they are associated with the membrane rather than when they are in the cytoplasm. The authors speculated that the reason for this might be the susceptibility of the cytoskeleton to membrane-associated proteases such as calpain when it is membrane bound. This may explain why I hardly see any expression of α(R22S) in the heterozygous stocks. If there is a mixed pool of α-spectrins, αβ dimers can be formed whether the α-spectrin is wild-type or carries the R22S mutation (since the mutation doesn't affect the dimerization site). However, while the membrane bound network may have a certain half-life when it is composed of wild-type spectrins, its half-life might be much less if it carries the α(R22S). Hence, at any given time, the probability of detecting the mutant network might be less than that of detecting a wild-type network and this might be why the myc-tagged α(R22S) is barely visible in the heterozygous stocks. It is also possible that the half life of α(R22S) is much less in the presence of the wild-type α-spectrin. The difference in the affinities to form a tetramer may be responsible for the exclusion of α(R22S) from the apical network and its selective degradation. Previous data from studies in erythrocytes from chicken (Blikstad *et al*., 1983) and rat (Hanspal and Palek, 1987) shows that α-spectrin is synthesized in excess over β-spectrin, although they are present in a 1:1 stoichiometry at the membrane. These studies also showed that the spectrin fraction that isn't associated with the membrane is rapidly degraded. Another possibility is that although the myc-tagged protein is observed by immunostaining the ovarioles, there could be an absence of staining in other tissues (which hasn't been attempted as yet) and this may be another contributing factor towards the low levels of the mutant protein on immunoblots.

In contrast, in the rescued females, the only source of α-spectrin is the construct carrying the mutant. If it's getting rapidly turned over at the membrane and it isn't being produced in sufficient quantities to reach the threshold required for a viable cell, in order to sustain life, the fly may compromise on other functions such as reproduction. For example, it is well known that the ovaries are extremely sensitive to nutrient availability and environmental factors (Spradling, 1993). One of the checkpoints in oogenesis is when yolk production (vitellogenesis) begins at Stage 8. It initially requires stored nutrients since the oldest chambers at eclosion are at Stage 7 and the flies don't feed for the first 12-24 hours. The ecdysone and juvenile hormones are required to turn on vitellogenesis (Terashima and Bownes, 2006) and an adequate amount of protein is paramount for enough yolk production. In case of limiting conditions, progression beyond Stage 8 is delayed and fertility is compromised (Spradling, 1993). This might explain why in rescued females that have only a mutant form of α-spectrin and reduced amounts of total α-spectrin compared to the wild-type, even though dying egg chambers are observed at a low frequency, there might be significant delays in egg chamber development, which might result in their inability to lay eggs.

To conclude, the R22S construct was remade and it rescued α-spectrin null mutants. The effects on oogenesis appear to be independent of temperature in the rescued flies. While the rescued progeny are unable to establish a stock, flies of the genotype *w; R22S/Cy; l(3)dre3*^{rg41}*R22S/TM6,* which have both, mutant and wild-type α-spectrin can. However, they exhibit the same phenotype in the ovaries as the rescued females- degenerating late stage egg chambers. This strongly resembles a nutritional phenotype and might have arisen from α-spectrin defects elsewhere. I decided to use flies of the genotype *w; R22S/Cy; l(3)dre3*^{rg41}*R22S/TM6* for proteomic analysis, since my results so far suggest that this mixed spectrin network has a very similar phenotype to the rescued females.

Chapter 5 The dominant effects of the R22S mutation on the PM proteome in *Drosophila* – quantitative proteomics by iTRAQ

5.1 Introduction

An introduction to proteomics, its applications, MS-based methods and its use to define the plasma membrane proteome of *Drosophila* heads has been described in Chapter 3. Chapter 3 focused on the qualitative aspects of proteomics, *viz*. optimizing methods for the identification of proteins with the aim of defining organism or organelle proteomes. There exists another aspect of proteomics called quantitative proteomics, which allows not only the identification of proteins but the determination of their relative quantities across multiple samples. The ability to determine relative amounts of proteins across samples opens up new realms in the field of proteomics. It allows for quantitative comparison of proteomes under different conditions, which could have implications for the determination of alterations in drug targets under diseased states to the identification of cellular pathways that might be altered under different environmental conditions.

Up until about 5-6 years ago, quantitative proteomics was almost exclusively gel-based. Difference gel electrophoresis (DIGE) is a 2D gel-based method first reported in 1997 (Unlu *et al*., 1997) and was developed with the aim of overcoming the challenge of irreproducibility in 2D gel electrophoresis. It compares proteins in two different samples on the same gel by differential labeling. Each of the two samples is labeled with a different cyanine-based fluorescent dye (Cy3-NHS or Cy5-NHS) that has the same molecular weight (Viswanathan *et al*., 2006). Thus, there is no electrophoretic mobility charge shift between identical proteins in the two samples, allowing for the comparison of protein profiles as well as relative amounts in the two samples using software that can calculate the changes in the intensities of the two dyes (Grant and Wu, 2007). The advantages of DIGE include the exclusion of gel-to-gel differences and its sensitivity – as less as 0.5 femtomole of a protein can be detected. However, one of its major shortcomings is its inability to resolve membrane proteins due to their precipitation during resolution in the first dimension (isoelectric focusing; Viswanathan *et al*., 2006).

Non gel-based methods are a good alternative to gel-based methods in their capability to provide an unbiased way to quantitate proteins, including membrane proteins. They can be further classified on the basis of whether or not a label (metabolic labeling or chemical modifications) has been employed. Label-free methods include spectrum counting and differential MS. Spectrum counting is based on the observation that during the MudPIT analysis of a complex protein mixture, there is a correlation between the amount of protein present in the sample and the number of peptides identified (Grant and Wu, 2007). Thus, a summation of the MS/MS observations for any peptide of a protein in multiple samples can be used to obtain relative quantities of that protein across samples. Differential MS uses LC-MS chromatography to compare and quantitate proteins across samples (Grant and Wu, 2007). The method makes use of software to compare intensities at each *m/z* (mass/charge) ratio to create a list with differences in the peptide intensities according to rank. The advantages of label-free methods lie in their ability to compare multiple samples while bypassing the use of costly labels. However, both methods require reproducibility of LC and sample preparation and a disadvantage of the spectrum counting method particularly is the listing of peptides in multiple entries in a database that for example report different isoforms of a protein, which may lead to inaccuracies (Grant and Wu, 2007). Non gel-based methods employing a label can be classified as those utilizing isotope labeling (ICAT and metabolic labeling) or then chemical modifications. Methods using chemical modifications can be further sorted on the basis of whether proteins or peptides are labeled.

The non gel-based method using Isotope Coded Affinity Tags (ICAT) consists of a tag which comprises three portions – a) a thiol reactive group which couples to the side chain of reduced cysteine residues b) an isotopically "heavy" (deuterium or ^{13}C) or "light" (^{12}C) ethylene glycol linker c) biotin, which allows for enrichment by avidin affinity chromatography. The tags are used to label protein samples that have been denatured and reduced. These are then combined and digested and the ICAT labeled peptides are isolated by avidin affinity chromatography. The peptides are then subjected to MS analysis – the peptides are sequenced and identified and the relative quantities of proteins in the two samples are reflected by the relative abundance of the labeled peptides

(Grant and Wu, 2007; Speers and Wu, 2007). While this method overcomes the disadvantages of sample complexity by isolating the tagged peptides, it is biased towards proteins that contain cysteine residues (Grant and Wu, 2007). The disadvantage of *in vitro* tagging methodologies can be overcome by *in vivo* metabolic labeling. Stable Isotope Labeling in Culture (SILAC) involves growing cells in culture media that contains an essential amino acid that contains a stable isotope. This allows all newly synthesized proteins to incorporate the labeled amino acid. Two protein samples, labeled and unlabeled can then be combined, co-digested and subjected to MS analysis. The sequence of the peptide leads to identification and the ratios of labeled and unlabeled peptides provide relative quantities of proteins corresponding to those peptides between the two samples (Grant and Wu, 2007; Sadowski *et al*., 2008). An extension of metabolic labeling involves feeding a whole organism with a diet containing labeled proteins (reviewed by Grant and Wu, 2007).

While the aforementioned non gel-based methods used protein labeling, relative quantitation of proteins across samples can also be done by peptide labeling. The use of Isobaric Tags for Relative and Absolute Quantitation (iTRAQ) was first reported in 2004 by a group at Applied Biosystems (Ross *et al*., 2004) as a method for quantitation of proteins from *Saccharomyces cerevisiae.* The method uses four isobaric tags to label the primary amines in four different digested protein samples. The labeled peptides are then mixed and separated by LC and analyzed by MS and MS/MS. Since the tags are isobaric, the same peptide from each sample will be represented by a single peak in the MS spectrum. However, upon collision induced dissociation (CID), the tagged peptides are fragmented, leading to the generation of reporter ions (114.1, 115.1, 116.1 and 117.1 *m/z*). While the fragmented peptides provide sequence information, the ratios of the reporter ions is a reflection of the relative amount of peptide (and hence corresponding protein) in the samples (Ross *et al*., 2004; Aggarwal *et al*., 2006; Casado-Vela *et al*., 2010). Up to eight samples can be compared using the 8-plex reagents (Pierce *et al*., 2008). While this method allows for the comparison of multiple samples simultaneously, it is recommended that replicates be included in the mix so as to exclude variations in sample handling (Unwin, 2010).

I chose to observe the differences between the plasma membrane proteome of *R22S/Cy; l(3)dre3^{rg41}R22S/TM6* flies at permissive and restrictive temperatures using iTRAQ. While it would have been ideal to study the role of an intact SBMS in maintaining plasma membrane protein levels using rescued flies (*R22S/Cy; l(3)dre3^{rg41}R22S/l(3)dre3^{1151}*), the inability of these flies to establish a stock lead me to the next best option – the use of a fly line that displayed the same phenotype as that observed in the rescued flies as depicted by immunostaining of the ovarioles (see Results in Chapter 4). This gave me an opportunity to study the effects of a mixed spectrin network (since there would be one wild-type copy of α-spectrin expressed from the balancer chromosome). Prior to this attempt, I had attempted to optimize the iTRAQ protocol as well as reproduce the plasma membrane protein preparation with heads of just wild-type flies (Oregon R, ORR) at 21 and 37°C. The details of that experiment, its results as well as the results from the actual comparison of wild-type and mutant flies are described in this chapter.

5.2 Materials and Methods

5.2.1 Plasma membrane protein purification by combined density gradient centrifugation and aqueous two-phase partitioning

ORR controls: Heads from approximately 15 grams of flies (at either 21°C (Non heat shock NHS) or 37°C (Heat shock HS) for 1 hour) were used to extract plasma membrane proteins by the density gradient+2PAP method described in Chapter 2. Proteins from three such preparations were combined for preparation for each iTRAQ labeling. Each NHS and HS sample had a duplicate.

yw vs. mutants: 400 whole flies of each genotype *viz.* yw and *R22S/Cy; l(3)dre3*^{rg41}*-R22S/TM6* (R) were used – 200 flies of each (approximately 100 males and 100 females) were kept at the permissive temperature (21°C) and at the restrictive temperature (29°C) for a period of 8 hours. Plasma membrane protein preparation was carried out for each set of flies using the density gradient centrifugation+2PAP method described in Chapter 2.

5.2.2 Preparation of samples for iTRAQ

The ConA pellets from each sample were resuspended in 20 µl of Dissolution Buffer (0.5M triethylammoniumbicarbonate pH 8.5). 1 µl from each resuspended sample was used for protein estimations using the Advanced Protein Assay Reagent (Cytoskeleton Inc., Denver CO) according to the manufacturer's instructions. To the remainder of the resuspended samples 1µl of 2% SDS was added and vortexed to allow denaturation. Following that, 1µl of the reducing agent tris-(2-carboxyethyl) phosphine was added. The samples were vortexed, spun and incubated at 60°C for 1 hour. After 1 hour, the samples were spun and 1µl of freshly prepared 84 mM iodoacetamide was added. The samples were vortexed, spun and incubated in the dark at room temperature for 30 min. The reduced and alkylated proteins were then digested with 10 µg of Promega Gold Trypsin (Promega Corp., Madison, WI) at 48°C for 3 hours followed by 37°C for 16 hours. Following digestion, the samples were labeled with an iTRAQ Multiplex (4-plex) Kit (Applied Biosystems, Framingham, MA). The labeling was as follows: Control experiment (NHS-1 (114), NHS-2 (115), HS-1(116) and HS-2 (117); Control vs. mutant (yw-21 (114), yw-29 (115), R-21 (116) and R-29 (117). Labeling was

carried out at room temperature for 1 hour and the reaction was quenched at room temperature for 30 minutes by the addition of 100 µl of Milli-Q water. Then, the contents of all 4 tubes were combined and dried and resuspended in 100 µl of distilled water. Drying and resuspension were done two more times and the pellet was then sent for Mass Spectrometry analysis. The sample was reconstituted in 20 µl of 2% acetonitrile/0.1% formic acid.

5.2.3 Mass Spectrometry and data interpretation

Mass spectrometry and data acquisition for the control experiment was done at The Mass Spectrometry Core Research Facility at Penn State, Hershey as described in Chapter 3. Mass spectrometry and data acquisition for Control vs. Mutant was done at AB SCIEX (Concord, ON, Canada) as part of a product demonstration for The AB SCIEX TripleTOF™ 5600 System. Peptides were separated by chromatography on Eksigent nanoLC-Ultra system fitted with cHiPLC-nanoflex station, using a Trap and Elute Scheme. The Trap was a Nano cHiPLC column (200 µm X 0.5 mm, ChromXP C18-CL, 3µm 120 Å) and Analytical column was a Nano cHiPLC (75 µm X 15 cm, ChromXP C18-CL, 3µm 120 Å). Buffers used were Buffer A (100% water/0.1% formic acid) and Buffer B (100% acetonitrile/0.1% formic acid). 10 µl of the reconstituted sample was injected. The gradient was a 60 minute ramp from 5-35% Buffer B at a flow rate of 300nL/minute. The data was processed with Protein Pilot software version 4.0 and false discovery rate (FDR) analysis was done by searching against a reverse database. Identified proteins were accepted only if they met our C.I. criterion and had an estimated FDR < 0.05. All identified proteins had an Unused Score of 1.3 or higher, which corresponds to a confidence of 95% or higher. All identified proteins also had an estimated local FDR of 5% or less, based on the number of IDs at any cutoff Unused Score from a "normal" database (database searched was the NCBI nr *Drosophila* Protein Sequences) compared to the number of IDs from a concatenated forward and decoy database plus a list of known or common contaminants.

5.3 Results

5.3.1 iTRAQ analysis of PM proteins expressed in ORR flies at control and heat shock temperatures

Protein estimations of the ConA pellets prior to reduction and digestion of proteins revealed the following total amounts of protein: NHS-1 (102.6 μg), NHS-2 (163 μg), HS-1 (121.7 μg) and HS-2 (98.3 μg). 592 proteins were identified with an Unused Score greater than 1.3 (greater than 95% confidence). In order to check for reproducibility of the plasma membrane protein preparation, the list of unique IDs from the published trial and the list from the control iTRAQ were compared using the BioVenn application (Hulsen *et al*., 2008). 252 proteins (close to 43% of the iTRAQ list and approximately 59% of the MudPIT list) were found to overlap (Fig. 5.1).

Statistical comparison ($p \leq 0.05$) of the proteins from each NHS sample with those from each HS sample revealed significant differential expression in 34 proteins between only one set of NHS and HS comparisons (Table 5.1) and in 9 proteins between two or more sets of NHS and HS comparisons (Table 5.2). Among the 34 proteins, 25 were down-regulated upon heat-shock. Among the 9 proteins, 4 were down-regulated and the remaining 5 were up-regulated.

5.3.2 iTRAQ analysis of proteins differentially expressed in *R22S/Cy; l(3)dre3^{rg41}R22S/TM6* at permissive and restrictive temperatures

Protein estimations of the ConA pellets prior to reduction and digestion of proteins revealed the following total amounts of protein: yw-21 (40 μg), yw-29 (49 μg), R-21 (49 μg) and R-29 (11 μg). 296 proteins were identified with an Unused Score greater than 1.3 (greater than 95% confidence). Statistical comparison ($p \leq 0.05$) revealed 18 proteins that showed significant differential expression between R-21 and R-29 (Table 5.3). 4 of these proteins showed down-regulation at 29^{o}C and the remaining 14 were up-regulated. Of the proteins that showed up-regulation, 4 were found to be associated with the plasma membrane (CG30035, Na^{+}/K^{+} ATPase, syntaxin 1A and vacuolar [H^{+}] ATPase). Two of the proteins that showed up-regulation (Na^{+}/K^{+} ATPase and CG30035) were found to be significantly down-regulated in the control flies at 29^{o}C (yw-29) versus those at 21^{o}C (yw-21).

Fig 5.1 Overlap of proteins isolated by density gradient centrifugation+2PAP in two different trials

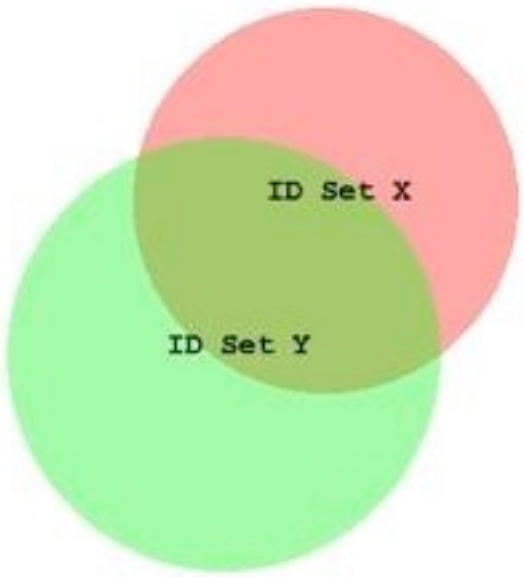

Fig 5.1 Overlap of proteins isolated by density gradient centrifugation+2PAP in two different trials ID Set X represents proteins from Trial 1 (published list of proteins obtained by MudPIT analysis of ConA pellets) and ID Set Y represents proteins from Trial 2 (NHS vs HS iTRAQ). The overlapping region represents 252 proteins, close to 43% of the proteins obtained from Trial 2 and approximately 59% of the proteins listed in Trial 1 (Biovenn was used to create this diagram; Hulsen *et al*., 2008)

Table 5.1 Differentially expressed proteins ($p \leq 0.05$) between ORR-NHS and ORR-HS in a single NHS vs HS comparison

Accession number	Protein	Compartment	Fold change
gi|34978339	14-3-3 protein epsilon	nucleus, cytoplasm	0.380189389
gi|7302124	Ac3, isoform A	integral to membrane; adenylate cyclase	0.420726597
gi|34922289	Acetyl-coenzyme A synthetase	cytoplasm	3.162277937
gi|7300478	ATP synthase, subunit d, isoform A	mitochondria	7.379042149
gi|161076803	basigin, isoform G	presynaptic active zone	0.630957425
gi|7302852	calbindin 53E	cellular calcium ion homeostasis, Ca ion binding	0.283139199
gi|62484414	Ca/calmodulin-dependent protein kinase II, isoform D	plasma membrane; calmodulin binding	0.432513803
gi|7300672	CG10830	plasma membrane; voltage gated K channel complex	0.591561615
gi|7303855	CG1648, isoform B	lipid particle	1.584892988
gi|45550877	CG1732, isoform A	plasma membrane; neurotransmitter transport	0.524807513
gi|71834216	CG1743	cytoplasm; glutamine synthetase 2	0.383707315
gi|24646943	CG3731, isoform A	mitochondrial respiratory chain complex III	6.486343861
gi|221329717	CG42265, isoform B	unknown	0.26546061
gi|161076922	CG4587, isoform C	membrane; voltage gated Ca channel activity	0.496592313
gi|7295470	CG4769	mitochondrial respiratory chain complex III	4.325138092

Table continued on next page.

Accession number	Protein	Compartment	Fold change
gi|7722	clathrin heavy chain	plasma membrane, synaptic vesicle	0.188799098
gi|281360039	complexin, isoform Y	membrane; synaptic vesicle exocytosis	0.095499262
gi|7481	conceptual protein of 1(1)ogre locus	integral to membrane; gap junction	0.524807513
gi|51704269	Disks large 1 tumor suppressor	plasma membrane, septate junction	0.758577585
gi|7301931	ferritin 2 light chain homologue, isoform A	Golgi; iron ion transport	4.168694019
gi|85724840	frequenin 1, isoform C	synapse; Ca ion binding	0.524807513
gi|7293756	G protein beta-subunit 76C	plasma membrane	0.260615289
gi|7292430	glutamic acid decarboxylase1,isoform A	glutamate decarboxylase activity	0.496592313
gi|7291098	imaginal disc growth factor 4, isoform A	extracellular region; chitinase activity	0.492039502
gi|269847881	MIP14966p (CG14762-RA)	unknown	0.231206506
gi|7298786	nervana 3, isoform B	plasma membrane, Na/K ATPase	1.106624007
gi|7295801	pdsw, isoform A	mitochondrial respiratory chain complex I	0.794328213
gi|73920219	l(2)37 (CG10691)	mitochondrial membrane	3.499452114
gi|21430682	RH08414p (CG4690) Tetraspanin 5D	integral to membrane	0.544502676
gi|996081	syntaxin 1A	plasma membrane	0.660693526
gi|76803826	Transient receptor potential	plasma membrane; light activated voltage gated Ca channel	2.654606104
gi|8810	vacuolar ATPase B subunit	plasma membrane, early endosome	0.602559626
gi|7296719	vacuolar H[+]-ATPase 26kD E subunit, isoform A	plasma membrane	0.461317599
gi|7297994	Vha68-1	plasma membrane	0.27289781

Down regulated proteins are in red; up regulated proteins are in blue.

Table 5.2 Differentially expressed proteins ($p \leq 0.05$) between ORR-NHS and ORR-HS in two or more NHS and HS comparisons

Accession number	Protein	Compartment	Fold change*
gi|7686	calreticulin	ER lumen; protein folding	7.358376105
gi|7293193	CG3560	mitochondrial respiratory chain complex III	3.46795702
gi|74871856	CTL-like protein 1	membrane glycoprotein	8.386881352
gi|7909	dynamnin-like protein	microtubule associated; GTPase	0.574163199
gi|458803	glutamate dehydrogenase, short peptide	mitochondrial matrix	0.351593942
gi|85857548	IP15876p	mitochondrial porin	2.21360298
gi|4028652	microsomal glutathione S-transferase-like protein Mgst1	mitochondrial outer membrane	19.09696961
gi|8250175	mitochondrial aconitase	mitochondria (TCA cycle)	0.485875502
gi|281359541	plasma membrane calcium ATPase, isoform L	pm, Ca ion transport	0.289441268

Down regulated proteins are in red; up regulated proteins are in blue.
* Denotes average fold change calculated by averaging the fold change by comparing each NHS sample with each HS sample.

Table 5.3 Differentially expressed proteins ($p \leq 0.05$) between R-21 and R-29.

Accession number	Protein	Compartment	Fold change
gi|24661344	arginine kinase, isoform C	cytoplasm/mitochondria	2.511885881
gi|7304361	ATP synthase-beta, isoform A	mitochondria	0.387257606
gi|7291679	calcium ATPase at 60A, isoform A	ER membrane	1.499685049
gi|24652789	CG30035, isoform A	Trehalose tansporter/plasma membrane	8.953647614
gi|28571792	CG31233	aminopeptidase	0.307609707
gi|7297573	CG5885	Sec61 translocon	85.50666809
gi|7290036	cytochrome P450-4g1	microsome	2.606153011
gi|62472216	failed axon connections, isoform C	axon bundle/Axonogenesis	3.221069098
gi|7301931	ferritin 2 light chain homologue, isoform A	Golgi/iron transport	0.331131101
gi|85857548	IP15876p /Porin	mitochondria	0.307609707
gi|54650752	LP07754p	aminopeptidase	0.544502676
gi|281427814	MIP15930p (CG8421)	ER	0.067920357
gi|28574239	myosin heavy chain, isoform H	myosin complex	0.401790798
gi|14424436	Na/K ATPase subunit alpha	plasma membrane	1.940886021
gi|135410	Tubulin alpha-2	microtubule	5.011871815

Table continued on next page.

Accession number	Protein	Compartment	Fold change
gi|7292133	ribosomal protein L23A	large ribosome	15.27565956
gi|996081	syntaxin 1A	plasma membrane	1.870682001
gi|7300533	vacuolar H[+] ATPase G-subunit	Plasma membrane (cell specific)	9.462371826

Down regulated proteins are in red; up regulated proteins are in blue.

5.4 Discussion

While the initial aim was to determine the changes in cell surface protein levels in the heads of flies with the genotype *R22S/Cy; l(3)dre3^{rg41}-R22S/l(3)dre3^{1151}* (Rescued), which carried α(R22S) as the sole source of α-spectrin, the results of this chapter are an initial look at changes in the cell surface proteome of whole flies of the genotype *R22S/Cy; l(3)dre3^{rg41}-R22S/TM6*, which express both, α(R22S) and wild-type α-spectrin (Heterozygous). This was because the rescued flies were unable to establish a stock. However, since the heterozygous females exhibited an identical phenotype in the ovary as the rescued females, I decided that they would be the next best option to get a preliminary look at changes in protein levels due to the presence of a defective spectrin network, albeit at a lower percentage than what might have been in the rescued flies. Using the heterozygous flies essentially allowed me to observe the effects of a mixed spectrin network.

Prior to preparing the R22S samples for iTRAQ, I attempted this technique to identify proteins from a plasma membrane protein preparation from just wild-type flies. The reasons for this were two-fold: First, it would allow me to work out the details of a new method, *viz* iTRAQ and determine if any modifications would have to be considered for the identification of membrane proteins. Second, the two duplicate experiments within the Control iTRAQ would serve as replicates of the plasma membrane protein preparation, bringing the total number of replicates for the method to three. It was gratifying to see an overlap of 252 proteins between the two experiments, which represented 59% of the initial protein list. It was even more encouraging to find 68 of the total 95 plasma membrane proteins that we reported via MudPIT analysis in the iTRAQ list (this represents 71.6% of the total known plasma membrane protein list reported by MudPIT analysis). The total number of proteins we found with iTRAQ (Unused Score > 1.3) was more than those we reported by MudPIT. This could be due to a smaller amount of protein in the MudPIT analysis (slightly less than 100 μg, which was the minimum amount labeled for each sample in iTRAQ), or differences due to a different batch of Dextran-ConA. However, the substantial overlap of the plasma membrane proteins was

particularly encouraging and I decided to use the technique as is in preparing the samples for comparison of wild-type versus mutant proteomes.

Comparison of the head proteomes of ORR flies that had been heat shocked versus those that hadn't showed a significant change ($p \leq 0.05$) in 9 proteins in two or more comparisons, of which only one was a plasma membrane protein. The majority were mitochondrial proteins. The function of each protein along with it's potential significance to heat shock is discussed:

a) Calreticulin: It is protein that resides in the lumen of the ER and is involved in protein folding. One of the cellular responses to heat shock is protein unfolding, which is caused even by a marginal increase in temperature (Richter *et al*., 2010). Hence, an upregulation of calreticulin might be a response to protein unfolding as a result of heat shock. Most likely a contaminant.

b) CG3560: This gene encodes a protein that is a component of the mitochondrial respiratory chain complex III (mitochondrial inner membrane) and catalyzes the oxidation of ubiquinol by cytochrome c. Heat shock is known to result in uncoupling of oxidative phosphorylation as well as loss of mitochondria and reduction in ATP levels (Richter *et al*., 2010). In eukaryotic cells, the respiratory chain complexes are the seats of oxidative phosphorylation and hence an upregulation of this protein might be a response to the drop in levels of ATP. Most likely a contaminant.

c) CTL-like protein 1: It is choline-transporter like membrane glycoprotein. It seems unclear why this protein might be upregulated in response to heat shock.

d) Dynamin-like protein: It has GTPase activity and is part of the microtubule associated complex. One of the responses to heat shock is the disruption of intracellular transport (Richter *et al*., 2010) and this phenomenon might explain the down regulation of this protein.

e) Glutamate dehydrogenase (Gdh), short peptide: It is a mitochondrial matrix protein that is involved in the process of aerobic respiration. It catalyzes the breakdown

of glutamate to 2-oxoglutarate. A decrease in levels of this protein upon heat shock might be a result of the number of mitochondria due to heat shock (Richter *et al*., 2010). Most likely a contaminant.

f) IP15876p (Porin): It is an outer mitochondrial membrane protein that forms a voltage-dependent anion selective channel. While it is most likely a contaminant in this experiment, the upregulation of this gene upon heat shock (37^{o}C, 10 minutes) has been demonstrated in *Saccharomyces cerevisae* (reviewed in Richter *et al*., 2010).

g) Microsomal glutathione S-transferase-like protein (Mgst1): A resident of the microsome, it catalyzes the following reaction: RX + glutathione ⇔ HX + R-S-glutathione, where X may be a sulfate, nitrile or halide group. Upregulation of this gene upon heat shock (37^{o}C, 10 minutes) has been demonstrated in *Arabidopsis thaliana* (reviewed in Richter *et al*., 2010), although it seems unclear why.

h) Mitochondrial aconitase: It is a mitochondrial protein and is part of the tricarboxylic acid (TCA) cycle. A decrease in levels of this protein upon heat shock might be a result of the number of mitochondria due to heat shock (Richter *et al*., 2010). Most likely a contaminant.

i) Plasma membrane calcium ATPase, isoform L (PMCA): A resident of the plasma membrane, it is one of the proteins responsible for maintaining intracellular calcium levels by removing calcium from the cell at the expense of ATP. Heat shock results in approximately 10-fold increase in intracellular calcium and it has been suggested that the plasma membrane is not particularly permeable to calcium upon heat shock (Drummond *et al*., 1986). A decrease in the levels of PMCA in this experiment might be a reflection of this phenomenon.

Comparison of the proteomes of the *R22S/Cy; l(3)dre3^{rg41}R22S/TM6* flies at the permissive and restrictive temperatures showed a significant ($p \leq 0.05$) change in 18 proteins, of which 4 were plasma membrane proteins, 3 were residents of the ER and all were up-regulated at the restrictive temperature. The remaining proteins that were up-

regulated were mitochondrial or cytoplasmic. Of the 18 proteins, 4 proteins were down-regulated. The function of all the proteins and their potential significance to spectrin, the phenotype observed in the ovarioles of R22S is discussed.

a) Arginine Kinase (AK): It is an enzyme that catalyzes the reaction

L-arginine + ATP $\longrightarrow$ N (omega)-phospho-L-arginine + ADP + $2H^+$

The enzyme is involved in regulating inorganic phosphate levels which has effects on cellular metabolism and proton buffering and in intracellular energy transport (Ellington, 2001). In *Drosophila*, the enzyme is found in the cytoplasm as well as mitochondria, with very high gene expression in the adult head, midgut, hindgut, heart and high gene expression in the ovaries and testes (Flybase.org). In the ovaries, the protein is expressed in the germline stem cells and later in the germ cells (Kai *et al*., 2005). One interesting physical interaction reported by The *Drosophila* Protein Interaction Mapping Project (Mintseris, 2009) is that of AK and a protein called Swallow (Swa). In adult flies, *swallow* gene expression is restricted to the ovaries and the protein is required for correct localization of the *bicoid* mRNA in the oocyte (Hegde and Stephenson, 1993). It was recently shown that this role might be an indirect one, whereby Swallow, which is localized at the plasma membrane of the oocyte, plays a role in organizing the actin cytoskeleton, which is in turn involved in anchoring the anterior microtubules to the cell cortex. *Bicoid* mRNA is tethered to microtubules and hence localizes in the anterior of the oocyte (Weil *et al*., 2010). One loss of function mutant allele of *bicoid* (bcd^6) results in female sterility (Struhl *et al*., 1989).

In the context of α(R22S), one might expect that a disruption in the spectrin network would disrupt the correct localization of *bicoid* mRNA by disrupting the interaction of Swallow with the cytoskeleton and potentially lead to defects in oogenesis. If AK indeed interacts with Swallow, then disruption of the cytoskeleton might lead to an effect on this interaction and a potential effect on one of these proteins viz. AK. Since the nature of the interaction isn't known as yet, nor is it clear what kind of interaction exists between these proteins and the cytoskeleton, it may be hard to explain why AK was up-regulated at the restrictive temperature. One possibility though is that it might be compensatory reaction to a direct inhibition of the interaction between AK and Swallow. Another possibility is that it is being up-regulated as a response to disturbed energy

metabolism that may have arisen at the nutritional checkpoint of the ovary at Stage 8 (where egg chamber defects are observed, see Chapter 4 Results and Discussion).

b) ATP synthase-beta isoform A (β-ATP): It is part of the catalytic core of the mitochondrial proton-transporting ATP synthase complex, which is involved in ATP synthesis during the process of oxidative phosphorylation. The β-ATP transcript is stored in oocytes in *Drosophila* and its levels increase during development (after 10 hours) and steady state levels are maintained in the larvae and adults (Pena *et al*., 1995). Mitochondria are maternally inherited and during *Drosophila* oogenesis, a fraction of these associate with the fusomes and move through the ring canals to enter the oocyte (like Balbiani bodies seen in other organisms; (Cox and Spradling, 2003). If β-ATP is reflective of the number of mitochondria, one reason for its down-regulation might be the disruption of the fusome structure observed in the presence of the α(R22S) since an intact fusome is required for formation of the Balbiani body and mitochondria are dispersed in hts mutants that result in structural disruption of fusomes (Cox and Spradling, 2003).

c) Calcium ATPase at 60A is a resident of the ER membrane and hydrolyzes ATP to pump calcium across the ER membrane, where it is normally stored and is thus responsible for maintaining the intracellular levels of calcium. Presumably, the inclusion of this protein is *via* residual ER in the PM preparation. It is known to play a role in neuromuscular physiology in *Drosophila* by terminating muscle contraction and controlling muscle excitability by regulating other calcium channels (Sanyal *et al*., 2006).

The importance of an up-regulation of this protein in the mutant at restrictive temperature and its connection to ischemia can be explained by the role that the endoplasmic reticulum plays in responding to ischemic insult. In the event of ischemia, the ER responds by triggering the Unfolded Protein Response (UPR), which is basically the expression of the ER stress genes (Lehotsky *et al*., 2009). In PC-12 cells, it has been demonstrated that following an UPR, there is an up-regulation of the calcium ATPase activity (Hojmann Larsen *et al*., 2001).

d) CG30035: This gene encodes the trehalose transporter protein, a resident of the plasma membrane. Trehalose is the main sugar in the hemolymph of *Drosophila* and it known to protect it from hypoxia and anoxia by preventing protein denaturation by through trehalose-protein interactions (Chen *et al*., 2002; Chen and Haddad, 2004). The trehalose transporter protein is highly expressed in the fat body and is probably involved in transporting the trehalose produced in the fat body into the hemolymph (Kanamori *et al*., 2010). The up-regulation of this protein might be reflective of a response to a cellular situation that mimics hypoxic or anoxic stress in some way.

e) CG31233: This gene encodes an aminopeptidase and is probably involved in proteolysis (Flybase.org). It is not immediately obvious why this would have a response to the disruption of the SBMS.

f) CG5885: This gene encodes the gamma subunit of the Sec61 translocon complex, which is involved in protein translocation to the ER. Besides its canonical role, Sec61β has also been implicated in the transport of Gurken (the ligand for the Epidermal Growth Factor Receptor in *Drosophila* oocytes; Kelkar and Dobberstein, 2009). The authors showed that reducing Sec61β in the oocytes reduces the level of Gurken at the plasma membrane due to a defect in transport from the Golgi to the plasma membrane. The effect is specific for Gurken. While these results are specific for Sec61β, the up-regulation of the γ subunit might actually be a compensatory response to a translocation defect in general due to impairment in spectrin tetramerization. However, being an ER protein, this is most likely a contaminant and may fluctuate widely between preparations.

g) Cytochrome P450-4g1: It is known to be associated with the microsomal membrane and has been predicted to have a role in lipid metabolism (Flybase.org). Its up-regulation might be indicative of some perturbation in lipid metabolism in the mutants.

h) Failed axon connections: It is a protein that is located in axon bundles and is known to be involved in axonogenesis (Flybase.org). It has also been shown to be enriched in border cells in the ovary (Gates *et al*., 2009)

i) Ferritin 2 Light Chain Homologue, isoform A (FLCH): It is a Golgi protein involved in iron ion transport (Flybase.org). Ferritin is an iron storage complex, consisting of heavy and light chains. The heavy chain is responsible for oxidation of soluble ferrous ions and its overexpression in mice results in protection from oxidative stress (Kaur *et al*., 2003; Wilkinson *et al*., 2006). An iron overload is known to induce ferritin expression in flies and ferritin has been found to be expressed in the middle midgut of third instar larvae (not overlapping with the copper cells; Missirlis *et al*., 2007). There is precedent for the involvement of α-spectrin in the copper cells in the regulation of copper homeostasis (Dubreuil *et al*., 1998) as well as the role of β_H-spectrin in maintaining the expression of the V-ATPase in the same cells (Phillips and Thomas, 2006). Thus, a down-regulation of FLCH in the mutant flies might actually be expected as a result of disrupted iron homeostasis due to defective tetramerization. Another possibility is a direct interaction between FLCH and the spectrin network, which might be disrupted due to a defective network since there is precedent for the Golgi localization of α-spectrin in *Drosophila* (Sisson *et al*., 2000).

j) Porin: It is an outer mitochondrial membrane protein that forms a voltage-dependent anion selective channel. It is most likely a contaminant.

k) LP07754p (CG31198): The gene encodes a protein that has metalloprotease activity. It's not obvious why this would have a response to the disruption of the SBMS.

l) CG8421: This gene encodes an aspartyl β-hydroxylase, integral to the ER membrane, most likely a contaminant.

m) myosin heavy chain, isoform H: It is part of the myosin complex and has been found to have a physical interaction with Swallow (see description of Arginine Kinase; (Mintseris, 2009). Its down-regulation at restrictive temperature might be reflective of a general disruption of the cytoskeleton in this mutant.

n) Na^+/K^+ ATPase is a plasma membrane protein and is the major sodium pump energizing cellular membranes. There is precedent for the role of spectrin in polarizing this protein in epithelial cells in Drosophila (Dubreuil *et al*., 2000). It's localization at the basolateral domain in MDCK cells has been shown to be due to the presence of the SBMS, to which it is anchored *via* Ankyrin (Hammerton *et al*., 1991). Thus one would expect a reduction of its expression in the absence of an intact spectrin network. However, in HEK-293 cells that were being used to model an anoxic response, Na^+/K^+ ATPase was observed in aggregates. Interestingly, these were dispersed when the cells were transfected with a construct encoding *Drosophila* trehalose-6-phosphate synthase, known to protect cells against hypoxic and anoxic stress (see discussion for trehalose transporter). It is possible that an up-regulation of this protein in the mutant fly at restrictive temperature might resemble the cellular effects of hypoxia or anoxia in some way.

o) α Tubulin 2: Component of the microtubule. Up-regulation might be a compensatory response to a defective spectrin network. It's not obvious why this would have a response to the disruption of the SBMS

p) Ribosomal protein L23A: It is a component of the large ribosomal subunit and its up-regulation might be expected, considering a majority of proteins in the list of changed proteins actually showed up-regulation, possibly indicating an increase in translation. However, it is a contaminant in the preparation.

q) Syntaxin 1A: It is a plasma membrane protein with canonical roles in neurotransmission. However, it also essential in oogenesis and has been found in the germarium and nurse cell membranes (Schulze and Bellen, 1996). A significant change (up-regulation) in this protein might be reflective of the necessity of an intact spectrin network in maintenance of its expression.

r) vacuolar H[+] ATPase G-subunit (V-ATPase): It is a vacuolar proton transporting V-type ATPAse found on the plasma membrane of certain cells (eg:

epithelial cells). In the apical brush border cells of the *Drosophila* larval middle midgut of *karst* mutant larvae, the V-ATPase is no longer present at the plasma membrane or the early endosome (Phillips and Thomas, 2006). Thus, there is precedent for it being affected in the absence of spectrin. However, its up-regulation in the presence of a mixed spectrin network suggests a different mode of regulation by α-spectrin or then just a compensatory response to a defective network.

This list of proteins seems to be the first insight into global changes in the proteome of an organism due to a defective spectrin network. While the use of rescued flies, that have α(R22S) as their sole source of α-spectrin would have provided an unambiguous look at changes in the proteome due to defective spectrin tetramerization, significant changes in proteins whose involvement have been reported in ischemic events (anoxia in flies or then ischemia in humans) with the use of heterozygous flies that still have one wild-type copy of α-spectrin is most encouraging. However, this list is by no means exhaustive; in fact the number of proteins (particularly plasma membrane proteins) is quite small and this might be due to low levels of the α(R22S) in the heterozygous stock. However, the use of this stock still made for an interesting experiment as any changes observed would be expected in only a minority population that actually contributed to the phenotype. With this list of proteins in hand, it would also be interesting to confirm changes in the expression of some of these proteins *via* immunostaining, not only in the heterozygous flies but also in rescued flies. Indeed, some of these proteins (e.g. Na^+/K^+ ATPase and trehalose transporter) could be used as markers to monitor the effects of temperature on the network *via* immunoblots.

Chapter 6 Conclusions and Future Perspectives

6.1 Applicability of the α(R22S) fly line to study ischemic events

The goal of this thesis was to develop *Drosophila* as a model system to study the effects of calpain-mediated proteolysis of the spectrin cytoskeleton, a characteristic of ischemic stroke, on the cell surface proteome. While vertebrate models of stroke exist in the form of rats and gerbils, invertebrate models have as yet to be fully explored in the study of this pathology. I wanted to introduce *Drosophila* as an effective model system to mimic and investigate some of the cellular effects of stroke. The plan was to induce spectrin breakdown in the fly and study the consequent effects on the expression of cell surface proteins that may be associated with spectrin, directly or indirectly. While this approach could have been used in any model system, *Drosophila* was particularly appealing due to the existence of a conditional mutant (temperature sensitive, TS) for spectrin integrity in this organism. A TS mutant offered the possibility of studying just the immediate effects of spectrin disruption, avoiding non-specific effects of proteolysis observed in ischemia as well as cellular compensations. This method would also allow me to skirt the embryonic- and larval- lethal effects of spectrin mutations in *Drosophila*. The genetic tractability of the organism as well as the fact that it has only a single gene for every spectrin isoform that it expresses also contribute to its attraction.

While it was not anticipated that the conditional mutant would have to be remade, doing so has provided us with a fly line that not only mimics the phenotype the original mutant exhibited, but also shows other interesting effects that might shed some light on the role of an intact spectrin network in certain *Drosophila* tissues. Perhaps the most striking observation is the way the mutant protein α(R22S) behaves in the presence of the wild-type protein. When expressed in the wild-type background, α(R22S) is excluded from the apicolateral spectrin network into the basal domain of the plasma membrane of the follicle cells. In the germaria, the mutant protein is completely excluded from the fusomes-it is seen in aggregates throughout the germarium instead of as a component of the tubulovesicular structures characteristic of fusomes. However, when the mutant protein is expressed in an α-spectrin null background, it behaves just like the wild-type protein – it localizes at the apicolateral membrane of the follicle cells and can

be seen in the fusomes as well. One possibility is that this is not an effect of the mutation but of too much α-spectrin. A simple way to test this would be to express wild-type α-spectrin as a transgene in a wild-type background. If the effect is just due to an over-expression of α–spectrin, then one might expect to see a similar effect in the germaria and follicle cells as seen when α(R22S) is expressed in a wild-type background. Another possibility is that a mixed tetramer, one which can contain wild-type and mutant α-spectrin, is more susceptible to proteolysis that a network that contains only wild-type α-spectrin or only mutant α-spectrin purely due to the lack of a "uniform" tetramer, which the cell might recognize as defective. In fact, this might be indicated by immunoblot analysis in wild-type flies, rescued flies and those from various heterozygous stocks (Fig 4.13 and 4.14), where a stable myc-tagged protein product is seen only in the rescued flies, barely visible in various heterozygous stocks. A third possibility is that due to defective tetramerization, certain signaling components known to be part of the fusome are disrupted and this leads to aggregation of the mutant protein instead of it being part of a tubulovesicular structure. A way to test this would be to try and rescue this phenotype with putative fusome components whose function might have been affected due to the presence of the α(R22S). One such fusome component is the recycling endosome GTPase Rab11. In germaria mosaic for *rab11* mutant alleles, the tubulovesicular structure of the fusome is greatly reduced in mutant clones and α-spectrin was seen as a spherical aggregate in these clones (Lighthouse *et al*., 2008). However, this cannot be an exclusive reason as it doesn't explain why then this α(R22S) aggregation isn't observed in germaria from rescued flies. In that context, the theory of the stability of a "uniform" network seems more plausible.

Although the work outlined in this thesis is limited in its use of a heterozygous fly line to test the efficacy of this model system in the study of ischemia, a significant change is certain proteins that may have functional significance in hypoxia/anoxia is encouraging. However, this examination of the proteome by iTRAQ needs to replicated in order to categorically claim that a certain protein is affected by a defective spectrin tetramers. In order to use rescued flies with α(R22S) as the sole source of α-spectrin, I would need to establish a viable stock of these flies in order to get them in large enough numbers for a proteomic analysis. While this isn't possible with the current R22S lines in

the lab, if this effect is a position effect (i.e. position of insertion of the transgene), it can be overcome by hopping out the transgene with the help of a transposase from its current position and its insertion in a position in the genome that allows the rescued progeny to procreate or for the addition of yet more copies of the transgene to the α-spectrin null background.

6.2 Alternative ways to mimic ischemia in *Drosophila*

6.2.1 Inducing cytoskeletal remodeling by Annexin

Annexins are a group of calcium-dependent phospholipids binding proteins present in all eukaryotes except yeast (Moss and Morgan, 2004). There are 12 annexins in vertebrates, 4 in *Drosophila*, 4-5 in *C.elegans*, 3 in Fungi (except yeast) and up to 13 in plants (Gerke and Moss, 2002; Moss and Morgan, 2004). All annexins have a conserved core domain that consists of 4 annexin repeats and a divergent amino terminal domain. The calcium binding domain lies in Repeat 2 (Moss and Morgan, 2004). Annexins have diverse cellular roles, including exocytosis, endocytosis, phagocytosis, organization of membrane domains by association with the cytoskeleton and regulation of ion channel activity, to name a few (reviewed by Gerke and Moss, 2002).

Annexins have been implicated in remodeling of the cytoskeleton – vertebrate Annexin 6 interacts with brain spectrin and actin (Watanabe *et al*., 1994), Annexin 2 binds to and helps bundle F-actin filaments (Hayes *et al*., 2004) and a study in human fibroblasts suggested that Annexin 6-mediated proteolysis of spectrin was required for coated-pit budding (Kamal *et al*., 1998). Our lab has contributed to annexin biology in *Drosophila* by showing that Annexin B9 physically interacts with β_H-spectrin (Tjota *et al*., 2011, in press.) and is involved in membrane trafficking and multivesicular body formation in conjunction with β_H-spectrin (Williams *et al*., 2004; Tjota *et al*., 2011, in press.). Since data from other labs suggests a role for Annexin in cytoskeletal remodeling and our own results in *Drosophila* demonstrate that it interacts with spectrin and is involved in protein trafficking, another way by which the effects of spectrin proteolysis in ischemia can be modeled in *Drosophila* is by the augmenting the action of Annexin on spectrin by overexpressing it in a wild-type background.

I attempted to induce remodeling of the spectrin network by introducing Annexin B9 as a transgene in the vector pUAST, putting it under the control of the Gal4 binary expression system, which would render its expression silent unless crossed to a Gal4-expressing driver fly line. Expression of Annexin B9 (fly line 9.1.a) was induced by use of the 69B-Gal4 driver line, which drives the expression of Gal4 in the embryonic epidermis and imaginal discs. The effects on spectrin as a result of the overexpression of Annexin were observed in the protein extracts from the larvae of this cross as well as the undriven control resolved by SDS-polyacryamide gel electrophoresis and blotted onto nitrocellulose membrane. Probing for α- and β_H-spectrin (rabbit anti-βH #675) revealed that β_H-spectrin was down-regulated in the lanes corresponding to proteins from larvae in which Annnexin B9 had been overexpressed in comparison to the undriven controls with a frequency of 60% (Fig 6.1). These preliminary results, although still slightly inconsistent (since spectrin down-regulation not observed with 100% frequency), seem to indicate that this approach might provide a suitable alternative to study the effects of spectrin degradation.

6.2.2 Activation of calpain

In order to mimic the effects of calpain-mediated spectrin proteolysis observed in ischemic events, a very obvious strategy would be to activate calpain in *Drosophila* and observe the subsequent effects on the cell surface proteome. I didn't use this as a primary strategy for reasons outlined in Section 1.5, *viz*. calpain has multiple targets, there are no reports of calpain-mediated degradation of spectrin in *Drosophila* to date and at the moment, the fly community lacks reagents such as mutant alleles and over-expression lines. However, recently, as part of the *Drosophila* Protein Interaction Mapping Project, a physical interaction was reported between Calpain and β_H-spectrin (Mintseris, 2009).

As a preliminary attempt to activate calpain, I tried to recapitulate calpain activation in *Drosophila* S2 cells (Farkas *et al*., 2004). Farkas *et al*. demonstrated the induction of Calpain B by the use of an ionophore (Ionomycin), which increases intracellular calcium levels and hence can activate calpain, a protease that responds to rise in levels of intracellular calcium. The induction of calpain was indicated by its autolysis in response to rise in calcium levels as observed by immunoblot analysis. Two major autolysis

Figure 6.1 Effect of Annexin B9 overexpression on spectrin levels

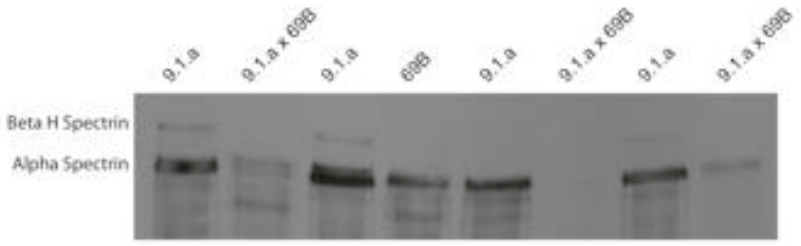

Fig 6.1 Effect of Annexin B9 overexpression on spectrin levels Immunoblot analysis of larval extracts for α- and βH spectrin when Annexin B9 is overexpressed in a wild-type background (9.1.a x 69B), 9.1.a is the undriven control and 69B is the Gal4 driver line. β_H-spectrin expression is reduced when Annexin B9 is overexpressed.

products can be seen (96 and 81 kDa) and within 60 minutes, only the 81 kDa product exists. I used the prescribed 10μM of Ionomycin to activate calpain in S2 cells and observed the 81 kDa autolytic product after 5 minutes up to 30 minutes (Fig 6.2). However, probing for α- and β_H-spectrin on blots with extracts from S2 cells treated with Ionomycin for up to 30 minutes revealed that the proteins were intact (Fig 6.3 and 6.4). However, there's no ruling out that activation of calpain might have lead to spectrin proteolysis since Fig 6.2 shows that all of the inactive calpain didn't undergo autolysis within 30 minutes and it's possible that there might be a lag period before spectrin protelysis begins after calpain is completely autolysed. In order to determine if spectrin is a target of calpain in S2 cells, this experiment would have to be repeated for longer periods of time.

To conclude, this was a novel attempt at determining the feasibility of using *Drosophila* as a model system for certain aspects of ischemic stroke. The aim was to document changes in the cell surface proteome of neuronal tissue as a response to loss of spectrin integrity. Within the scope of this dissertation, I introduced a novel method to isolate cell surface proteins from *Drosophila* tissue, developed a fly line that potentially mimics spectrin degradation characteristic of ischemic strokes and have provided a preliminary list of proteins that show significant change in their expression as a result of defective spectrin tetramerization (amongst those proteins are some that have functional significance in response to ischemia). It will be exciting to track the progress of this attempt in the future. I envision this project to point the way for further studies in vertebrate model systems and ultimately the development of alternative therapies or compensatory treatments for stroke patients, thus improving their quality of life and more effective rehabilitation.

Figure 6.2 Calpain activation in *Drosophila* S2 cells

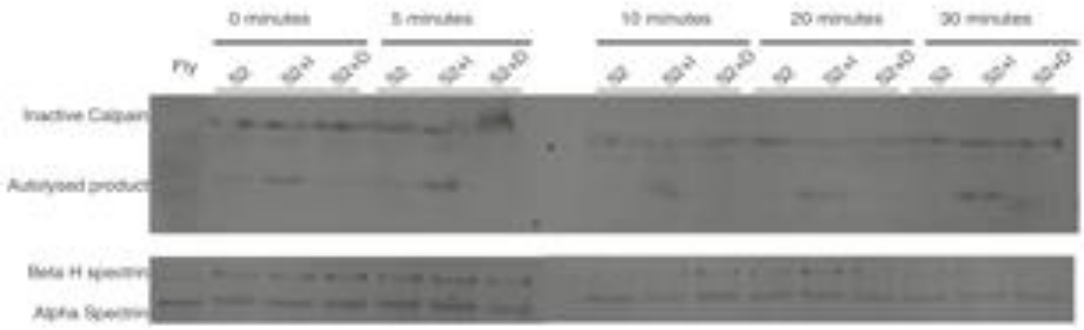

Fig 6.2 Calpain activation in Drosophila S2 cells S2 cells were exposed to the ionophore Ionomycin (S2+I) for 30 minutes. Samples were taken at regular time intervals (indicated on immunoblot) and extracts were probed for Calpain, α- and βH spectrin. Activated calpain (autolysed product) is only observed when S2 cells are exposed to Ionomycin. S2 cells without treatment (S2) and those treated with the solvent DMSO (S2+D) do not show activation of Calpain. The spectrins are intact even after 30 minutes of exposure to Ionomycin.

BIBLIOGRAPHY

Abedinpour, P. and Jergil, B. (2003). Isolation of a caveolae-enriched fraction from rat lung by affinity partitioning and sucrose gradient centrifugation. *Anal Biochem* **313**, 1-8.

Aggarwal, K., Choe, L. H. and Lee, K. H. (2006). Shotgun proteomics using the iTRAQ isobaric tags. *Brief Funct Genomic Proteomic* **5**, 112-20.

Akcakaya, H., Aroymak, A. and Gokce, S. (2007). A quantitative colorimetric method of measuring alkaline phosphatase activity in eukaryotic cell membranes. *Cell Biol Int* **31**, 186-90.

Alonso, J., Rodriguez, J. M., Baena-Lopez, L. A. and Santaren, J. F. (2005). Characterization of the Drosophila melanogaster mitochondrial proteome. *J Proteome Res* **4**, 1636-45.

Alonso, J. and Santaren, J. F. (2006). Characterization of the Drosophila melanogaster ribosomal proteome. *J Proteome Res* **5**, 2025-32.

An, X., Gauthier, E., Zhang, X., Guo, X., Anstee, D. J., Mohandas, N. and Chasis, J. A. (2008). Adhesive activity of Lu glycoproteins is regulated by interaction with spectrin. *Blood* **112**, 5212-8.

Apodaca, G. (2002). Modulation of membrane traffic by mechanical stimuli. *Am J Physiol Renal Physiol* **282**, F179-90.

Armario, P. and de la Sierra, A. (2009). Blood pressure as a therapeutic target in stroke. *Curr Top Med Chem* **9**, 1278-84.

Ashburner, M. (1989). Drosophila A Laboratory Handbook: Cold Spring Harbor Laboratory Press.

Ayalon, G., Hostettler, J. D., Hoffman, J., Kizhatil, K., Davis, J. Q. and Bennett, V. (2010). Ankyrin-B interactions with spectrin and dynactin-4 are required for dystrophin-based protection of skeletal muscle from exercise injury. *J Biol Chem* **286**, 7370-8.

Bae, T. J., Kim, M. S., Kim, J. W., Kim, B. W., Choo, H. J., Lee, J. W., Kim, K. B., Lee, C. S., Kim, J. H., Chang, S. Y. *et al.* (2004). Lipid raft proteome reveals ATP synthase complex in the cell surface. *Proteomics* **4**, 3536-48.

Baines, A. J. (2010). The spectrin-ankyrin-4.1-adducin membrane skeleton: adapting eukaryotic cells to the demands of animal life. *Protoplasma* **244**, 99-131.

Barone, F. C. (2009). Ischemic stroke intervention requires mixed cellular protection of the penumbra. *Curr Opin Investig Drugs* **10**, 220-3.

Beller, M., Riedel, D., Jansch, L., Dieterich, G., Wehland, J., Jackle, H. and Kuhnlein, R. P. (2006). Characterization of the Drosophila lipid droplet subproteome. *Mol Cell Proteomics* **5**, 1082-94.

Bennett, V. and Baines, A. J. (2001). Spectrin and ankyrin-based pathways: metazoan inventions for integrating cells into tissues. *Physiol Rev* **81**, 1353-92.

Bennett, V. and Gilligan, D. M. (1993). The spectrin-based membrane skeleton and micron-scale organization of the plasma membrane. *Annu Rev Cell Biol* **9**, 27-66.

Bevers, E. M., Comfurius, P., Dekkers, D. W. and Zwaal, R. F. (1999). Lipid translocation across the plasma membrane of mammalian cells. *Biochim Biophys Acta* **1439**, 317-30.

Beziat, F., Touraille, S., Debise, R., Morel, F., Petit, N., Lecher, P. and Alziari, S. (1997). Biochemical and molecular consequences of massive mitochondrial gene loss in different tissues of a mutant strain of Drosophila subobscura. *J Biol Chem* **272**, 22583-90.

Binder, W. H., Barragan, V. and Menger, F. M. (2003). Domains and rafts in lipid membranes. *Angew Chem Int Ed Engl* **42**, 5802-27.

Blikstad, I., Nelson, W. J., Moon, R. T. and Lazarides, E. (1983). Synthesis and assembly of spectrin during avian erythropoiesis: stoichiometric assembly but unequal synthesis of alpha and beta spectrin. *Cell* **32**, 1081-91.

Bozoky, Z., Alexa, A., Dancsok, J., Gogl, G., Klement, E., Medzihradszky, K. F. and Friedrich, P. (2009). Identifying calpain substrates in intact S2 cells of Drosophila. *Arch Biochem Biophys* **481**, 219-25.

Brunner, E., Ahrens, C. H., Mohanty, S., Baetschmann, H., Loevenich, S., Potthast, F., Deutsch, E. W., Panse, C., de Lichtenberg, U., Rinner, O.*et al.* (2007). A high-quality catalog of the Drosophila melanogaster proteome. *Nat Biotechnol* **25**, 576-83.

Butters, T. D. and Hughes, R. C. (1981). Phospholipids and glycolipids in subcellular fractions of mosquito *Aedes aegypti* cells. *In Vitro* **17**, 831-38.

Caetano, F. H., Zara, F. J. and Gregório, E. A. (2002). The origin of lipid droplets in the post-pharyngeal gland of *Dinoponera australis* (Formicidae: Ponerinae). *Cytologia* **67**, 301-8.

Cairo, C. W., Das, R., Albohy, A., Baca, Q. J., Pradhan, D., Morrow, J. S, Coombs, D. and Golan, D. E. (2010). Dynamic regulation of CD45 lateral mobility by the spectrin-ankyrin cytoskeleton of T cells. *J Biol Chem* **285**, 11392-401.

Casado-Vela, J., Martinez-Esteso, M. J., Rodriguez, E., Borras, E., Elortza, F. and Bru-Martinez, R. (2010). iTRAQ-based quantitative analysis of protein mixtures with large fold change and dynamic range. *Proteomics* **10**, 343-7.

Chandra, N. C., Spiro, M. J. and Spiro, R. G. (1998). Identification of a glycoprotein from rat liver mitochondrial inner membrane and demonstration of its origin in the endoplasmic reticulum. *J Biol Chem* **273**, 19715-21.

Chen, A., Liao, W. P., Lu, Q., Wong, W. S. and Wong, P. T. (2007). Upregulation of dihydropyrimidinase-related protein 2, spectrin alpha II chain, heat shock cognate protein 70 pseudogene 1 and tropomodulin 2 after focal cerebral ischemia in rats--a proteomics approach. *Neurochem Int* **50**, 1078-86.

Chen, Q. and Haddad, G. G. (2004). Role of trehalose phosphate synthase and trehalose during hypoxia: from flies to mammals. *J Exp Biol* **207**, 3125-9.

Chen, Q., Ma, E., Behar, K. L., Xu, T. and Haddad, G. G. (2002). Role of trehalose phosphate synthase in anoxia tolerance and development in Drosophila melanogaster. *J Biol Chem* **277**, 3274-9.

Cherry, L., Menhart, N. and Fung, L. W. (1999). Interactions of the alpha-spectrin N-terminal region with beta-spectrin. Implications for the spectrin tetramerization reaction. *J Biol Chem* **274**, 2077-84.

Chichili, G. R. and Rodgers, W. (2007). Clustering of membrane raft proteins by the actin cytoskeleton. *J Biol Chem* **282**, 36682-91.

Chichili, G. R. and Rodgers, W. (2009). Cytoskeleton-membrane interactions in membrane raft structure. *Cell Mol Life Sci* **66**, 2319-28.

Chichili, G. R., Westmuckett, A. D. and Rodgers, W. (2010). T cell signal regulation by the actin cytoskeleton. *J Biol Chem* **285**, 14737-46.

Clarkson, Y. L., Gillespie, T., Perkins, E. M., Lyndon, A. R. and Jackson, M. (2010). Beta-III spectrin mutation L253P associated with spinocerebellar ataxia type 5 interferes with binding to Arp1 and protein trafficking from the Golgi. *Hum Mol Genet* **19**, 3634-41.

Collins, C. (2007). Pathophysiology and classification of stroke. *Nurs Stand* **21**, 35-9.

Cox, R. T. and Spradling, A. C. (2003). A Balbiani body and the fusome mediate mitochondrial inheritance during Drosophila oogenesis. *Development* **130**, 1579-90.

Czogalla, A. and Sikorski, A. F. (2005). Spectrin and calpain: a 'target' and a 'sniper' in the pathology of neuronal cells. *Cell Mol Life Sci* **62**, 1913-24.

de Cuevas, M., Lee, J. K. and Spradling, A. C. (1996). alpha-spectrin is required for germline cell division and differentiation in the Drosophila ovary. *Development* **122**, 3959-68.

de Cuevas, M., Lilly, M. A. and Spradling, A. C. (1997). Germline cyst formation in Drosophila. *Annu Rev Genet* **31**, 405-28.

De Matteis, M. A. and Morrow, J. S. (2000). Spectrin tethers and mesh in the biosynthetic pathway. *J Cell Sci* **113 (Pt 13)**, 2331-43.

Deng, H., Lee, J. K., Goldstein, L. S. and Branton, D. (1995). Drosophila development requires spectrin network formation. *J Cell Biol* **128**, 71-9.

Deng, W. and Lin, H. (1997). Spectrosomes and fusomes anchor mitotic spindles during asymmetric germ cell divisions and facilitate the formation of a polarized microtubule array for oocyte specification in Drosophila. *Dev Biol* **189**, 79-94.

Devarajan, P., Stabach, P. R., De Matteis, M. A. and Morrow, J. S. (1997). Na,K-ATPase transport from endoplasmic reticulum to Golgi requires the Golgi spectrin-ankyrin G119 skeleton in Madin Darby canine kidney cells. *Proc Natl Acad Sci U S A* **94**, 10711-6.

Devaux, P. F. (2000). Is lipid translocation involved during endo- and exocytosis? *Biochimie* **82**, 497-509.

Distler, A. M., Kerner, J. and Hoppel, C. L. (2008). Proteomics of mitochondrial inner and outer membranes. *Proteomics* **8**, 4066-82.

Domanitskaya, E. V., Liu, H., Chen, S. and Kubli, E. (2007). The hydroxyproline motif of male sex peptide elicits the innate immune response in Drosophila females. *FEBS J* **274**, 5659-68.

Dosemeci, A. and Reese, T. S. (1995). Effect of calpain on the composition and structure of postsynaptic densities. *Synapse* **20**, 91-7.

Drummond, I. A., McClure, S. A., Poenie, M., Tsien, R. Y. and Steinhardt, R. A. (1986). Large changes in intracellular pH and calcium observed during heat shock are not responsible for the induction of heat shock proteins in Drosophila melanogaster. *Mol Cell Biol* **6**, 1767-75.

Dubreuil, R. R., Byers, T. J., Sillman, A. L., Bar-Zvi, D., Goldstein, L. S. and Branton, D. (1989). The complete sequence of Drosophila alpha-spectrin: conservation of structural domains between alpha-spectrins and alpha-actinin. *J Cell Biol* **109**, 2197-205.

Dubreuil, R. R., Frankel, J., Wang, P., Howrylak, J., Kappil, M. and Grushko, T. A. (1998). Mutations of alpha spectrin and labial block cuprophilic cell differentiation and acid secretion in the middle midgut of Drosophila larvae. *Dev Biol* **194**, 1-11.

Dubreuil, R. R., Wang, P., Dahl, S., Lee, J. and Goldstein, L. S. (2000). Drosophila beta spectrin functions independently of alpha spectrin to polarize the Na,K ATPase in epithelial cells. *J Cell Biol* **149**, 647-56.

Ekblad, L. and Jergil, B. (2001). Localization of phosphatidylinositol 4-kinase isoenzymes in rat liver plasma membrane domains. *Biochim Biophys Acta* **1531**, 209-21.

Ellington, W. R. (2001). Evolution and physiological roles of phosphagen systems. *Annu Rev Physiol* **63**, 289-325.

Emori, Y. and Saigo, K. (1994). Calpain localization changes in coordination with actin-related cytoskeletal changes during early embryonic development of Drosophila. *J Biol Chem* **269**, 25137-42.

Endres, M. and Dirnagl, U. (2002). Ischemia and stroke. *Adv Exp Med Biol* **513**, 455-73.

Eroglu, C., Brugger, B., Wieland, F. and Sinning, I. (2003). Glutamate-binding affinity of Drosophila metabotropic glutamate receptor is modulated by association with lipid rafts. *Proc Natl Acad Sci U S A* **100**, 10219-24.

Fabini, G., Freilinger, A., Altmann, F. and Wilson, I. B. (2001). Identification of core alpha 1,3-fucosylated glycans and cloning of the requisite fucosyltransferase cDNA from Drosophila melanogaster. Potential basis of the neural anti-horseadish peroxidase epitope. *J Biol Chem* **276**, 28058-67.

Farkas, A., Tompa, P., Schad, E., Sinka, R., Jekely, G. and Friedrich, P. (2004). Autolytic activation and localization in Schneider cells (S2) of calpain B from Drosophila. *Biochem J* **378**, 299-305.

Feany, M. B. and Bender, W. W. (2000). A Drosophila model of Parkinson's disease. *Nature* **404**, 394-8.

Featherstone, D. E., Davis, W. S., Dubreuil, R. R. and Broadie, K. (2001). Drosophila alpha- and beta-spectrin mutations disrupt presynaptic neurotransmitter release. *J Neurosci* **21**, 4215-24.

Fleming, J. E., Quattrocki, E., Latter, G., Miquel, J., Marcuson, R., Zuckerkandl, E. and Bensch, K. G. (1986). Age-dependent changes in proteins of Drosophila melanogaster. *Science* **231**, 1157-9.

Friedrich, P., Tompa, P. and Farkas, A. (2004). The calpain-system of Drosophila melanogaster: coming of age. *Bioessays* **26**, 1088-96.

Fritz, J. D., Swartz, D. R. and Greaser, M. L. (1989). Factors affecting polyacrylamide gel electrophoresis and electroblotting of high-molecular-weight myofibrillar proteins. *Anal Biochem* **180**, 205-10.

Gates, J., Nowotarski, S. H., Yin, H., Mahaffey, J. P., Bridges, T., Herrera, C., Homem, C. C., Janody, F., Montell, D. J. and Peifer, M. (2009). Enabled and Capping protein play important roles in shaping cell behavior during Drosophila oogenesis. *Dev Biol* **333**, 90-107.

Gerke, V. and Moss, S. E. (2002). Annexins: from structure to function. *Physiol Rev* **82**, 331-71.

Glantz, S. B., Cianci, C. D., Iyer, R., Pradhan, D., Wang, K. K. and Morrow, J. S. (2007). Sequential degradation of alphaII and betaII spectrin by calpain in glutamate or maitotoxin-stimulated cells. *Biochemistry* **46**, 502-13.

Grant, K. J. and Wu, C. C. (2007). Advances in neuromembrane proteomics: efforts towards a comprehensive analysis of membrane proteins in the brain. *Brief Funct Genomic Proteomic* **6**, 59-69.

Greaser, M. L. and Gergely, J. (1971). Reconstitution of troponin activity from three protein components. *J Biol Chem* **246**, 4226-33.

Grewal, T., Koese, M., Rentero, C. and Enrich, C. (2010). Annexin A6-regulator of the EGFR/Ras signalling pathway and cholesterol homeostasis. *Int J Biochem Cell Biol* **42**, 580-4.

Gstaiger, M. and Aebersold, R. (2009). Applying mass spectrometry-based proteomics to genetics, genomics and network biology. *Nat Rev Genet* **10**, 617-27.

Hammerton, R. W., Krzeminski, K. A., Mays, R. W., Ryan, T. A., Wollner, D. A. and Nelson, W. J. (1991). Mechanism for regulating cell surface distribution of Na+,K(+)-ATPase in polarized epithelial cells. *Science* **254**, 847-50.

Hansen, C. G. and Nichols, B. J. (2010). Exploring the caves: cavins, caveolins and caveolae. *Trends Cell Biol* **20**, 177-86.

Hansen, J. C., Skalak, R., Chien, S. and Hoger, A. (1996). An elastic network model based on the structure of the red blood cell membrane skeleton. *Biophys J* **70**, 146-66.

Hanspal, M. and Palek, J. (1987). Synthesis and assembly of membrane skeletal proteins in mammalian red cell precursors. *J Cell Biol* **105**, 1417-24.

Hardy, B., Bensch, K. G. and Schrier, S. L. (1979). Spectrin rearrangement early in erythrocyte ghost endocytosis. *J Cell Biol* **82**, 654-63.

Harris, A. S. and Morrow, J. S. (1990). Calmodulin and calcium-dependent protease I coordinately regulate the interaction of fodrin with actin. *Proc Natl Acad Sci U S A* **87**, 3009-13.

Hayes, M. J., Rescher, U., Gerke, V. and Moss, S. E. (2004). Annexin-actin interactions. *Traffic* **5**, 571-6.

Heck, M. M., Pereira, A., Pesavento, P., Yannoni, Y., Spradling, A. C. and Goldstein, L. S. (1993). The kinesin-like protein KLP61F is essential for mitosis in Drosophila. *J Cell Biol* **123**, 665-79.

Hegde, J. and Stephenson, E. C. (1993). Distribution of swallow protein in egg chambers and embryos of Drosophila melanogaster. *Development* **119**, 457-70.

Hojmann Larsen, A., Frandsen, A. and Treiman, M. (2001). Upregulation of the SERCA-type Ca2+ pump activity in response to endoplasmic reticulum stress in PC12 cells. *BMC Biochem* **2**, 4.

Holleran, E. A., Ligon, L. A., Tokito, M., Stankewich, M. C., Morrow, J. S. and Holzbaur, E. L. (2001). beta III spectrin binds to the Arp1 subunit of dynactin. *J Biol Chem* **276**, 36598-605.

Hulsen, T., de Vlieg, J. and Alkema, W. (2008). BioVenn-a web application for the comparison and visualization of biological lists using area-proportional Venn diagrams. *BMC Genomics* **9**, 488-93

Hulsmeier, J., Pielage, J., Rickert, C., Technau, G. M., Klambt, C. and Stork, T. (2007). Distinct functions of alpha-Spectrin and beta-Spectrin during axonal pathfinding. *Development* **134**, 713-22.

Ikeda, Y., Dick, K. A., Weatherspoon, M. R., Gincel, D., Armbrust, K. R., Dalton, J. C., Stevanin, G., Durr, A., Zuhlke, C., Burk, K. *et al.* (2006). Spectrin mutations cause spinocerebellar ataxia type 5. *Nat Genet* **38**, 184-90.

Indraswari, F., Wong, P. T., Yap, E., Ng, Y. K. and Dheen, S. T. (2009). Upregulation of Dpysl2 and Spna2 gene expression in the rat brain after ischemic stroke. *Neurochem Int* **55**, 235-42.

Iskratsch, T., Braun, A., Paschinger, K. and Wilson, I. B. (2009). Specificity analysis of lectins and antibodies using remodeled glycoproteins. *Anal Biochem* **386**, 133-46.

Jiang, Q. Y., Gnagey, A., Tandler, B. and Jacobs-Lorena, M. (1986). Isolation of plasma membranes from Drosophila embryos. *Mol Biol Rep* **11**, 19-24.

Josic, D. and Clifton, J. G. (2007). Mammalian plasma membrane proteomics. *Proteomics* **7**, 3010-29.

Josic, D., Clifton, J. G., Kovac, S. and Hixson, D. C. (2008). Membrane proteins as diagnostic biomarkers and targets for new therapies. *Curr Opin Mol Ther* **10**, 116-23.

Kai, T., Williams, D. and Spradling, A. C. (2005). The expression profile of purified Drosophila germline stem cells. *Dev Biol* **283**, 486-502.

Kallappagoudar, S., Varma, P., Pathak, R. U., Senthilkumar, R. and Mishra, R. K. (2010). Nuclear matrix proteome analysis of *Drosophila melanogaster*. *Mol Cell Proteomics* **9**, 2005-18.

Kamal, A., Ying, Y. and Anderson, R. G. (1998). Annexin VI-mediated loss of spectrin during coated pit budding is coupled to delivery of LDL to lysosomes. *J Cell Biol* **142**, 937-47.

different kinetic properties involved in trehalose import into peripheral tissues. *Insect Biochem Mol Biol* **40**, 30-7.

Kastrykina, T. F., Malysheva, M.K. (2000). Calpain as one of the calcium signal mediators in the cell *Neurophysiology* **32**, 111-123.

Kaur, D., Yantiri, F., Rajagopalan, S., Kumar, J., Mo, J. Q., Boonplueang, R., Viswanath, V., Jacobs, R., Yang, L., Beal, M. F. ***et al.*** (2003). Genetic or pharmacological iron chelation prevents MPTP-induced neurotoxicity in vivo: a novel therapy for Parkinson's disease. *Neuron* **37**, 899-909.

Kelkar, A. and Dobberstein, B. (2009). Sec61beta, a subunit of the Sec61 protein translocation channel at the endoplasmic reticulum, is involved in the transport of Gurken to the plasma membrane. *BMC Cell Biol* **10**, 11.

Khanna, M. R., Stanley, B.A. and Thomas, G.H. (2010). Towards a Membrane Proteome in Drosophila: A Method for the Isolation of Plasma Membrane. *BMC Genomics* **In Press**.

Kizhatil, K., Davis, J. Q., Davis, L., Hoffman, J., Hogan, B. L. and Bennett, V. (2007). Ankyrin-G is a molecular partner of E-cadherin in epithelial cells and early embryos. *J Biol Chem* **282**, 26552-61.

Kodippili, G. C., Spector, J., Sullivan, C., Kuypers, F. A., Labotka, R., Gallagher, P. G., Ritchie, K. and Low, P. S. (2009). Imaging of the diffusion of single band 3 molecules on normal and mutant erythrocytes. *Blood* **113**, 6237-45.

Koles, K., Lim, J. M., Aoki, K., Porterfield, M., Tiemeyer, M., Wells, L. and Panin, V. (2007). Identification of N-glycosylated proteins from the central nervous system of Drosophila melanogaster. *Glycobiology* **17**, 1388-403.

Kotula, L., DeSilva, T. M., Speicher, D. W. and Curtis, P. J. (1993). Functional characterization of recombinant human red cell alpha-spectrin polypeptides containing the tetramer binding site. *J Biol Chem* **268**, 14788-93.

Kusumi, A., Nakada, C., Ritchie, K., Murase, K., Suzuki, K., Murakoshi, H., Kasai, R. S., Kondo, J. and Fujiwara, T. (2005). Paradigm shift of the plasma membrane concept from the two-dimensional continuum fluid to the partitioned fluid: high-speed single-molecule tracking of membrane molecules. *Annu Rev Biophys Biomol Struct* **34**, 351-78.

Kyte, J. and Doolittle, R. F. (1982). A simple method for displaying the hydropathic character of a protein. *J Mol Biol* **157**, 105-32.

Laemmli, U. K. (1970). Cleavage of structural proteins during the assembly of the head of bacteriophage T4. *Nature* **227**, 680-5.

Lajoie, P. and Nabi, I. R. (2010). Lipid rafts, caveolae, and their endocytosis. *Int Rev Cell Mol Biol* **282**, 135-63.

Lasko, P. (2002). Diabetic flies? Using Drosophila melanogaster to understand the causes of monogenic and genetically complex diseases. *Clin Genet* **62**, 358-67.

Lawson, E. L., Clifton, J. G., Huang, F., Li, X., Hixson, D. C. and Josic, D. (2006). Use of magnetic beads with immobilized monoclonal antibodies for isolation of highly pure plasma membranes. *Electrophoresis* **27**, 2747-58.

Lee, H. G., Zarnescu, D. C., MacIver, B. and Thomas, G. H. (2010). The cell adhesion molecule Roughest depends on beta(Heavy)-spectrin during eye morphogenesis in Drosophila. *J Cell Sci* **123**, 277-85.

Lee, J. K., Coyne, R. S., Dubreuil, R. R., Goldstein, L. S. and Branton, D. (1993). Cell shape and interaction defects in alpha-spectrin mutants of Drosophila melanogaster. *J Cell Biol* **123**, 1797-809.

Lehotsky, J., Racay, P., Pavlikova, M., Tatarkova, Z., Urban, P., Chomova, M., Kovalska, M. and Kaplan, P. (2009). Cross-talk of intracellular calcium stores in the response to neuronal ischemia and ischemic tolerance. *Gen Physiol Biophys* **28 Spec No Focus**, F104-14.

Lighthouse, D. V., Buszczak, M. and Spradling, A. C. (2008). New components of the Drosophila fusome suggest it plays novel roles in signaling and transport. *Dev Biol* **317**, 59-71.

Lin, H., Yue, L. and Spradling, A. C. (1994). The Drosophila fusome, a germline-specific organelle, contains membrane skeletal proteins and functions in cyst formation. *Development* **120**, 947-56.

Lippincott-Schwartz, J. and Phair, R. D. (2010). Lipids and cholesterol as regulators of traffic in the endomembrane system. *Annu Rev Biophys* **39**, 559-78.

Lipton, P. (1999). Ischemic cell death in brain neurons. *Physiol Rev* **79**, 1431-568.

Lopez, M. F., Kristal, B. S., Chernokalskaya, E., Lazarev, A., Shestopalov, A. I., Bogdanova, A. and Robinson, M. (2000). High-throughput profiling of the mitochondrial proteome using affinity fractionation and automation. *Electrophoresis* **21**, 3427-40.

Lu, B., McClatchy, D. B., Kim, J. Y. and Yates, J. R., 3rd. (2008). Strategies for shotgun identification of integral membrane proteins by tandem mass spectrometry. *Proteomics* **8**, 3947-55.

Lusitani, D. M., Qtaishat, N., LaBrake, C. C., Yu, R. N., Davis, J., Kelley, M. R. and Fung, L. W. (1994). The first human alpha-spectrin structural domain begins with serine. *J Biol Chem* **269**, 25955-8.

Manes, S., del Real, G., Lacalle, R. A., Lucas, P., Gomez-Mouton, C., Sanchez-Palomino, S., Delgado, R., Alcami, J., Mira, E. and Martinez, A. C. (2000). Membrane raft microdomains mediate lateral assemblies required for HIV-1 infection. *EMBO Rep* **1**, 190-6.

Marchesi, V. T. and Steers, E., Jr. (1968). Selective solubilization of a protein component of the red cell membrane. *Science* **159**, 203-4.

Matsumoto, H., Takemori, N., Thompson, J. N. j., Yamamoto, M.-T. and Komori, N. (2007). *Drosophila* proteome atlas. *Drosophila Information Service* **90**, 162-4.

Maurer, M. H., Berger, C., Wolf, M., Futterer, C. D., Feldmann, R. E., Jr., Schwab, S. and Kuschinsky, W. (2003). The proteome of human brain microdialysate. *Proteome Sci* **1**, 7.

Medina, E., Lemmers, C., Lane-Guermonprez, L. and Le Bivic, A. (2002). Role of the Crumbs complex in the regulation of junction formation in Drosophila and mammalian epithelial cells. *Biol Cell* **94**, 305-13.

Mintseris, J., Obar, R.A., Celniker, S., Gygi, S.P., VijayRaghavan, K., Artavanis-Tsakonas, S. (2009). DPiM: the Drosophila Protein Interaction Mapping project.

Missirlis, F., Kosmidis, S., Brody, T., Mavrakis, M., Holmberg, S., Odenwald, W. F., Skoulakis, E. M. and Rouault, T. A. (2007). Homeostatic mechanisms for iron storage revealed by genetic manipulations and live imaging of Drosophila ferritin. *Genetics* **177**, 89-100.

Molloy, M. P. (2000). Two-dimensional electrophoresis of membrane proteins using immobilized pH gradients. *Anal Biochem* **280**, 1-10.

Montreuil, J., Vliegenthart, J. F. G. and Schachter, H. (1995). Glycoproteins. Amsterdam ; New York: Elsevier.

Moss, S. E. and Morgan, R. O. (2004). The annexins. *Genome Biol* **5**, 219.

Muller, H., Schmidt, D., Steinbrink, S., Mirgorodskaya, E., Lehmann, V., Habermann, K., Dreher, F., Gustavsson, N., Kessler, T., Lehrach, H. *et al.* (2010). Proteomic and functional analysis of the mitotic Drosophila centrosome. *EMBO J* **29**, 3344-57.

Munujos, P., Coll-Canti, J., Gonzalez-Sastre, F. and Gella, F. J. (1993). Assay of succinate dehydrogenase activity by a colorimetric-continuous method using iodonitrotetrazolium chloride as electron acceptor. *Anal Biochem* **212**, 506-9.

Nakada, C., Ritchie, K., Oba, Y., Nakamura, M., Hotta, Y., Iino, R., Kasai, R. S., Yamaguchi, K., Fujiwara, T. and Kusumi, A. (2003). Accumulation of anchored proteins forms membrane diffusion barriers during neuronal polarization. *Nat Cell Biol* **5**, 626-32.

Nicolas, G., Fournier, C. M., Galand, C., Malbert-Colas, L., Bournier, O., Kroviarski, Y., Bourgeois, M., Camonis, J. H., Dhermy, D., Grandchamp, B. *et al.* (2002). Tyrosine phosphorylation regulates alpha II spectrin cleavage by calpain. *Mol Cell Biol* **22**, 3527-36.

Odell, A. F., Van Helden, D. F. and Scott, J. L. (2008). The spectrin cytoskeleton influences the surface expression and activation of human transient receptor potential channel 4 channels. *J Biol Chem* **283**, 4395-407.

Oh, Y. and Fung, L. W. (2007). Brain proteins interacting with the tetramerization region of non-erythroid alpha spectrin. *Cell Mol Biol Lett* **12**, 604-20.

Ohno-Iwashita, Y., Shimada, Y., Hayashi, M. and Inomata, M. (2010). Plasma membrane microdomains in aging and disease. *Geriatr Gerontol Int* **10 Suppl 1**, S41-52.

Overington, J. P., Al-Lazikani, B. and Hopkins, A. L. (2006). How many drug targets are there? *Nat Rev Drug Discov* **5**, 993-6.

Papoulas, O., Hays, T. S. and Sisson, J. C. (2005). The golgin Lava lamp mediates dynein-based Golgi movements during Drosophila cellularization. *Nat Cell Biol* **7**, 612-8.

Patterson, G. H., Hirschberg, K., Polishchuk, R. S., Gerlich, D., Phair, R. D. and Lippincott-Schwartz, J. (2008). Transport through the Golgi apparatus by rapid partitioning within a two-phase membrane system. *Cell* **133**, 1055-67.

Pedersen, K. S., Codrea, M. C., Vermeulen, C. J., Loeschcke, V. and Bendixen, E. (2010). Proteomic characterization of a temperature-sensitive conditional lethal in Drosophila melanogaster. *Heredity* **104**, 125-34.

Pellikka, M., Tanentzapf, G., Pinto, M., Smith, C., McGlade, C. J., Ready, D. F. and Tepass, U. (2002). Crumbs, the Drosophila homologue of human CRB1/RP12, is essential for photoreceptor morphogenesis. *Nature* **416**, 143-9.

Pena, P., Ugalde, C., Calleja, M. and Garesse, R. (1995). Analysis of the mitochondrial ATP synthase beta-subunit gene in Drosophilidae: structure, transcriptional regulatory features and developmental pattern of expression in Drosophila melanogaster. *Biochem J* **312 (Pt 3)**, 887-97.

Persson, A. and Jergil, B. (1992). Purification of plasma membranes by aqueous two-phase affinity partitioning. *Anal Biochem* **204**, 131-6.

Persson, A., Johansson, B., Olsson, H. and Jergil, B. (1991). Purification of rat liver plasma membranes by wheat-germ-agglutinin affinity partitioning. *Biochem J* **273(Pt 1)**, 173-7.

Phillips, M. D. and Thomas, G. H. (2006). Brush border spectrin is required for early endosome recycling in Drosophila. *J Cell Sci* **119**, 1361-70.

Pielage, J., Fetter, R. D. and Davis, G. W. (2006). A postsynaptic spectrin scaffold defines active zone size, spacing, and efficacy at the Drosophila neuromuscular junction. *J Cell Biol* **175**, 491-503.

Pierce, A., Unwin, R. D., Evans, C. A., Griffiths, S., Carney, L., Zhang, L., Jaworska, E., Lee, C. F., Blinco, D., Okoniewski, M. J. *et al.* (2008). Eight-channel iTRAQ enables comparison of the activity of six leukemogenic tyrosine kinases. *Mol Cell Proteomics* **7**, 853-63.

Pike, B., Flint, J., Jitendra, D., Lu, X., Wang, K., Tortella, F, Hayes, R. (2003). Accumulation of calpain and caspase-3 proteolyic fragments of brain-derived αII-spectrin in cerebral spinal fluid after middle cerebral artery occlusion in rats. *Journal of Cerebral Blood Flow and Metabolism* **24**, 98-106.

Pike, L. J. (2006). Rafts defined: a report on the Keystone Symposium on Lipid Rafts and Cell Function. *J Lipid Res* **47**, 1597-8.

Pinter, M. and Friedrich, P. (1988). The calcium-dependent proteolytic system calpain-calpastatin in Drosophila melanogaster. *Biochem J* **253**, 467-73.

Pradhan, D. and Morrow, J. (2002). The spectrin-ankyrin skeleton controls CD45 surface display and interleukin-2 production. *Immunity* **17**, 303-15.

Rafii, M. S. and Hillis, A. E. (2006). Compendium of cerebrovascular diseases. *Int Rev Psychiatry* **18**, 395-407.

Rao, R. P., Yuan, C., Allegood, J. C., Rawat, S. S., Edwards, M. B., Wang, X., Merrill, A. H., Jr., Acharya, U. and Acharya, J. K. (2007). Ceramide transfer protein function is essential for normal oxidative stress response and lifespan. *Proc Natl Acad Sci U S A* **104**, 11364-9.

Rendić, D., Wilson, I. B. H. and Paschinger, K. (2008). The glycosylation capacity of insect cells. *Croatica Chemica Acta* **81**, 7-21.

Richter, K., Haslbeck, M. and Buchner, J. (2010). The heat shock response: life on the verge of death. *Mol Cell* **40**, 253-66.

Rietveld, A., Neutz, S., Simons, K. and Eaton, S. (1999). Association of sterol- and glycosylphosphatidylinositol-linked proteins with Drosophila raft lipid microdomains. *J Biol Chem* **274**, 12049-54.

Rolls, M. M., Marquardt, M.T., Kielian, M. and Machamer, C.E. (1997). Cholesterol-independent Targeting of Golgi Membrane Proteins in Insect Cells. *Mol Biol Cell* **8**, 2111-2118.

Ross, P. L., Huang, Y. N., Marchese, J. N., Williamson, B., Parker, K., Hattan, S., Khainovski, N., Pillai, S., Dey, S., Daniels, S. *et al.* (2004). Multiplexed protein quantitation in Saccharomyces cerevisiae using amine-reactive isobaric tagging reagents. *Mol Cell Proteomics* **3**, 1154-69.

Rustin, G. J., Wilson, P. D. and Peters, T. J. (1979). Studies on the subcellular localization of human neutrophil alkaline phosphatase. *J Cell Sci* **36**, 401-12.

Saatman, K. E., Creed, J. and Raghupathi, R. (2010). Calpain as a therapeutic target in traumatic brain injury. *Neurotherapeutics* **7**, 31-42.

Sadowski, P. G., Groen, A. J., Dupree, P. and Lilley, K. S. (2008). Sub-cellular localization of membrane proteins. *Proteomics* **8**, 3991-4011.

Sangerman, J., Gard, A. L., Shah, A. and Goodman, S. R. (1999). Synthesis, assembly, and turnover of alpha and beta-erythroid and nonerythroid spectrins in rat hippocampal neurons. *Brain Res* **849**, 128-38.

Sanyal, S., Jennings, T., Dowse, H. and Ramaswami, M. (2006). Conditional mutations in SERCA, the Sarco-endoplasmic reticulum Ca2+-ATPase, alter heart rate and rhythmicity in Drosophila. *J Comp Physiol B* **176**, 253-63.

Schindler, J., Lewandrowski, U., Sickmann, A., Friauf, E. and Nothwang, H. G. (2006). Proteomic analysis of brain plasma membranes isolated by affinity two-phase partitioning. *Mol Cell Proteomics* **5**, 390-400.

Schroeder, F., Nemecz, G., Wood, W. G., Joiner, C., Morrot, G., Ayraut-Jarrier, M. and Devaux, P. F. (1991). Transmembrane distribution of sterol in the human erythrocyte. *Biochim Biophys Acta* **1066**, 183-92.

Schulze, K. L. and Bellen, H. J. (1996). Drosophila syntaxin is required for cell viability and may function in membrane formation and stabilization. *Genetics* **144**, 1713-24.

Shcherbata, H. R., Yatsenko, A. S., Patterson, L., Sood, V. D., Nudel, U., Yaffe, D., Baker, D. and Ruohola-Baker, H. (2007). Dissecting muscle and neuronal disorders in a Drosophila model of muscular dystrophy. *EMBO J* **26**, 481-93.

Sheetz, M. P. (2001). Cell control by membrane-cytoskeleton adhesion. *Nat Rev Mol Cell Biol* **2**, 392-6.

Shilov, I. V., Seymour, S. L., Patel, A. A., Loboda, A., Tang, W. H., Keating, S. P., Hunter, C. L., Nuwaysir, L. M. and Schaeffer, D. A. (2007). The Paragon Algorithm, a next generation search engine that uses sequence temperature values and feature probabilities to identify peptides from tandem mass spectra. *Mol Cell Proteomics* **6**, 1638-55.

Sisson, J. C., Field, C., Ventura, R., Royou, A. and Sullivan, W. (2000). Lava lamp, a novel peripheral golgi protein, is required for Drosophila melanogaster cellularization. *J Cell Biol* **151**, 905-18.

Spadoni, C., Farkas, A., Sinka, R., Tompa, P. and Friedrich, P. (2003). Molecular cloning and RNA expression of a novel Drosophila calpain, Calpain C. *Biochem Biophys Res Commun* **303**, 343-9.

Speers, A. E., Blackler, A. R. and Wu, C. C. (2007). Shotgun analysis of integral membrane proteins facilitated by elevated temperature. *Anal Chem* **79**, 4613-20.

Speers, A. E. and Wu, C. C. (2007). Proteomics of integral membrane proteins--theory and application. *Chem Rev* **107**, 3687-714.

Speicher, D. W., DeSilva, T. M., Speicher, K. D., Ursitti, J. A., Hembach, P. and Weglarz, L. (1993). Location of the human red cell spectrin tetramer binding site and detection of a related "closed" hairpin loop dimer using proteolytic footprinting. *J Biol Chem* **268**, 4227-35.

Spradling, A. C. (1993). Developmental Genetics of Oogenesis. In *The Development of Drosophila Melanogaster*, vol. I (ed. M. B. a. A. M. Arias), pp. 1-70: Cold Spring Harbor Laboratory Press.

Stabach, P. R., Devarajan, P., Stankewich, M. C., Bannykh, S. and Morrow, J. S. (2008). Ankyrin facilitates intracellular trafficking of alpha1-Na+-K+-ATPase in polarized cells. *Am J Physiol Cell Physiol* **295**, C1202-14.

Stark, W. S., Lin, T. N., Brackhahn, D., Christianson, J. S. and Sun, G. Y. (1993). Phospholipids in Drosophila heads: effects of visual mutants and phototransduction manipulations. *Lipids* **28**, 23-8.

Stasyk, T. and Huber, L. A. (2004). Zooming in: fractionation strategies in proteomics. *Proteomics* **4**, 3704-16.

Struhl, G., Struhl, K. and Macdonald, P. M. (1989). The gradient morphogen bicoid is a concentration-dependent transcriptional activator. *Cell* **57**, 1259-73.

Sumandea, C. A. and Fung, L. W. (2005). Mutational effects at the tetramerization site of nonerythroid alpha spectrin. *Brain Res Mol Brain Res* **136**, 81-90.

Sun, B. and Salvaterra, P. M. (1995). Characterization of nervana, a Drosophila melanogaster neuron-specific glycoprotein antigen recognized by anti-horseradish peroxidase antibodies. *J Neurochem* **65**, 434-43.

Tang, W. H., Shilov, I. V. and Seymour, S. L. (2008). Nonlinear fitting method for determining local false discovery rates from decoy database searches. *J Proteome Res* **7**, 3661-7.

Taraszka, J. A., Gao, X., Valentine, S. J., Sowell, R. A., Koeniger, S. L., Miller, D. F., Kaufman, T. C. and Clemmer, D. E. (2005a). Proteome profiling for assessing diversity: analysis of individual heads of Drosophila melanogaster using LC-ion mobility-MS. *J Proteome Res* **4**, 1238-47.

Taraszka, J. A., Kurulugama, R., Sowell, R. A., Valentine, S. J., Koeniger, S. L., Arnold, R. J., Miller, D. F., Kaufman, T. C. and Clemmer, D. E. (2005b). Mapping the proteome of Drosophila melanogaster: analysis of embryos and adult heads by LC-IMS-MS methods. *J Proteome Res* **4**, 1223-37.

Tateno, H., Nakamura-Tsuruta, S. and Hirabayashi, J. (2009). Comparative analysis of core-fucose-binding lectins from Lens culinaris and Pisum sativum using frontal affinity chromatography. *Glycobiology* **19**, 527-36.

Terashima, J. and Bownes, M. (2006). E75A and E75B have opposite effects on the apoptosis/development choice of the Drosophila egg chamber. *Cell Death Differ* **13**, 454-64.

Theopold, U., Pinter, M., Daffre, S., Tryselius, Y., Friedrich, P., Nassel, D. R. and Hultmark, D. (1995). CalpA, a Drosophila calpain homolog specifically expressed in a small set of nerve, midgut, and blood cells. *Mol Cell Biol* **15**, 824-34.

Thiele, C. and Spandl, J. (2008). Cell biology of lipid droplets. *Curr Opin Cell Biol* **20**, 378-85.

Thomas, G. H., Zarnescu, D. C., Juedes, A. E., Bales, M. A., Londergan, A., Korte, C. C. and Kiehart, D. P. (1998). Drosophila betaHeavy-spectrin is essential for development and contributes to specific cell fates in the eye. *Development* **125**, 2125-34.

Tomishige, M., Sako, Y. and Kusumi, A. (1998). Regulation mechanism of the lateral diffusion of band 3 in erythrocyte membranes by the membrane skeleton. *J Cell Biol* **142**, 989-1000.

Tse, W. T., Lecomte, M. C., Costa, F. F., Garbarz, M., Feo, C., Boivin, P., Dhermy, D. and Forget, B. G. (1990). Point mutation in the beta-spectrin gene associated with

alpha I/74 hereditary elliptocytosis. Implications for the mechanism of spectrin dimer self-association. *J Clin Invest* **86**, 909-16.

Tse, W. T. and Lux, S. E. (1999). Red blood cell membrane disorders. *Br J Haematol* **104**, 2-13.

Tsuji, A. and Ohnishi, S. (1986). Restriction of the lateral motion of band 3 in the erythrocyte membrane by the cytoskeletal network: dependence on spectrin association state. *Biochemistry* **25**, 6133-9.

Unlu, M., Morgan, M. E. and Minden, J. S. (1997). Difference gel electrophoresis: a single gel method for detecting changes in protein extracts. *Electrophoresis* **18**, 2071-7.

Unwin, R. D. (2010). Quantification of proteins by iTRAQ. *Methods Mol Biol* **658**, 205-15.

Vaccari, T., Rusten, T. E., Menut, L., Nezis, I. P., Brech, A., Stenmark, H. and Bilder, D. (2009). Comparative analysis of ESCRT-I, ESCRT-II and ESCRT-III function in Drosophila by efficient isolation of ESCRT mutants. *J Cell Sci* **122**, 2413-23.

van Meer, G., Voelker, D. R. and Feigenson, G. W. (2008). Membrane lipids: where they are and how they behave. *Nat Rev Mol Cell Biol* **9**, 112-24.

Vanderklish, P. W. and Bahr, B. A. (2000). The pathogenic activation of calpain: a marker and mediator of cellular toxicity and disease states. *Int J Exp Pathol* **81**, 323-39.

Viswanathan, S., Unlu, M. and Minden, J. S. (2006). Two-dimensional difference gel electrophoresis. *Nat Protoc* **1**, 1351-8.

Washburn, M. P., Wolters, D. and Yates, J. R., 3rd. (2001). Large-scale analysis of the yeast proteome by multidimensional protein identification technology. *Nat Biotechnol* **19**, 242-7.

Watanabe, T., Inui, M., Chen, B. Y., Iga, M. and Sobue, K. (1994). Annexin VI-binding proteins in brain. Interaction of annexin VI with a membrane skeletal protein, calspectin (brain spectrin or fodrin). *J Biol Chem* **269**, 17656-62.

Weil, T. T., Xanthakis, D., Parton, R., Dobbie, I., Rabouille, C., Gavis, E. R. and Davis, I. (2010). Distinguishing direct from indirect roles for bicoid mRNA localization factors. *Development* **137**, 169-76.

Wilkinson, J. t., Di, X., Schonig, K., Buss, J. L., Kock, N. D., Cline, J. M., Saunders, T. L., Bujard, H., Torti, S. V. and Torti, F. M. (2006). Tissue-specific expression of ferritin H regulates cellular iron homoeostasis in vivo. *Biochem J* **395**, 501-7.

Williams, J. A., MacIver, B., Klipfell, E. A. and Thomas, G. H. (2004). The C-terminal domain of Drosophila (beta) heavy-spectrin exhibits autonomous membrane association and modulates membrane area. *J Cell Sci* **117**, 771-82.

Winkelmann, J. C. and Forget, B. G. (1993). Erythroid and nonerythroid spectrins. *Blood* **81**, 3173-85.

Wodarz, A., Hinz, U., Engelbert, M. and Knust, E. (1995). Expression of crumbs confers apical character on plasma membrane domains of ectodermal epithelia of Drosophila. *Cell* **82**, 67-76.

Wood, W. G., Igbavboa, U., Muller, W. E. and Eckert, G. P. (2011). Cholesterol asymmetry in synaptic plasma membranes. *J Neurochem* **116**, 684-9.

Wu, C. C., MacCoss, M. J., Howell, K. E. and Yates, J. R., 3rd. (2003). A method for the comprehensive proteomic analysis of membrane proteins. *Nat Biotechnol* **21**, 532-8.

Xun, Z., Kaufman, T. C. and Clemmer, D. E. (2009). Stable isotope labeling and label-free proteomics of Drosophila parkin null mutants. *J Proteome Res* **8**, 4500-10.

Xun, Z., Sowell, R. A., Kaufman, T. C. and Clemmer, D. E. (2007). Lifetime proteomic profiling of an A30P alpha-synuclein Drosophila model of Parkinson's disease. *J Proteome Res* **6**, 3729-38.

Yao, H., Ginsberg, M. D., Eveleth, D. D., LaManna, J. C., Watson, B. D., Alonso, O. F., Loor, J. Y., Foreman, J. H. and Busto, R. (1995). Local cerebral glucose utilization and cytoskeletal proteolysis as indices of evolving focal ischemic injury in core and penumbra. *J Cereb Blood Flow Metab* **15**, 398-408.

Yates, J. R., Ruse, C. I. and Nakorchevsky, A. (2009). Proteomics by mass spectrometry: approaches, advances, and applications. *Annu Rev Biomed Eng* **11**, 49-79.

Zaccai, M. and Lipshitz, H. D. (1996). Differential distributions of two adducin-like protein isoforms in the Drosophila ovary and early embryo. *Zygote* **4**, 159-66.

Zachowski, A. (1993). Phospholipids in animal eukaryotic membranes: transverse asymmetry and movement. *Biochem J* **294 (Pt 1)**, 1-14.

Zhang, Z., Weed, S. A., Gallagher, P. G. and Morrow, J. S. (2001). Dynamic molecular modeling of pathogenic mutations in the spectrin self-association domain. *Blood* **98**, 1645-53.

Zhao, Z., Zhang, W., Stanley, B. A. and Assmann, S. M. (2008). Functional proteomics of Arabidopsis thaliana guard cells uncovers new stomatal signaling pathways. *Plant Cell* **20**, 3210-26.

Zwaal, R. F. and Schroit, A. J. (1997). Pathophysiologic implications of membrane phospholipid asymmetry in blood cells. *Blood* **89**, 1121-32.

APPENDIX

PART I

Link to chapter 2	Procedure	Lagniappe
2.2.1	Extract preparation	▪ After the first spin to pellet the nuclei, the supernatant is covered by a layer of "scum" (probably fat). In order to remove the supernatant for the next spin, insert the pipette tip below the scum layer and withdraw liquid till about 0.5 ml of liquid remains over the pellet. Make sure the pellet isn't disturbed. ▪ The microsome pellet (100,000xg) is comprised of 2 concentric circles (3 if the mitochondria haven't been removed)-the outer circle is mostly translucent and has a gel like consistency. The inner circle is darker in colour. ▪ It may take about 30 minutes to resuspend the microsome pellet. This step should be performed on ice! Wash continuously with a pipettor. If the mitochondria haven't been removed by centrifugation prior to pelleting out the microsomes, avoid the innermost circle.
2.2.2	Preparation of ConA-dextran	See part II of Appendix for protocol
2.2.3	2PAP	▪ The phases should be made the night before. ▪ The phases will separate only at 4^{o}C. ▪ To make a phase separation system, use pre-made master stocks of Dextran (20%) and PEG (40%). These stocks can be stored at 4^{o}C.

2.2.4	Density gradient centrifugation	▪ The amount of protein per gradient should be between 12 and 20 milligrams. ▪ Add protease inhibitor cocktail at 1:1000 in the buffer used to make the gradients. ▪ The gradients should be centrifuged at 4^{o}C with **slow acceleration** and **slow deceleration**. The slow deceleration is **VERY** important so as to avoid mixing of the different layers of the gradient once they've formed.
2.2.5	Combined density gradient centrifugation and 2PAP	▪ Remember to sample fractions 15-20 before combining them so that they can be used for immunoblots. ▪ For each 1g system, resuspend the pellet from fractions 15-20 in 100 ul of buffer (with 1:1000 protease inhibitors).

PART II PREPARATION OF ConA-Dextran

A Activation of dextran (preparation of tresyl-dextran)

Preparation of materials

1) Dissolve 5 grams of dextran in about 20 ml distilled water (D/W) and freeze dry. Store at -20^{o}C. Can be stored for up to 6 months.

2) Dry solvents with silica gel (0.02 grams per ml of solvent) for at least 5 hours. The flasks in which the solvents are to be dried should be washed and dried at 65^{o}C the night before with silica gel.

Solvents- DMSO (50 ml), Triethylamine (5 ml) and Dichloromethane (400 ml).

Preparation of tresyl-dextran

1) Dissolve the freeze-dried dextran in 25 ml of DMSO in a glass beaker (the beaker should also be dried overnight) at room temperature (stir with stir bar). **This can take from 30 mins up to an hour.** Cover with parafilm.

2) Add 1 ml of triethylamine slowly followed by 5 ml of dichloromethane. This should be done within 10 minutes with stirring (with a stir bar) so as to prevent the precipitation of dextran. Cover the beaker with parafilm. Continue to stir on

ice or at 4°C.

3) Slowly add tresyl chloride (0.35 g) while stirring vigorously on ice. Continue stirring on ice for 1 hour. **Precaution: Tresyl chloride is harmful! Wear gloves and work in the fume hood.**

4) Stir the solution overnight at room temperature. Remember to cover with parafilm.

5) Precipitate the dextran with 25 ml of dichloromethane. **Note: The precipitate is a white, sticky solid, which gets tough with subsequent washes. During and after precipitation, stir with a spatula or glass rod as the precipitate is too viscous for a stir bar.**

6) Wash the precipitate thoroughly with dichloromethane (4 times with 25 ml of solvent for each wash), kneading and breaking up the mass with a glass rod/spatula until firm at the end.

7) Dissolve the washed precipitate in D/W (5-10 ml; may take 30-35 mins) and dialyze against D/W. Freeze dry the tresyl-dextran and store at -20°C. Can be stored for up to 6 months. Note: Activate the dialysis bags (MwCO 12-14,000) by boiling in 10mM EDTA and wash thoroughly with D/W until no odor remains.

Coupling of ConA

1) Dissolve 2 g of freeze-dried tresyl-dextran in 10 ml of **Coupling Buffer** (0.1 M sodium phosphate / 0.5 M sodium chloride pH 7.5). This may take about 15 mins.

2) Dissolve 10 mg of ConA in 1 ml of **Coupling Buffer**.

3) Add 1 ml of ConA to the dissolved tresyl-dextran drop wise (very important!) with vigorous stirring/vortexing. Add OVER 10 MINUTES and incubate at 4°C overnight with gentle agitation.

4) Terminate the reaction with Tris-Cl to a final concentration of 400mM pH 7.5. Incubate at 4°C for 2 hours.

5) Divide the volume between 2 Jumbosep filtration devices (MwCO 100,000) and add D/W to make up volume to 60 ml in each filter. Centrifuge until the volume is 20 ml. Repeat 2 more times. **Note: The first wash might take up to an hour. The centrifuge to be used is a Sorvall 32B which is in Althouse (contact Bob Boor).**

6) Remove the retentate in a clean glass bottle and freeze dry the ConA-dextran. Store at -20^{o}C. Can be stored for up to 6 months.

Determining coupling efficiency

1) Dissolve 0.02 g of ConA-dextran in 250 ul of D/W and another 0.02 g in 250 ul of 0.1 M glucose.

2) Filter through a micron filter (14,000 rpm in microfuge for 30 minutes).

3) Vacuum dry the filtrate and resuspend in 50 ul of 1X LB.

4) Boil for 10 minutes, centrifuge in microfuge at max speed for 2 minutes. Load on a 12% SDS polyacrylamide gel.

5) Use unbound ConA (also filtered through micron filter) and BSA as controls.

6) Stain the gel with colloidal Coomassie Blue and destain.

7) To calculate the coupling efficiency:

a) First determine filtration efficiency by comparing the amount of unbound ConA filtered through the micron filter using different amounts of BSA as controls.

b) Compare the intensity of the ConA band after the glucose wash (this is the amount of ConA that can leach off) to BSA to determine its amount. This is the amount of ConA that is not bound to 0.02 g of dextran assuming the filtration efficiency is 100%. Extrapolate to calculate the amount that isn't bound to 2 g of dextran (the amount that was used for the coupling reaction).

Table 3.1

Accession number	CG number	Name	Subcellular compartment	Predicted tm domains	% sequence coverage (95%)	No. of peptides at CI>95%	No.of peptides at CI<95%	Peptide sequence	Precursor m/z	Charge	Score	Spectrum Number in Additional File
gi|24648576	CG5670-PA	Sodium pump alpha subunit	plasma membrane, nucleus	yes (1)	51.48895383	70	16					
gi|7291679	CG3725-PA	Calcium ATPase at 60A	ER membrane, nuc envelope	yes (2)	24.85029995	28	9					
gi|7293373	CG5870-PA	Beta-spectrin	plasma membrane, cytoskeleton	no	11.39240488	20	18					
gi|7292157	CG1977-PA	Alpha-spectrin	plasma membrane, cytoskeleton, Golgi	no	8.074533939	17	21					
gi|7291477	CG3612-PA	Bellwether	mitochondrial proton-transporting ATP synthase complex, catalytic core F(1)	no	34.78260934	18	3					
gi|7298786	CG8663-PB	Nervana 3	plasma membrane	yes (3)	28.61736417	18	3					
gi|24647500	CG6588-PC	Fasciclin 1	plasma membrane	yes (4)	24.12213683	17	6					
gi|7302024	CG1744-PA	Chaoptic	plasma membrane	yes (5)	13.76425922	16	5					
gi|73920239	CG5125	Neither inactivation nor afterpotential protein C	cytoskeleton (myosin complex), cytoplasm,	no	11.39240488	14	19					
gi|7290947	CG1634-PA	Neuroglian	plasma membrane	yes (6)	13.64003271	15	6					
gi|24661336	CG32031-PA	Arginine kinase	unknown	no	24.55516011	14	7					
gi|507752	CG1618	N-ethylmaleimide-sensitive fusion protein	cytoplasm	no	21.342282	13	7					
gi|161082106	CG34416-PJ	Ankyrin 2	plasma membrane	no	4.129863903	13	14					
gi|7290649	CG4027-PA	Actin 5C	cytoskeleton (actin filament), lipid particle	no	33.24468136	12	8					
gi|7301454	CG8058-PB	Aldolase	unknown	no	36.84210479	12	6					
gi|7304361	CG11154-PA	ATP synthase-β	lipid particle, mitochondrial proton-transporting ATP synthase complex, catalytic core F(1)	no	32.67326653	12	2					
gi|82471615	CG9261-PF	Nervana 2	plasma membrane	yes (7)	36.84210479	11	3					
gi|7298859	CG1913-PA	Alpha-tubulin	cytoskeleton (microtubule)	no	31.11111224	11	3					
gi|82471697	CG17870-PI	14-3-3zeta	nucleus	no	42.74193645	11	3					
gi|82090586	CG16944	Stress-sensitive B	mitochondrial inner memb	yes (8)	30.76923192	10	5					
gi|7295053	CG5962-PA	Phosrestin-1	membrane fraction, cytoplasm	no	26.68329179	11	4					
gi|8250175	CG9244	Aconitase	lipid particle,mitochondria	no	17.7890718	10	4					
gi|82484401	CG2165-PB		plasma membrane	yes (9)	9.553023428	10	9					
gi|7302471	CG9277-PA	Beta-Tubulin at 56D	cytoskeleton (microtubule)	no	28.94736826	10	5					
gi|996081	CG31136	Syntaxin 1A	plasma membrane	yes (10)	22.68041223	10	1					
gi|46409210	CG5594-PD		integral to membrane	yes (11)	7.914339006	8	11					
gi|77403899	CG4264		lipid particle, mitochondria, nuc	no	17.6651299	9	5					
gi|7664	CG7088	bangles and beads	unknown	no	35.06787419	9	4					
gi|7303741	CG2204-PA	G protein oα 47A	plasma membrane (heterotrimeric G-protein complex)	no	22.88135588	8	6					
gi|7297994	CG12403-PA	Vha68-1	plasma membrane (V-type ATPase, V0 domain)	no	15.63517898	8	3					
gi|7290601	CG11473-PA		membrane (Kyte and Doolittle)	yes (12)	11.57205254	9	3					
gi|24581228	CG3139-PC	Synaptotagmin	membrane, integral to synaptic vesicle membrane	yes (13)	17.7966103	8	2					
gi|24584716	CG17927-PM	Myosin heavy chain	cytoskeleton (myosin complex)	no	6.611569971	8	9					
gi|157981	CG3620	Phospholipase C	membrane fraction	no	8.127854019	8	7					
gi|7293146	CG10545-PA	G protein β-subunit 13F	plasma membrane (heterotrimeric G-protein complex)	no	24.41176474	8	3					
gi|7293147	CG8893-PA	Glyceraldehyde 3 phosphate dehydrogenase 2	lipid particle, cytoplasm	no	24.39759076	7	3					
gi|161076920	CG4587-PB		membrane (voltage-gated ion channel activity)	yes (14)	7.030604035	7	6					
gi|21627755	CG14762-PA		unknown	no	22.55319208	8	1					
gi|45550877	CG1732-PA		plasma membrane	yes (15)	13.67924511	7	3					
gi|48429216	CG1743	Glutamine synthetase 2	cytoplasm	no	22.49322534	7	4					
gi|3128475	CG7070	Pyruvate kinase	lipid particle, cytoplasm	no	20.82551569	7	2					
gi|24640124	CG3861-PB	Knockdown	mitochondrial matrix	no	17.43295044	7	3					
gi|7298967	CG2791-PA		membrane (Kyte and Doolittle)	yes (16)	18.76106262	7	1					
gi|85857592	CG42314		plasma membrane	no	19.83002871	7	3					
gi|51961046	CG40049-PA	Synapse protein 25	plasma membrane	no	40.56603909	6	6					
gi|28574660	CG33113-PF	Rtnl1	lipid particle, ER	yes (17)	22.18487412	7	3					
gi|85857548	CG6647	Porin	lipid particle, mitochondrial outer membrane	no	17.37588644	6	1					
gi|45554791	CG1725-PH	Discs large 1	plasma membrane	no	9.989023209	6	6					
gi|7294089	CG4169-PA		lipid particle, mitochondrial respiratory chain complex III	no	15.90909064	6	3					
gi|7291243	CG9394-PA		unknown	no	9.720176458	5	4					
gi|78706474	CG33950-PF	Terribly reduced optic lobes	lipid particle, basement membrane	no	0.885720458	4	16					
gi|7291098	CG1780-PA	Imaginal disc growth factor 4	Extracellular region	no	18.32579225	6	2					
gi|7783	CG17903	Cytochrome c proximal	mitochondrial inner memb	no	41.66666567	6	1					
gi|7293756	CG8770-PA	G protein β-subunit 76C	plasma membrane (heterotrimeric G-protein complex)	no	19.9421972	5	4					
gi|82484414	CG18069-PD	Calcium/calmodulin-dependent protein kinase II	plasma membrane(postsynaptic)	yes (18)	16.22641534	6	4					
gi|66804035	CG8983	Erp60	lipid particle, ER	no	16.76891595	6	1					
gi|47117835	CG9916	Cyclophilin 1	cytoplasm	no	25.99118948	6	3					
gi|7293665	CG6625-PA	Soluble NSF attachment protein	Golgi, ER, extrinsic to membrane	no	30.13698757	5	2					
gi|384212	CG9325	hu-li tai shao	plasma membrane	no	4.238754511	5	6					
gi|24668878	CG32230-PB		mitochondrial respiratory chain complex I	no	43.37349534	5	2					
gi|7301749	CG1709-PC	Vha100-1	membrane (Kyte and Doolittle)	yes (19)	6.432748586	5	7					
gi|7299734	CG1790-PA	Acetylcholine esterase	plasma membrane	yes (20)	12.17257306	5	5					
gi|24581914	CG14028-PA	Cyclope	lipid particle, mitochondrial respiratory chain complex IV	yes (21)	28.90625	5	1					
gi|8785	CG2960	Ribosomal protein L40	lipid particle, ribosome	no	42.85714328	5	2					
gi|4101653	CG1506	Adenylyl cyclase isoform DAC39E	integral to memb	yes (22)	6.169665977	5	2					
gi|82484222	CG31795-PA	la2	plasma membrane	yes (23)	5.594405532	5	7					
gi|7301957	CG2239-PA	Jdp	unknown	no	26.15384758	5	1					
gi|458803	CG5320	glutamate dehydrogenase	mitochondrial matrix	no	14.75409865	5	3					
gi|93141332	CG3762	V-ATPase 69 kDa subunit 2	plasma membrane (V-type ATPase, V0 domain)	no	12.05211729	4	2					
gi|8441	CG3481	Alcohol dehydrogenase	lipid particle	no	26.171875	5	1					
gi|7302861	CG6518-PA	Inactivation no afterpotential C	plasma membrane (inaD receptor complex)	yes (24)	7.999999821	5	1					
gi|7292118	CG17248-PB	n-synaptobrevin	plasma membrane	yes (25)	47.91666567	5						
gi|7294126	CG4899-PA	Photoreceptor dehydrogenase	membrane (Kyte and Doolittle)	yes (26)	22.30215818	5						
gi|7299915	CG2286-PA	NADH:ubiquinone reductase 75kD subunit precursor	mitochondrial respiratory chain complex I	no	8.618330956	4	2					
gi|7300560	CG4550-PA	Neither inactivation nor afterpotential E	plasma membrane (inaD receptor complex)	yes (27)	11.52814999	4	1					
gi|7294388	CG4994-PA	Mitochondrial phosphate carrier protein	lipid particle, mitochondrial inner memb, membrane, lipid particle	yes (28)	8.707865328	4	2					
gi|7303429	CG8604-PA	Amphiphysin	plasma membrane, cytoplasm	no	7.97342211	4	5					
gi|7833	CG18102	Dynamin	plasma membrane	no	4.53001149	3	7					
gi|47271230	CG3665	Fasciclin 2	plasma membrane, cytoplasm	yes (29)	5.692108721	4	4					
gi|7302996	CG8416-PB	Rho1	cytoplasm (cell cortex)	no	27.60416567	4	2					
gi|7302306	CG3283-PA	Succinate dehydrogenase B	mitochondrial respiratory chain complex II	no	12.45791242	4	2					
gi|8127	CG1242	Heat shock protein 83	lipid particle, cytoplasm, centrosome	no	7.531380653	4	6					
gi|8163739	CG9474	Synapse protein 24	cytoplasm (vesicle-)secretory granule	no	31.60377443	4	2					
gi|6013202	CG3988	Gamma-soluble NSF attachment protein	Golgi, ER, cytoplasm	no	16.88741744	4	2					
gi|24762461	CG2835-PC	G protein sα 60A	plasma membrane, heterotrimeric G-protein complex	no	15.44502676	4	4					
gi|6782318	CG3694	G protein γ30A	plasma membrane (heterotrimeric G-protein complex)	no	77.7777791	4	1					
gi|7293593	CG12233-PB	Lethal (1) G0156	lipid particle, mitochondrial matrix	no	13.7931034	3	2					
gi|41019545	CG1065	Succinyl coenzyme A synthetase α subunit	mitochondrion	yes (30)	14.02439028	4	1					
gi|7291601	CG17280-PA	Levy	lipid particle, mitochondrial respiratory chain complex IV, microsome	no	34.8623842	4	2					
gi|24583867	CG6579-PA		membrane (Kyte and Doolittle)	yes (31)	36.21621728	5						
gi|24641679	CG32638-PA		membrane (Kyte and Doolittle)	yes (32)	30.65693378	4						
gi|30580507	CG8884	Synapse-associated protein 47kD	synapse	no	7.259528339	4						
gi|7291663	CG11303-PA	Transmembrane 4 superfamily	plasma membrane	yes (33)	8.041957766	4	1					
gi|7297135	CG11015-PA		lipid particle, mitochondrial respiratory chain complex IV	no	27.5000006	3	3					
gi|7304088	CG2297-PA	Obp44a	unknown	no	20.27972043	3	3					
gi|7292924	CG11111-PB	retinal degeneration B	plasma membrane, intracellular	no	5.840000138	4	2					
gi|7298751	CG1099-PA	Dynamin associated protein 160	plasma membrane (presynaptic memb)	yes (34)	4.466727376	4	6					
gi|7296504	CG7145-PA		mitochondrial matrix	no	7.491289079	4	4					
gi|8810	CG17369	Vacuolar H+-ATPase 55kD B subunit	plasma membrane (V-tvoe ATPase. V0 domain)	no	7.551020384	3	9					
gi|881340	CG9258	Nervous system antigen 1	plasma membrane	yes (35)	6.472492218	3	2					
gi|34978339	CG31196	14-3-3 protein epsilon	nucleus, cytoplasm	no	19.46564913	3	3					
gi|7291816	CG4692-PB		lipid particle, mitochondrial proton-transporting ATP synthase complex, coupling factor F(o)	no	31.77570105	3	3					
gi|7290447	CG2934-PA	VhaAC39	plasma membrane (V-type ATPase, V0 domain)	no	11.71428561	4						
gi|7292440	CG15811-PA	Ras opposite	membrane, cytoplasm	no	4.187604785	3	5					
gi|7296719	CG1088-PA	Vacuolar H+-ATPase 26kD E subunit	plasma membrane (V-tvoe ATPase. V0 domain)	no	14.60177004	3	3					
gi|161077652	CG34344-PC	Retinal degeneration A	membrane	yes (36)	4.00390625	3	9					
gi|46019969	CG6803	Myofilin	cytoplasm (A-band (sarcomere))	no	9.890110046	3	4					
gi|5404981	CG7708	High-affinity choline transporter 1	integral to membrane	yes (37)	8.14332217	3	2					
gi|7297522	CG4422-PA	GDP dissociation inhibitor	synaptic vesicle	no	10.38374752	3	3					
gi|60678203	CG34120		membrane (ATP-binding cassette (ABC) transporter complex)	yes (38)	2.612152137	3	5					
gi|74871832	CG32245	Band 7 protein	membrane	yes (39)	9.504950792	3	5					

Table 3.1

Accession number	CG number	Name	Subcellular compartment	Predicted tm domains	% sequence coverage (95%)	No. of peptides at CI>95%	No.of peptides at CI<95%	Peptide sequence	Precursor m/z	Charge	Score	Spectrum Number in Additional File
gi|24643379	CG14235-PC		mitochondrial respiratory chain complex IV	no	41.55844152	3	2					
gi|9295510	CG15862	cAMP-dependent protein kinase R2	cytoplasm	no	8.488063514	2	5					
gi|28571173	CG17762-PC	Tomosyn	integral to membrane, synaptic vesicle	yes (40)	3.333333507	3	3					
gi|7294615	CG9762-PA	Lethal (3) neo18	mitochondrial respiratory chain complex I	yes (41)	17.74193496	3	1					
gi|7301553	CG5889-PA	Malate dehydrogenase (NADP-dependent oxaloacetate decarboxylating)	mitochondrion	no	7.61750415	3	2					
gi|85724874	CG33979-PB	Capulet	unknown	no	5.236270651	3	3					
gi|7300478	CG6030-PA	ATP synthase, subunit d	lipid particle, mitochondrial proton-transporting ATP synthase complex, coupling factor F(o)	no	21.34831399	3	2					
gi|24645604	CG3940-PA		unknown	no	17.10526347	3	1					
gi|73920742	CG1417	Sluggish-A	mitochondrial matrix	no	6.02055788	3	4					
gi|24642061	CG32593-PC	Flotillin 2	plasma membrane	no	10.47381535	3	3					
gi|24624873	CG32848	VAChT (Vesicular acetylcholine transporter)	integral to membrane	yes (42)	7.958477736	3	1					
gi|4105503	CG4123	Multiple inositol polyphosphate phosphatase 1	membrane (Kyte and Doolittle)	yes (43)	8.565310389	3	2					
gi|17945344	CG11001	FK506-binding protein 2	cytoplasm	no	21.08433694	3	1					
gi|25012931	CG32490	Complexin	membrane	no	20.27972043	3	1					
gi|7767570	CG10181	Multiple drug resistance 65	plasma membrane	yes (44)	2.534562163	2	7					
gi|24659386	CG30415-PB		unknown	no	56.09756112	3						
gi|28557669	CG6330		cytoplasm	yes (45)	7.336956263	3	1					
gi|7290603	CG42265-PA		membrane (Kyte and Doolittle)	yes (46)	6.998445094	3						
gi|7293712	CG7433-PA		mitochondrial matrix	no	4.938271642	3						
gi|7295470	CG4769-PA		lipid particle, mitochondrial respiratory chain complex III	yes (47)	15.96091241	3	1					
gi|7297508	CG3747-PA	Excitatory amino acid transporter 1	plasma membrane	yes (48)	9.185803682	3	1					
gi|7302495	CG7461-PA		lipid particle	no	6.71755746	3	1					
gi|7302893	CG5210-PA	Chitinase-like	Extracellular	no	7.964602113	4						
gi|73920223	CG10443	Leukocyte-antigen-related-like	plasma membrane	yes (49)	2.020699903	3						
gi|77403931	CG3127	Phosphoglycerate kinase	cytoplasm	no	8.915662766	3						
gi|24641539	CG42258-PD		unknown	no	37.27810681	3	1					
gi|51092023	CG2140-PB	Cyt-b5	membrane, microsome, lipid particle	yes (50)	15.67164212	3	2					
gi|7291724	CG4254-PA	Twinstar	cytoplasm (intracellular)	no	21.62162215	3						
gi|4972752	CG18617	Vha100-2	plasma membrane (V-type ATPase, V0 domain)	yes (51)	3.956834599	3	3					
gi|7294560	CG10620-PA	Transferrin 2	Extracellular region	yes (52)	5.128205195	3	2					
gi|7294780	CG7888-PA		membrane (Kyte and Doolittle)	yes (53)	6.92640692	3	2					
gi|7299809	CG9287-PA		unknown	no	5.053763464	3						
gi|161077675	CG34352-PA		membrane	no	0.948684756	3	4					
gi|24655647	CG17246-PC	Succinyl coenzyme A synthetase flavoprotein subunit	mitochondrial respiratory chain complex II	yes (54)	3.328290582	2	6					
gi|7292056	CG2248-PA	Rac1	cytoplasm (intracellular)	no	15.625	3						
gi|7301823	CG7610-PB	ATP synthase-γ chain	lipid particle, mitochondrial proton-transporting ATP synthase complex, catalytic core F(1)	no	12.12121248	3	1					
gi|7304364	CG11081-PA	Plexin A	membrane, intracellular	yes (55)	1.439588703	2	3					
gi|23397467	CG10260-PB		membrane (Kyte and Doolittle)	yes (56)	1.147842035	2	7					
gi|7301734	CG1954-PA	Protein C kinase 98E	unknown	no	3.112313896	2	2					
gi|24650122	CG5028-PA		mitochondrial matrix	no	7.213930041	2	1					
gi|7292012	CG13807-PA		membrane (Kyte and Doolittle)	yes (57)	2.573529445	2	5					
gi|7302508	CG11949-PA	Coracle	plasma membrane, cytoskeleton	no	2.120141312	2	10					
gi|28316876	CG4260	Alpha-adaptin	plasma membrane	no	3.128911182	2	3					
gi|161076458	CG34146-PB	Bruchpilot	membrane, nucleus	no	0.744132791	1	9	KLQDTDTFGRETR	1566.75	1	13	1
gi|7722	CG9012	Clathrin heavy chain	synaptic vesicle, lipid particle	no	2.026221715	2	2					
gi|4028652	CG1742	Microsomal glutathione S-transferase-like	lipid particle, microsome, mitochondrial outer membrane	yes (58)	7.894736528	2	2					
gi|7303826	CG12140-PA		lipid particle, mitochondrial inner membrane	no	3.311258182	2	1					
gi|8488	CG5502	60S ribosomal protein L4	lipid particle, ribosome	no	6.142506003	2	7					
gi|24762736	CG16932-PB	Eps-15	synaptic vesicle	no	3.24675329	2	3					
gi|7807	CG4379	cAMP-dependent protein kinase 1	plasma membrane	no	5.099150166	2	6					
gi|62471689	CG8732-PD	Lethal (2) 44DEa	lipid particle	yes (59)	2.928870358	2	2					
gi|78706832	CG7254-PB	Glycogen phosphorylase	unknown	no	2.725118399	2	3					
gi|76803826	CG7875	Transient receptor potential protein	plasma membrane	yes (60)	2.352941222	1	7	DAPAPPTKPGDTKPAAPKPGESAKPEAAAK	2895.373	1	12	2
gi|111145307	CG1721	Phosphoglyceromutase	unknown	no	13.33333403	2	2					
gi|45553479	CG31140-PB		membrane (Kyte and Doolittle)	yes (61)	2.180094831	2	3					
gi|28316937	CG11958	Calnexin 99A	plasma membrane, ER	yes (62)	6.351550668	2	3					
gi|6901844	CG16857		membrane (Kyte and Doolittle)	yes (63)	1.112656482	1	5	AFLNIQYK	996.5359	1	12	3
gi|7299519	CG14724-PA	Cytochrome c oxidase subunit Va	lipid particle, mitochondrial inner membrane	no	16.77852422	2	3					
gi|27819851	CG13636		membrane (Kyte and Doolittle)	yes (64)	11.82795689	2	2					
gi|7297382	CG7781-PA		membrane (Kyte and Doolittle)	yes (65)	6.12244904	2	2					
gi|7303222	CG8331-PA		membrane (Kyte and Doolittle)	yes (66)	14.04494345	2	1					
gi|7915	CG8280	Elongation factor 1α48D	lipid particle, cytoplasm	no	5.395568006	2	3					
gi|7300357	CG7998-PA		lipid particle, mitochondrial matrix	no	6.547619402	2	1					
gi|78706449	CG6963-PG	Gilgamesh	plasma membrane	no	7.352941483	2	3					
gi|7290857	CG1527-PA	Ribosomal protein S14b	ribosome	no	11.25827804	2	1					
gi|7303058	CG8186-PA	Vha36	plasma membrane (V-type ATPase, V0 domain)	no	9.34959352	2	2					
gi|45550690	CG1090-PB		integral to membrane	yes (67)	6.074766442	2	1					
gi|7296215	CG4574-PB	Phospholipase C at 21C	unknown	no	2.36280486	2	2					
gi|7303816	CG2331-PA	Transitional endoplasmic reticulum ATPase TER94	lipid particle, ER	no	3.245942667	2	2					
gi|78706848	CG17263-PA	Protein phosphatase 2A at 29B	cytoplasm (intracellular)	no	3.384094685	2	1					
gi|160715156	CG40625-PA		membrane (Kyte and Doolittle)	yes (68)	9.081935138	2	2					
gi|7290454	CG5014-PB	Vap-33-1	lipid particle, synaptic vesicle	yes (69)	4.460966587	2	1					
gi|32172424	CG1560	Myospheroid	plasma membrane (integrin complex)	yes (70)	3.309692815	2	1					
gi|7294533	CG10960-PB		integral to membrane	yes (71)	6.307977438	2	1					
gi|77403907	CG7050	Neurexin 1	plasma membrane	yes (72)	1.413043495	2	1					
gi|24639048	CG14622-PA	Dishevelled Associated Activator of Morphogenesis	unknown	no	3.231597692	2	1					
gi|25012528	CG11901	Ef1γ	lipid particle, cytoplasm	no	8.260869235	2	2					
gi|7301882	CG7920-PA		lipid particle	no	7.966457307	2	2					
gi|24584958	CG5803-PA	Fasciclin 3	plasma membrane	yes (73)	4.724409431	2						
gi|24655079	CG5226-PA		plasma membrane	yes (74)	3.999999911	2	1					
gi|27820101	CG3269	Rab2	cytoplasm (intracellular)	no	11.26760542	2						
gi|28573018	CG9796-PA		membrane (Kyte and Doolittle)	yes (75)	11.20000035	2	1					
gi|41058170	CG6827	Neurexin IV	plasma membrane	yes (76)	1.869158819	2						
gi|54650560	CG8048	Vacuolar H+ ATPase 44kD C subunit	plasma membrane (V-type ATPase, V0 domain)	no	3.229665011	2						
gi|60677949	CG1084	Contactin	plasma membrane (septate junction)	yes (77)	1.942446083	2						
gi|62862658	CG40002-PA		unknown	no	22.34042585	2						
gi|62900602	CG16935		mitochondrion	no	11.76470593	2	1					
gi|68067447	CG17654	Enolase	lipid particle	no	4.399999976	2						
gi|7291832	CG3683-PC		mitochondrial respiratory chain complex I	no	26.85714364	2						
gi|7293367	CG5703-PA		mitochondrial respiratory chain complex I	no	14.46280926	2						
gi|7294489	CG11051-PA	Neuropeptide-like precursor 2	Extracellular	no	29.0697664	2						
gi|7295655	CG12787-PA	Hoepel1	integral to membrane	yes (78)	4.234122112	2						
gi|7296533	CG6395-PA	Cysteine string protein 3	plasma membrane	yes (79)	16.5919289	2						
gi|7296954	CG10833-PA	Cyp28d1	membrane, microsome	no	4.780876637	2						
gi|7298248	CG13240-PA	Lethal (2) 35Di	mitochondrial respiratory chain complex I	no	9.58083868	2						
gi|7299757	CG9813-PB		membrane(proton-transporting two-sector ATPase complex, catalytic domain)	no	5.575539544	2						
gi|7301393	CG6120-PA	Tetraspanin 96F	integral to membrane	yes (80)	10.07462665	2						
gi|7302003	CG1715-PA	Lethal (3) 03670	unknown	no	21.52466327	2	1					
gi|7302707	CG5036-PA		unknown	no	5.904059112	2						
gi|7303046	CG8210-PA	Vacuolar H" ATPase 14kD subunit	plasma membrane (V-tvoe ATPase. V0 domain)	no	15.32258093	2						
gi|7304188	CG1358-PA		membrane (Kyte and Doolittle)	yes (81)	4.564315453	2						
gi|730537	CG6510	60S ribosomal protein L18a	ribosome	no	14.12429363	2						
gi|73621361	CG32498	Dunce	membrane (Kyte and Doolittle)	yes (82)	4.651162773	2						
gi|8111	CG4463	Heat shock protein 23	unknown	no	20.43010741	2						
gi|8248425	CG4636	SCAR	unknown	no	2.936378494	2						
gi|8647	CG11793	Cu-Zn superoxide dismutase	cytoplasm	no	20.26143819	2						
gi|46409160	CG11661	Neural conserved at 73EF	mitochondrial oxoglutarate dehydrogenase complex	no	1.376597863	1	4	SPFSEMSEGSEFQR	1617.679	1	13	4
gi|7290874	CG2254-PA		lipid particle	yes (83)	6.875000149	2	1					
gi|7303207	CG8542-PA	Heat shock protein cognate 5	lipid particle, mitchondrion	no	3.790087625	2	2					
gi|23171448	CG6126-PA		membrane	yes (84)	3.783783689	1	2	QNSVYPDDPEQMVPLKNIESK	2431.168	1	12	5
gi|7301648	CG5520-PA	Glycoprotein 93	lipid particle	no	3.684879467	2	1					

Table 3.1

Accession number	CG number	Name	Subcellular compartment	Predicted tm domains	% sequence coverage (95%)	No. of peptides at CI>95%	No.of peptides at CI<95%	Peptide sequence	Precursor m/z	Charge	Score	Spectrum Number in Additional File
gi|7290869	CG2233-PA		unknown	no	5.072463676	2	1					
gi|7303987	CG8261-PA	G protein γ 1	plasma membrane (heterotrimeric G-protein complex)	no	27.14285851	1	3	YITEHEQEDYLLTGFTSQK	2302.078	1	24	6
gi|7291403	CG3413-PD	Windpipe	plasma membrane	yes (85)	4.874446243	2	1					
gi|62484397	CG2381-PE	Syt7	membrane (synaptic vesicle)	no	8.894230425	2	1					
gi|7295936	CG3210-PA	Dynamin related protein 1	cytoskeleton (microtubule associated)	yes (86)	3.809523955	2						
gi|7299548	CG3359-PB	Midline fascicilin	plasma membrane	no	3.553921729	2	1					
gi|161078090	CG17816-PG		unknown	no	4.195011407	1	5	TTGPDVEEGALLPSPTR	1739.857	1	11	7
gi|45553437	CG5670-PG	Sodium pump alpha subunit	plasma membrane, nucleus	yes (87)	52.39520669	1	3	DPYRDNLVNRR	1417.698	1	12	8
gi|7299435	CG5214-PA		lipid particle, mitochondrial oxoglutarate dehydrogenase complex	no	6.410256773	1	3	AAPAPAAAPKPAPPPPAAGAPKPPPPPPPK	2723.576	1	13	9
gi|7686	CG9429	Calreticulin	ER lumen, lipid particle	no	2.463054098	1	2	MKEAQDEVQR	1233.652	1	13	10
gi|7298308	CG4559-PA	Imaginal disc growth factor 3	Extracellular	no	7.482992858	2						
gi|51338816	CG15792	Zipper	cytoskeleton	no	1.847350597	2	2					
gi|78706754	CG6783-PB		unknown	no	18.46153885	1	2	YKLDKSENFDEYMKELGVGLVTRK	2862.181	1	14	11
gi|7301355	CG4685-PA		mitochondrion	no	7.072691619	2	1					
gi|7300799	CG6439-PA		mitochondrion	no	6.216216087	2	2					
gi|2295756	CG13279	Cytochrome b5-related	lipid particle, mitochondrion	yes (88)	7.246376574	1	3	GTDITEAFEAHHLTTAPEK	2068.002	1	12	12
gi|21358627	CG3360-PA	Cyp313a1	membrane, microsome, ribosome	no	4.67479676	1	3	TDSDPESNIVINR	1459.699	1	13	13
gi|24582192	CG11567-PB	Cytochrome P450 reductase	lipid particle, ER	no	6.545454264	1	4	NKQPQGSEEVKVPVFIR	1955.079	1	12	14
gi|7289861	CG17947-PA	alpha Catenin	plasma membrane	no	4.58015278	1	3	KVQNPIHALSEFQSPADAV	2051.011	1	12	15
gi|7296536	CG5837-PA	HEM-protein	plasma membrane, cytoplasm	yes (89)	2.13143881 4	1	1	LAEEFIPHQR	1239.632	1	11	16
gi|7294943	CG3922-PB	Ribosomal protein S17	lipid particle, ribosome	no	10.68702266	1	2	GLQLTQPNTNNFGR	1559.762	1	11	17
gi|28317033	CG6703	Calcium/calmodulin-dependent protein kinase	membrane	no	1.440576185	1	5	THLADTVEELKR	1411.747	1	14	18
gi|45553057	CG18815-PB		unknown	no	8.5561499	2						
gi|85726415	CG14274-PA		membrane (Kyte and Doolittle)	yes (90)	16.20370299	1	1	FCQLDTGDSDACEILR	1899.845	1	13	19
gi|7298842	CG2520-PA	Like-AP180	synaptic vesicle, clathrin coat	no	1.923076995	1	2	MDRVGEFLK	1094.563	1	11	20
gi|90855663	CG2165-RC		plasma membrane	yes (91)	21.48997188	1	1	NLTGENDGRSQIK	1431.774	1	12	21
gi|7293142	CG9032-PA	Stunted	mitochondrial proton-transporting ATP synthase complex, catalytic core F(1)	no	29.50819731	1	3	DASHVKFTPWANGKPAQR	2011.016	1	13	22
gi|7302882	CG8905-PA	Manganese superoxide dismutase	mitochondrial matrix	no	3.225806355	1	1	AIESQQWK	861.4528	1	11	23
gi|116007958	CG32464-PP	l(3)82Fd	membrane (Kyte and Doolittle)	yes (92)	1.217656024	1	2	SVDHGLAAPFDLDSLR	1712.843	1	14	24
gi|28574881	CG9674-PD		unknown	no	0.520340586	1	6	AQDNPWPQWPK	1366.664	1	10	25
gi|116875733	CG30164	Prominin	integral to membrane	yes (93)	1.031894889	1	3	SIFSNFPQQVK	1294.681	1	10	26
gi|85856081	CG11064	Retinoid- and fatty acid-binding glycoprotein	lipid particle, endocytic vesicle, extracellular	no	0.477469433	1	8	VSHDTTVVYELGNKPK	1786.863	1	15	27
gi|7303053	CG8200-PB	Flotillin-1	plasma membrane(caveolar)	no	2.790697664	1	2	AFVWPVGQQVQR	1414.761	1	17	28
gi|24639032	CG3638-PD	Protein tweety-2	membrane (Kyte and Doolittle)	yes (94)	0.925925933	1	2	SPYVDFLNCGTPR	1525.715	1	13	29
gi|17945679	CG9603		mitochondrial respiratory chain complex IV	no	17.52577275	1	2	SAAVPKDQIEKGYFEIR	1950.982	1	7	30
gi|7300469	CG6008-PA	NP15.6	unknown	no	14.66666609	1	1	KDETTAPTSLTTEDFANPSPK	2363.161	1	11	31
gi|73920745	CG10975	Protein tyrosine phosphatase 69D	plasma membrane	yes (95)	0.683994545	1	2	NLPYMFDKLK	1268.641	1	12	32
gi|51704243	CG4634	Nucleosome remodeling factor - 38kD	nucleus, cytoplasm	no	3.254437819	1	1	ALYETVEKGAK	1250.673	1	14	33
gi|7303926	CG8024-PB	Lightoid	unknown	no	1.603498496	1	1	YVHQFFSQNYR	1488.689	1	13	34
gi|85857428	CG33129		lipid particle	yes (96)	5.063291267	1	1	NAALEYYNQFHK	1497.713	1	19	35
gi|85700964	CG10233	Retinophilin	unknown	no	3.535353392	1	3	SQCEHPY	920.3999	1	10	36
gi|7298421	CG5711-PA	Arrestin 1	membrane fraction, cytoplasm	yes (97)	4.120879248	1	1	ASDESQPCGVQYFVK	1714.771	1	18	37
gi|7297923	CG6601-PA	Rab6	unknown	no	5.288461596	1	2	LQLWDTAGQER	1316.67	1	11	38
gi|24648516	CG31195-PA		membrane (Kyte and Doolittle)	yes (98)	1.831501909	1	1	DAFDEIKR	993.505	1	9	39
gi|78709078	CG7217-PA		nucleus, cytoplasm, mitochondrion	no	8.421052992	1	1	VIIFGVDGAFTPGCSK	1649.851	1	11	40
gi|33112444	CG10844	Ryanodine receptor 44F	ER, integral to membrane	yes (99)	0.234055007	1	5	KMPEYDVIEFAR	1497.726	1	11	41
gi|7297072	CG9159-PA	Kruppel homolog 2	integral to membrane	yes (100)	6.88405782	1	3	SSQQQEQPQQSQSQNVPAK	2127.085	1	13	42
gi|7293455	CG6186-PA	Transferrin 1	Extracellular	no	2.808112279	1	2	KADVLATEPEDMYIAYHR	2122.015	1	15	43
gi|8484	CG4897	Ribosomal protein L7	ribosome	no	7.949791104	1	5	ANHYVNGGDFGNREDQINR	2175.976	1	17	44
gi|25013052	CG32368		unknown	no	15.90909064	1	1	DPARAKMIEEHIEK	1698.86	1	12	45
gi|45825129	CG2171	Triose phosphate isomerase	unknown	no	2.58620698	1	2	KFCVGGNWK	1095.464	1	7	46
gi|51316120	CG34387	Futsch	cytoskeleton (microtubule associated)	no	0.351071684	1	5	ESHTDTPESSPKPTSPFPR	2096.999	1	11	47
gi|73863346	CG32017		unknown	no	4.522613063	1	3	IGNSPYNNKEFDTNKELK	2123.135	1	14	48
gi|201066275	CG2979	Yolk protein 2	lipid particle	no	3.485838696	1	3	ITALDPTKIYGKPEER	1830.987	1	11	49
gi|62484475	CG3985-PD	Synapsin	terminal button (synapse)	no	1.921229623	1	4	MQNVCRPSMAQTGPGKLPSR	2215.101	1	11	50
gi|7292470	CG1268-PA		plasma membrane (V-type ATPase, V0 domain)	yes (101)	9.41176489	1	2	DVVAMIGR	860.4683	1	12	51
gi|62484538	CG12345-PB	Choline acetyltransferase	unknown	no	1.540616248	1	2	GFTGATPTVHR	1143.606	1	15	52
gi|54650746	CG8036		lipid particle	no	2.076677233	1	1	KIDSDLEGHPTPR	1464.684	1	7	53
gi|944924	CG17759	G protein alpha49B	plasma membrane (heterotrimeric G-protein complex)	no	17.56373942	1	1	VAQPAYLPTEQDILR	1713.894	1	14	54
gi|7290843	CG18624-PA		mitochondrial respiratory chain complex I	no	30.35714328	1	1	SALYGRPAGSEGKAPSW	1733.859	1	13	55
gi|729733	CG17950	High mobility group protein D	nucleus	no	24.10714328	1	1	AKDDYDRAVKEFEANGGSSAANGGGAK	2685.247	1	11	56
gi|24585263	CG10132-PA		unknown	no	1.175606158	1	5	YIRDSTAGPLVVSGAR	1732.955	1	8	57
gi|24662337	CG6409-PA		ER	no	3.88888903	1	1	AIESLAGGKAPEQR	1426.786	1	10	58
gi|7300703	CG5771-PA	Rab11	terminal button (synapse), lipid particle, endosome, trans-Golgi network transport vesicle	no	6.074766442	1	2	AQIWDTAGQERYR	1593.776	1	11	59
gi|40714549	CG12473	Stoned B	plasma membrane, endocytic vesicle, clathrin adaptor complex	no	1.743264683	1	3	FAQYAIAGDYEGVKEFGSDLKK	2436.177	1	15	60
gi|24639550	CG2849-PB	Ras-related protein	cytoplasm (intracellular)	no	7.1065992 12	1	1	AQQWAVPYVETSAK	1577.802	1	11	61
gi|7293168	CG9172-PA		mitochondrial respiratory chain complex I	no	4.07239832	1	1	KGYSPFGTK	984.4777	1	8	62
gi|7299191	CG9375-PA	Ras1	plasma membrane	no	7.407407463	1	2	SFEDIGTYREQIKR	1741.764	1	8	63
gi|24652789	CG30035-PA		integral to membrane	yes (102)	1.633605547	1	3	MSSVANIKPLSFNM	1538.761	1	14	64
gi|7294479	CG10724-PA	Flare	unknown	no	3.125	1	1	AQPQPPAKENKNIYATLPR	2213.16	1	11	65
gi|7302105	CG2098-PA	Ferrochelatase	mitochondrial inner membrane	no	2.083333395	1	2	LGPWIAQR	940.5369	1	11	66
gi|161076367	CG2093-PA		membrane (Kyte and Doolittle)	yes (103)	0.240891287	1	4	NFHEGLAR	943.4778	1	12	67
gi|78214285	CG14509		membrane (Kyte and Doolittle)	yes (104)	1.96463652	1	2	DSKLLHGQER	1182.619	1	14	68
gi|24648572	CG31191-PA		cytoplasm (intracellular)	no	3.529411927	1	1	YTMLKDMIK	1142.575	1	12	69
gi|7295848	CG3523-PA		lipid particle	no	0.533223944	1	4	FAEEVITAEPAQR	1460.751	1	8	70
gi|7648816	CG4464	Ribosomal protein S19	ribosome	no	8.333333582	1	1	DAAKQTGPIVISK	1327.765	1	20	71
gi|78706950	CG7100-PI	N-cadherin	plasma membrane	yes (105)	0.451612892	1	6	ASSGIEGNPTVFYR	1497.734	1	13	72
gi|7293150	CG9066-PA	Membrane steroid binding protein	plasma membrane	yes (106)	5.645161122	1	1	FYGPGGPYATFAGR	1460.7	1	15	73
gi|832109790	CG9261	Nervana 2	plasma membrane	yes (107)	31.6770196	1	2	SKPVPMSPSFVDEDLHNLRKPKPFK	2935.26	1	12	74
gi|7292698	CG4147-PA	Heat shock protein cognate 3	lipid particle, ER	no	5.182926729	1	3	VTHAVVTVPAYFNDAQR	1887.949	1	14	75
gi|994753	CG5779	Black cells	unknown	no	2.173913084	1	2	DARQEASVIGESGAR	1545.769	1	13	76
gi|161078546	CG34355-PA		membrane (Kyte and Doolittle)	yes (108)	2.46376805	1	2	YHPFYITDSPEGGLGDK	1908.855	1	7	77
gi|28574063	CG13388-PD	A kinase anchor protein 200	lipid particle	no	2.747909166	1	1	SAVAEGGDAVAETAKGEEGSPK	2131.004	1	21	78
gi|45550723	CG31352-PA		unknown	no	1.364764292	1	1	TPSASKEPLYK	1220.679	1	17	79
gi|28317158	CG8996	Walrus	lipid particle, mitochondria	no	5.588235334	1	1	AAVDAGFVPNDLQIGQTGK	1901.002	1	11	80
gi|7293014	CG9512-PA		membrane (Kyte and Doolittle)	yes (109)	3.370786458	1	1	MGPSTDPTAVVDPQLRVHGAK	2176.132	1	11	81
gi|8896016	CG3504	Inactivation no afterpotential D	plasma membrane (InaD receptor complex)	no	2.670623176	1	3	HSNYADEDDEDTRDMTGR	2126.868	1	11	82
gi|7300860	CG7057-PA	AP-50	synaptic vesicle	no	2.059496567	1	3	TFITQQGIK	1035.568	1	13	83
gi|24659853	CG32387-PA		membrane (Kyte and Doolittle)	yes (110)	0.790960435	1	1	SGEYEEVRERPFTK	1726.831	1	12	84
gi|33589406	CG4467		membrane (Kyte and Doolittle)	yes (111)	1.011029445	1	3	RAPSYTFYAPR	1328.637	1	8	85
gi|4574736	CG10382	Wrapper	plasma membrane (extrinsic to)	yes (112)	2.999999933	1	1	ELDFNNDLENSQKFK	1840.852	1	17	86
gi|54650756	CG5355		unknown	no	2.513227426	1	1	KDESVAEDFHGTQIKDVYR	2237.079	1	17	87
gi|7293979	CG7580-PA		lipid particle, mitochondrial respiratory chain complex III	no	10.11235937	1	1	GQHFGNLAK	971.5056	1	14	88
gi|7298728	CG9338-PA		membrane (Kyte and Doolittle)	yes (113)	7.482992858	1	1	SCYFGNIADTK	1275.562	1	13	89
gi|45645191	CG18405	Semaphorin-1A	plasma membrane	yes (114)	1.411764696	1	2	GKDEEACQNYIR	1482.706	1	16	90
gi|7297383	CG14275-PA		unknown	no	10.13513505	1	1	TVINFEQNDERRIER	1918.965	1	11	91
gi|78707176	CG1865-PB	Serine protease inhibitor 43Ab	unknown	no	2.544529177	1	2	SGSYQQALTR	1110.561	1	13	92
gi|24658811	CG12781-PB	Nahoda	membrane (Kyte and Doolittle)	yes (115)	0.898876414	1	3	GVTQINFFEKEK	1439.751	1	16	93
gi|24580788	CG4577-PA		unknown	no	3.820224851	1	1	SSPEVPASFSNAPSAR	1716.844	1	9	94
gi|7294310	CG6988-PA	Protein disulfide isomerase	lipid particle, ER	no	3.225806355	1	1	AAQQLAEKESPIKLAK	1724.94	1	19	95
gi|74865931	CG8399		integral to membrane	yes (116)	1.391035505	1	1	DAVTNVQGR	959.5087	1	12	96
gi|710417	CG8203	Cyclin-dependent kinase 5	nucleus	no	6.802721322	1	2	ISAEAAMQHPYFTDSSSSGH	2122.914	1	13	97
gi|7293981	CG7603-PA		unknown	no	19.67213154	1	1	VKDTFQDFAQSPAACGAESSPPK	2448.198	1	18	98
gi|7296323	CG6020-PA		mitochondrial respiratory chain complex I	no	4.326923192	1	1	SGTQMILPYRGDDSDVIR	2022.986	1	11	99
gi|7297791	CG6105-PA	Lethal (2) 06225	lipid particle, mitochondrial proton-transporting ATP synthase complex, coupling factor F(o)	no	15.1515156	1	1	VELTPPTPADIPAIR	1589.873	1	8	100
gi|85724748	CG17471-PA		unknown	no	4.702970386	1	1	YGSNVDGISTCDPEQYAKR	2159.945	1	10	101
gi|7303012	CG8322-PA	ATP citrate lyase	lipid particle, cytoplasm	no	1.841620542	1	1	VVPKEEVPPPTVPMDYSWAR	2297.174	1	12	102
gi|47117880	CG6455		mitochondrial inner membrane	yes (117)	1.307966746	1	2	GVYPEDALRER	1304.655	1	8	103
gi|45553375	CG4898-PL	Tropomyosin 1	cytoplasm	no	5.281690136	1	2	LIAEEADKKYEEVAR	1763.903	1	12	104
gi|7303306	CG6050-PA	Elongation factor Tu mitochondrial	mitochondria	no	2.862985618	1	2	KYNEIDNAPEEKAR	1676.827	1	10	105
gi|78706750	CG6782-PA		lipid particle, mitochondrial envelope, mitochondrial inner membrane	yes (118)	2.523659356	1	1	FGAFEFLK	958.4904	1	12	106

Table 3.1

Accession number	CG number	Name	Subcellular compartment	Predicted tm domains	% sequence coverage (95%)	No. of peptides at CI>95%	No.of peptides at CI<95%	Peptide sequence	Precursor m/z	Charge	Score	Spectrum Number in Additional File
gi|24656228	CG12187-PA		unknown	no	3.576982766	1	2	SAYDVFAPGLTQGGATPATQLQR	2349.187	1	14	107
gi|24661475	CG32039-PA		unknown	no	15.85365832	1	1	AEEMQRREEEAAR	1604.75	1	13	108
gi|40882587	CG6084		unknown	no	5.142857134	1	1	AGDPVLEEAKKEIAAK	1895.028	1	17	109
gi|74867920	CG1976	Rho GTPase-activating protein 100F	cytoplasm (intracellular)	no	0.86767897	1	3	MSTGTGNVGLAQQHAR	1627.828	1	11	110
gi|45550786	CG16791-PA		unknown	no	1.80505421	1	1	LAQSGDATCNGLDSAEVGSR	2007.9	1	11	111
gi|557084	CG1651	Ankyrin	plasma membrane	yes (119)	1.549386699	1	2	LLLQHDPNADIVSK	1562.843	1	11	112
gi|7298049	CG9306-PA		mitochondrial respiratory chain complex I	no	6.25	1	2	AQYPEYFAK	1116.584	1	11	113
gi|7301693	CG9990-PA		plasma membrane	yes (120)	1.73267331	1	2	TYYEDLDDAKEAVR	1687.774	1	13	114
gi|74871594	CG5627	Rab3-GEF	integral to membrane,synaptic vesicle	yes (121)	0.481927721	1	1	ASQFLNQFAR	1181.608	1	11	115
gi|841262	CG4609	Failed axon connections	unknown	no	3.110047802	1	1	SEAPPAQKFNVHK	1452.769	1	20	116
gi|7300672	CG10830-PA		plasma membrane	no	6.140350923	1	2	GSFQFGKDGLADVK	1468.744	1	9	117
gi|7302754	CG14482-PA		mitochondrial respiratory chain complex III	no	17.54385978	1	1	HAEIASSFIR	1130.494	1	7	118
gi|8840	CG2985	Yolk protein 1	lipid particle	no	6.150341779	1	1	NAPAQKQSSYHGVHQAWNTNQDSKDYQ	3102.404	1	11	119
gi|9501917	CG1448	Innexin 3	plasma membrane (gap junction)	yes (122)	5.063291267	1	2	ISHPIYPPVETFGGGKETET	2158.935	1	9	120
gi|24645646	CG3996-PA		cytoplasm (intracellular)	no	0.578592112	1	1	FRDEDEDEDQFEEAPRPK	2251.984	1	15	121
gi|24653164	CG8772-PC	No extended memory	mitochondria	no	1.975683868	1	1	VVHSYVGQEPSGR	1414.762	1	16	122
gi|25012987	CG32032		membrane (Kyte and Doolittle)	yes (123)	3.536977619	1	1	GYGYGNQDYNR	1306.579	1	12	123
gi|28380884	CG12013	PHGPx	cytoplasm,mitochondria	no	5.042016879	1	2	FLVNKEGVPINR	1385.776	1	11	124
gi|28573864	CG8889-PB		membrane (Kyte and Doolittle)	yes (124)	6.442577392	1	2	VHVPGDNDIGGENGDYISNSNQR	2457.091	1	11	125
gi|45774381	CG9339-PH		cytoplasm (intracellular)	no	2.268760838	1	2	SYTEIQQLLQDGK	1535.798	1	12	126
gi|5052532	CG9075	Eukaryotic initiation factor-4a	nucleus, cytoplasm	no	3.970223293	1	2	GIYGYGFEKPSAIQQR	1813.918	1	12	127
gi|7291447	CG2852-PA		lipid particle	no	10.24390236	1	1	IIKDFMIQGGDFTKGDGTGGR	2213.087	1	13	128
gi|7292402	CG10849-PA	Sc2	integral to membrane, cytoplasm	yes (125)	4.635761678	1	1	VKVPSGATPIGDLR	1409.802	1	12	129
gi|7292862	CG1633-PB	Thioredoxin peroxidase 1	cytoplasm	no	8.762886375	1	2	TMVADFTKSKEYFETTS	1934.886	1	13	130
gi|7295801	CG8844-PA	Pdsw	mitochondrial respiratory chain complex I	no	10.69182381	1	2	ESIVEPNQQKQNWYHQR	2184.095	1	11	131
gi|7296023	CG4233-PA	Glutamate oxaloacetate transaminase 2	lipid particle, mitochondria	no	4.009433836	1	1	TFEADGHDFCLAQSFAK	1943.854	1	13	132
gi|7298307	CG4475-PA	Imaginal disc growth factor 2	Extracellular region	no	3.409091011	1	1	ASNLVCYYDSSSYTR	1785.812	1	6	133
gi|7300071	CG4225-PA		integral to membrane, mitochondrial inner membrane, ABC transporter complex	yes (126)	2.309948761	1	1	LDNDTANESQGNVQTGSAFR	2123.932	1	15	134
gi|7301299	CG10423-PA	Ribosomal protein S27	lipid particle, ribosome	yes (127)	15.47619104	1	1	LVQHPNSYFMDVK	1577.766	1	12	135
gi|73920219	CG10691	Lethal (2) 37Cc	lipid particle, membrane, mitochondria	no	3.623188287	1	1	FVVEKAEQQK	1205.632	1	13	136
gi|77415712	CG11390	Ejaculatory bulb protein 3	Extracellular region	no	10.31746045	1	1	CLVDNGKCTPEGR	1505.741	1	7	137
gi|78214248	CG3380	Organic anion transporting polypeptide 58Dc	integral to membrane	yes (128)	2.027883381	1	2	IVQHEEEKANNEKNTEI	1896.966	1	13	138
gi|116008402	CG18208-PA		integral to membrane	yes (129)	2.002861165	1		KTNNEQVTSFTTAK	1568.803	1	22	139
gi|116008557	CG17839-PB		membrane (Kyte and Doolittle)	yes (130)	0.905797072	1		SANGNVAFENPTYTR	1641.732	1	11	140
gi|124248352	CG32234		membrane (Kyte and Doolittle)	yes (131)	6.321839243	1	1	NGDIASRIEEEEEEEDEAPAQK	2488.081	1	11	141
gi|161077626	CG32717-PG	Stardust	plasma membrane	no	0.693069305	1		EGEVPGVDYYHFITR	1618.792	1	11	142
gi|21358031	CG11306-PA		unknown	no	2.52631586	1		FSEQEFEKNFLR	1573.742	1	12	143
gi|24582467	CG4675-PB	Na[+]-driven anion exchanger 1	plasma membrane	yes (132)	1.728844456	1		TGGEDFTQQFTENDFEGHR	2214.931	1	15	144
gi|24640179	CG4094-PB	Lethal (1) G0255	cytoplasm,mitochondria	no	2.783725969	1		SQINFPIGGATER	1389.684	1	14	145
gi|24649622	CG6356-PA		membrane (Kyte and Doolittle)	yes (133)	2.280701697	1		SLEPEEGFSFGQK	1454.649	1	6	146
gi|25012513	CG9834	Endophilin B	cytoplasm	no	3.439153158	1	1	FLDGEMKTIGKER	1523.763	1	14	147
gi|25012545	CG1250	Sec23	Golgi, ER	no	3.622251004	1		GAAPGPQQQQHLPGQPAGAAAPVPPAHR	2706.405	1	11	148
gi|28573410	CG33138-PA		unknown	no	1.605839469	1		SNFIEVYTPSR	1312.653	1	11	149
gi|28574697	CG15630-PA		unknown	no	4.222222045	1		TTRLEQGEKPPSPANFQLR	2169.132	1	11	150
gi|4378008	CG7434	Ribosomal protein L22	lipid particle, ribosome	no	8.333333582	1		AAAPAAAAPAPAAAAPAWAKPAPKPK	2247.311	1	18	151
gi|45549584	CG6867-PA		membrane (Kyte and Doolittle)	yes (134)	1.264488976	1		DGKDGLHGKDGK	1226.574	1	11	152
gi|45551165	CG2727-PB	Epithelial membrane protein	plasma membrane, lysosome	yes (135)	1.814882085	1		YGIIDNFNGR	1168.584	1	15	153
gi|45553439	CG5670-PF	Sodium pump alpha subunit	plasma membrane, nucleus	yes (136)	52.0958066	1		NPFQDKLVNER	1359.682	1	19	154
gi|552138	CG4843	Tropomyosin 2	cytoplasm	no	5.836575851	1		MLAEDADTKSDEVSR	1666.766	1	15	155
gi|62471695	CG17870-PJ	14-3-3zeta	nucleus	no	5.759162456	11	3					
gi|7290254	CG4199-PA		cytoplasm	yes (137)	7.766990364	1		CTHYGAPLQTGALGLGR	1771.876	1	12	156
gi|7291015	CG9022-PA	Oligosaccharyl transferase 48 kDa subunit	lipid particle, ER membrane	yes (138)	3.378378227	1	1	QADAAPLLYR	1117.621	1	10	157
gi|7293032	CG9067-PA	Lipid storage droplet-2	lipid particle	no	1.592718996	1		SKVEDVVQPHLER	1519.846	1	11	158
gi|7293278	CG9634-PA		membrane (Kyte and Doolittle)	yes (139)	2.44755242	1		EADLFADDIFHYER	1740.779	1	11	159
gi|7293861	CG3979-PA	I'm not dead yet	plasma membrane	yes (140)	6.293706596	1		INHEPQYQIVGGNK	1596.807	1	16	160
gi|7294125	CG4893-PA		unknown	no	4.247104377	1		NVVDGSGYVSGYQHKDTYDNAH	2426.041	1	18	161
gi|7294903	CG8329-PA		unknown	no	5.078125	1	1	VSDHLDWREK	1397.686	1	14	162
gi|7295074	CG6822-PA	Ergic53	membrane	yes (141)	3.125	1	1	NAGQALPPPAAGGVPQQQLPVGAVSR	2480.319	1	15	163
gi|7295158	CG7962-PA	CDP diglyceride synthetase	plasma membrane, ER, nuclear envelope	yes (142)	3.245436028	1		KGEDEPLEDTAISGSDAANKR	2203.077	1	13	164
gi|7295846	CG8822-PA	Protein phosphatase D6	unknown	no	1.590457186	1		AHQVVEDGYEFFAKR	1795.889	1	14	165
gi|7297534	CG4389-PA		lipid particle	yes (143)	18.18181872	1		GIFLYDGQK	1040.546	1	10	166
gi|7298528	CG10470-PA	Allastin	membrane (Kyte and Doolittle)	no	6.593406945	1		QGVGLGPAPGQFK	1402.746	1	12	167
gi|7298641	CG10664-PA		lipid particle, mitochondrial respiratory chain complex IV	yes (144)	8.783783764	1	1	FREPTNEINALR	1459.63	1	12	168
gi|7298801	CG1112-PA	Alpha-Esterase-7	lipid particle, cytoplasm	no	22.34042585	1		FKAPQRPIPWER	1524.716	1	10	169
gi|7299171	CG9354-PA	Ribosomal protein L34a	ribosome	no	5.249343812	1		LVQYVK	912.5043	1	10	170
gi|7299735	CG11686-PA		unknown	no	14.81481493	1		AMLEGKQAF	994.5297	1	13	171
gi|7299873	CG3321-PB		lipid particle, mitochondrial proton-transporting ATP synthase complex, coupling factor F(o)	no	6.69856444	1		ALAELSKPTPKH	1291.671	1	16	172
gi|7299984	CG4307-PA	Oligomycin sensitivity-conferring protein	lipid particle, mitochondrial proton-transporting ATP synthase, central stalk	no	12.5	1		VMATALKEASEKLR	1546.872	1	14	173
gi|7300661	CG15693-PA	40S ribosomal protein S20	lipid particle, ribosome	no	2.402957529	1		DIEKPHVGDSASVHR	1646.834	1	15	174
gi|7301186	CG6666-PA	Allastin	membrane (Kyte and Doolittle)	yes (145)	9.852216393	1		LALADTGKKPFQR	1444.805	1	12	175
gi|7301302	CG11857-PA		integral to membrane	yes (146)	2.117647044	1	1	YQRVNDLAGSGPGSVAGNSK	1976.989	1	13	176
gi|7301322	CG10550-PB		unknown	no	5.641025677	1		TFINPYYAK	1116.572	1	12	177
gi|7301609	CG5588-PA	Mig-2-like	cytoplasm (intracellular)	no	3.470031545	1		GLKPVFEEAVR	1244.7	1	17	178
gi|7301797	CG1907-PA		lipid particle, mitochondrial inner membrane	no	3.365384787	1		NVTNVANALAR	1206.611	1	13	179
gi|7302989	CG8430-PA	Glutamate oxaloacetate transaminase 1	mitochondria	no	14.00000006	1		AFGVQTISGTGALR	1377.729	1	10	180
gi|7303165	CG10130-PA	Sec61beta	ER membrane (rough er)	yes (147)	6.169665977	1	1	SRAPGGAGTGGMWR	1360.645	1	11	181
gi|7303250	CG13349-PA		nucleus, cytoplasm	no	9.803921729	1		SSSNVNSQVDEGAGSSVDADAPGR	2248.015	1	18	182
gi|7303630	CG13220-PA		membrane (Kyte and Doolittle)	yes (148)	4.564315453	1	1	VGTDYIQDVDKLQKN	1735.886	1	12	183
gi|7303910	CG1975-PA	DNA fragmentation factor-related protein 2	cytoplasm (intracellular)	no	2.688172087	1		KGLSAQSSLDNKSVSSQSSQPR	2291.126	1	12	184
gi|7303982	CG8251-PA	Phosphoglucose isomerase	lipid particle, cytoplasm	no	1.604278013	1		DAMFSGQHINITENR	1732.81	1	12	185
gi|7304213	CG11140-PA	Aldehyde dehydrogenase type III	lipid particle	yes (149)	3.947368264	1		VINANNFQR	1075.576	1	13	186
gi|7304277	CG10106-PA	Tetraspanin 42Ee	integral to membrane	yes (150)	5.292478949	1		GGVFDTIQK	964.5661	1	14	187
gi|73920221	CG12369	Lachesin	plasma membrane (septate junction)	yes (151)	0.786639252	1		ENNALPTDSATYVGNTLR	2049.035	1	21	188
gi|73920746	CG11516	Protein tyrosine phosphatase 99A	plasma membrane	yes (152)	12.58278191	1		GAIFPIEGSR	1046.561	1	10	189
gi|743005	CG18319	Bendless	unknown	no	4.419889674	1		LMQEPVPGINAIPDENNAR	2078.067	1	16	190
gi|7481	CG3039	Optic ganglion reduced	plasma membrane (gap junction)	yes (153)	3.47071588	1		NLDPVIYKDVMSEFAK	1884.942	1	13	191
gi|74870777	CG3967		unknown	no	3.703703731	1		VGTKNLYLFDEAGKTR	1811.954	1	14	192
gi|7595904	CG9195	Secretory carrier membrane protein	integral to membrane	yes (154)	14.28571492	1		AQAEFTTEFLR	1312.659	1	12	193
gi|7739793	CG5730	Annexin B9b	unknown	no	11.18421033	1		TIAQFYEQSFGK	1418.683	1	18	194
gi|8067	CG33865	Histone H2A	nucleus	no	3.735144436	1	1	AGLQFPVGR	944.5371	1	12	195
gi|81175197	CG1210	Synaptotrevin	plasma membrane	yes (155)	8.791209012	1		ADQLEQGASQFEQQAGK	1834.84	1	14	196
gi|82407248	CG1411	Collapsin Response Mediator Protein	unknown	no	3.735144436	1		SLAYDDLQLTGSDNCTFNKEHK	2556.183	1	15	197
gi|8408	CG1956	Roughened	lipid particle	no	8.791209012	1		NLATQFNCAFMETSAK	1832.812	1	15	198
gi|85724868	CG3662-PB		membrane (Kyte and Doolittle)	yes (156)	3.717472032	1		TVEPFALNWR	1232.649	1	14	199
gi|85725000	CG12055-PB	Glyceraldehyde 3 phosphate dehydrogenase 1	lipid particle	no	2.422907576	1		DGRGAAQNIIPAATGAAK	1681.873	1	15	200
gi|85725242	CG7535-PD	GluClalpha	plasma membrane (postsynaptic)	yes (157)	2.400000021	1		HPGDPLALEKR	1232.665	1	11	201
gi|8855	CG3533	Unzipped	plasma membrane	yes (158)	3.346456587	1	1	KFDAGVPVGAIR	1229.688	1	16	202
gi|92109834	CG2151	Thioredoxin reductase 1	cytoplasm,mitochondria	no	2.895752899	1		TVPLSVEKQDDGKLLVK	1869.059	1	19	203
gi|92109994	CG34353		membrane (Kyte and Doolittle)	yes (159)	2.895752899	1		GLPDQHYEATVQSR	1715.784	1	16	204
The proteins listed in the shaded section below have a >95% confidence but >5% FDR and were therefore excluded from our analysis. They are included here for completeness.												
gi|21356183	CG5023-PA		unknown	no	9.467455745	1		ITQKHPEYTGPTLGPK	1763.848	1	15	205
gi|21358513	CG7630-PA		lipid particle	yes (160)	14.44444507	1		SSGIIHFNYYAPK	1496.718	1	20	206
gi|22946384	CG16820-PA		unknown	no	4.854368791	1		LVPKGPFNITIDNIK	1669.918	1	12	207
gi|25012844	CG11876		lipid particle, cytoplasm	no	2.465753444	1		TLEAHALPR	1007.573	1	11	208
gi|28571140	CG7033-PC		lipid particle, cytoplasm	no	2.063789777	1		QTLGLDMELGK	1205.583	1	11	209
gi|28573762	CG8306-PA		membrane (Kyte and Doolittle)	yes (161)	2.519379929	1		LLKDHPNTYTFTK	1577.838	1	11	210
gi|28573957	CG13743-PA		membrane (Kyte and Doolittle)	yes (162)	2.27272734	1		NTATEFSYILQR	1442.723	1	15	211
gi|41713668	CG11500	Spase 12-subunit	ER, integral to membrane	yes (163)	14.28571492	1		NALKWQKPIDTDAK	1627.887	1	14	212
gi|45550736	CG6666-PA	Succinate dehydrogenase C	mitochondrial respiratory chain complex II	yes (164)	11.11111119	1		VVSVAETQKDESFFEKNER	2242.103	1	16	213
gi|50403790	CG18279	Immune induced molecule 10	Extracellular region	no	6.716418266	1		NAGGPASHTISGPNFSAK	1712.828	1	24	214
gi|6851385	CG13057	Retinin	membrane (Kyte and Doolittle)	yes (165)	4.787234217	1		LVTPIVAPAVR	1135.724	1	11	215

Table 3.1

Accession number	CG number	Name	Subcellular compartment	Predicted tm domains	% sequence coverage (95%)	No. of peptides at CI>95%	No.of peptides at CI<95%	Peptide sequence	Precursor m/z	Charge	Score	Spectrum Number in Additional File
gi|7263022	CG14996	Chd64	cytoplasm	no	3.079710156	1		SGFAAEAQR	936.4918	1	13	216
gi|7290278	CG3621-PA		mitochondrial respiratory chain complex I	no	2.22717151	1		DVSPLIQR	927.5477	1	11	217
gi|7291234	CG10627-PA		unknown	no	6.578947604	1		WYDNVITVGR	1222.611	1	12	218
gi|7292067	CG9160-PA	Mitochondrial acyl carrier protein 1	mitochondria	no	1.520270295	1		YVADKEDVYE	1230.572	1	10	219
gi|7292579	CG2145-PA		unknown	no	11.50442511	1		QAMLFLQQK	1106.568	1	11	220
gi|7292608	CG15201-PA		unknown	no	3.693181649	1		RGQDYVDFGKDGK	1484.715	1	13	221
gi|7294118	CG4729-PD		membrane (Kyte and Doolittle)	yes (166)	11.45833358	1		SVEPHLLMR	1081.564	1	11	222
gi|7295109	CG7176-PA	Isocitrate dehydrogenase	lipid particle, mitochondria	no	4.697986692	1		LVTGWQKPVIGR	1466.877	1	17	223
gi|7295657	CG3036-PA		integral to membrane	yes (167)	4.464285821	1		ISDVTQEEGVPLKNEK	1785.913	1	11	224
gi|7296273	CG11372-PA	Galectin	cytoplasm	no	5.49450554	1		LPQNYIVR	1002.576	1	11	225
gi|7296592	CG8385-PB	ADP ribosylation factor 79F	cytoplasm (intracellular)	no	3.720930219	1		IGEAREELMR	1203.618	1	12	226
gi|7296785	CG2804-PB		lipid particle	yes (168)	5.541561544	1		STEVDKVCLPFPGSDR	1806.874	1	18	227
gi|7297162	CG11324-PB	Homer	unknown	no	1.149425283	1		SANGSNAVTPTTSANTSPISGR	2091.011	1	14	228
gi|7297880	CG14933-PA		unknown	no	5.740181357	1		TLNIRKDGPCNETN	1631.808	1	11	229
gi|7298392	CG5094-PA	Small glutamine-rich tetratricopeptide containing protein	unknown	no	7.650273293	1		AIELEPDNEVYKSNLEAAR	2161.059	1	16	230
gi|7298726	CG9336-PA		membrane (Kyte and Doolittle)	yes (169)	2.097902074	1		TLESVAGHPQIVR	1406.783	1	16	231
gi|7299097	CG8369-PA		unknown	no	4.166666791	1		KPATNSCQHNCGEVYEPVCAK	2449.019	1	13	232
gi|7299540	CG10007-PA	Transport and Golgi organization 9	Golgi, integral to membrane	yes (170)	12.85714358	1		YVDLGTENAAAPNSRPADVI	2073.035	1	16	233
gi|7293642	CG12532-PA	Beta Adaptin	plasma membrane	yes (171)	1.08577637	1	3	TDSKYFTTTK	1233.641	1	7	234
gi|24641620	CG32648-PA	Phosphodiesterase 9	cytoskeleton	yes (172)	1.142263785	1	2	FKVDTEGSSNR	1239.646	1	9	235
gi|125660072	CG14714		membrane (Kyte and Doolittle)	yes (173)	1.119664125	1	1	SQQGPLTVHCSPGTGR	1681.826	1	10	236
gi|24583465	CG7400-PB	Fatty acid (long chain) transport protein	plasma membrane	no	1.277955249	1	3	IYPISIIR	974.6174	1	10	237
gi|116007602	CG17800-PAY	Down syndrome cell adhesion molecule	plasma membrane	yes (174)	0.7433102	1	4	VVYAPSDEWYDETKR	1857.868	1	10	238
gi|25012863	CG31030		membrane	yes (175)	3.98009941	1	1	GDEYTLPSAPLGFSYR	1772.817	1	7	239
gi|24648943	CG3731-PA		lipid particle, mitochondria	no	1.489361748	1	1	QILCYNR	966.4969	1	9	240
gi|7296247	CG11455-PB		mitochondrial respiratory chain complex I	no	14.85148519	1	1	KGQEFFADPPRVDAY	1739.84	1	10	241
gi|7290966	CG1787-PA	Hexosaminidase 2	plasma membrane	no	1.607717015	1	2	YIETYLPKER	1311.698	1	10	242
gi|7341376	CG5269	Phosphatidylinositol transfer protein (Vibrator)	cytoplasm (intracellular)	no	5.147058889	1	1	AIEDQTKEELDKAR	1645.837	1	10	243
gi|7494853	CG9128	Sac1	membrane (Kyte and Doolittle)	yes (176)	1.858108118	1	1	RTKSGAMQDGK	1194.587	1	11	244
gi|22026914	CG13506-PA		membrane (Kyte and Doolittle)	yes (177)	3.578528762	1		NVSPEDSDDYYCEILPQR	2200.036	1	10	245
gi|24580953	CG31663-PA		membrane (Kyte and Doolittle)	yes (178)	0.724637695	1		FGEFCQR	943.4237	1	9	246
gi|45551810	CG9391-PB		unknown	no	3.264094889	1		NNEQRQDFVCK	1437.722	1	9	247
gi|62484226	CG9887-PA	Vesicular glutamate transporter	integral to membrane	yes (179)	1.265822817	1		FWAPPMER	1033.504	1	10	248
gi|7298957	CG2943-PA		membrane (Kyte and Doolittle)	yes (180)	0.983606558	1		VDLNHFQPR	1125.579	1	10	249
gi|7302341	CG8994-PC	Exuperantia	cytoplasm	no	2.067669109	1		QSSKNAVQGKR	1186.563	1	11	250
gi|74876618	CG33090		unknown	no	1.371308044	1		SWTEYDLSHYGVR	1612.737	1	10	251
gi|7302479	CG7563-PB	Calpain	cytoplasm	no	2.536231838	1	3	VFSETQNNMEENDDHVGYGGK	2369.971	1	10	252
gi|24584673	CG17332-PB	Vacuolar H+-ATPase SFD subunit	plasma membrane (V-type ATPase, V0 domain)	no	3.505535051	1	3	LQNSVQDLSSFDEYATEVR	2201.034	1	10	253
gi|7188753	CG9423	Karyopherin α3	cytoplasm	no	3.696497902	1	2	AAADATKPEQQLAAVQAAR	1910	1	10	254
gi|7303217	CG8394-PA		membrane (Kyte and Doolittle)	yes (181)	3.642987087	1	1	AMEAGMDGGDTTEMSSNPFR	2103.852	1	10	255
gi|194369501	CG33472	Quiver	plasma membrane	yes (182)	4.430379719	1	1	SPYEVVR	849.4479	1	9	256
gi|82510651	CG1086	Glucose transporter 1	integral to membrane, nucleus	yes (183)	1.21951215	1	1	HSFSYAPK	936.4551	1	9	257
gi|73853449	CG5261		lipid particle, mitochondria	no	2.9296875	1	1	AAGARYEDIPVTNMR	1663.824	1	8	258
gi|94400531	CG12218	Mei-P26	cytoplasm (intracellular)	no	0.6728432	1	1	FQFGVAGK	853.4534	1	10	259
gi|45551451	CG1640-PB		unknown	no	1.565217413	1		QVAQYIEKR	1134.637	1	10	260
gi|54650748	CG30359		unknown	no	2.063492127	1		TANWVLGNHDQPR	1507.728	1	10	261
gi|7294514	CG11267-PA		lipid particle, mitochondria	no	16.50485396	1		NASTGNHIPIGVKEGDR	1764.879	1	10	262
gi|7295604	CG1467-PA	Syntaxin 16	plasma membrane, golgi	yes (184)	4.26136367	1		MTQQQLLLFEEENTR	1879.923	1	10	263
gi|7298203	CG4170-PA	Vasa intronic gene	cytoplasm (intracellular)	no	2.653061226	1		GGPRPGGFGGGPR	1168.595	1	9	264
gi|7298683	CG2493-PA		unknown	no	2.52631586	1		TSSWNFKDYAEK	1475.681	1	10	265
gi|7301577	CG3373-PA	Hemomucin	plasma membrane (cell surface), lipid particle	no	2.245250344	1		IGQPCEDIYEESR	1595.683	1	6	266
gi|7302897	CG8098-PB	Picot	integral to membrane	yes (185)	4.725898057	1		QYWDNPEDDEQKPALQTTVTTSPAR	2890.353	1	11	267
gi|7635	CG2210	Abnormal wing discs	cytoskeleton	no	7.843137532	1		TFIMVKPDGVQR	1390.736	1	9	268
gi|161081617	CG34418-PF	Still life	cytoplasm (intracellular), synapse	yes (186)	0.752728619	1	5	SSFDSHGESDHNLDVPHGSR	2179.916	1	10	269
gi|7291847	CG16936-PA		unknown	no	7.174888253	1		YGQKEQQLYPKELVQR	2007.065	1	10	270
gi|74891743	CG3832	Peptidylglycine-α-hydroxylating monooxygenase	membrane	no	2.739726007	1		TTWNCGEMNR	1268.533	1	9	271
gi|8860	CG2621	Shaggy	unknown	no	6.920415163	1		TSSFAEGNKQSPSLVLGGVK	2006.04	1	5	272
gi|7290707	CG15894-PA		unknown	no	1.620220393	1	4	SKERPMTATGGLGGGGGSQNVTPSK	2314.156	1	10	273
gi|161077439	CG34372-PB		integral to membrane	yes (187)	0.990098994	1	1	RVDIDQCPQR	1286.675	1	9	274
gi|45549251	CG16973-PA	Misshapen	cytoplasm (cell cortex)	no	0.598404277	1	3	NFQQIQEGR	1119.565	1	9	275
gi|161077242	CG15081-PE	Lethal (2) 03709	membrane, lipid particle	no	2.071005851	1	1	AVFFVER	867.4809	1	9	276
gi|76803819	CG11276	40S ribosomal protein S4	lipid particle, ribosome	no	4.214559495	1	1	GVPFLVTHDGR	1197.616	1	6	277
gi|160715095	CG41555-PA		unknown	no	0.633640541	1		NEIDLQQEEAK	1316.675	1	8	278
gi|24662306	CG6463-PA		mitochondrial respiratory chain complex I	no	9.677419066	1		AVSKMPQDASYR	1352.693	1	9	279
gi|25089940	CG31040	Cog7	Golgi	yes (188)	1.752021536	1		LSSNQATPSDGVR	1333.613	1	9	280
gi|5881825	CG11130	Rtc1	nucleus	no	6.382978708	1		VLMACVGIGYTNINK	1669.866	1	7	281

Table 3.3

Accession no.	CG number	Name	Function
gi|161077626	CG32717-PG	Stardust	protein binding, establishment or maintenance of epithelial cell apical/basal polarity
gi|161082106	CG34416-PJ	Ankyrin 2	signal transduction
gi|24582467	CG4675-PB	Na[+]-driven anion exchanger 1	transport, sodium:bicarbonate symporter activity, anion exchanger
gi|24584673	CG17332-PB	Vacuolar H+-ATPase SFD subunit	transport, proton transporting V-type ATPase
gi|24584958	CG5803-PA	Fasciclin 3	adehsion, cell adhesion
gi|24642061	CG32593-PC	Flotillin 2	structural
gi|24647500	CG6588-PC	Fasciclin 1	adhesion, neuron adhesion, neuron recognition
gi|24648576	CG5670-PA	Sodium pump alpha subunit	transport, sodium:potassium-exchanging ATPase activity
gi|24655079	CG5226-PA		neurotransmitter transport
gi|24762461	CG2835-PC	G protein sα 60A	signal transduction
gi|28316876	CG4260	Alpha-adaptin	neurotransmitter secretion, intracellular protein transport
gi|28316937	CG11958	Calnexin 99A	protein folding
gi|32172424	CG1560	Myospheroid	adhesion, heterophilic cell adesion
gi|384212	CG9325	hu-li tai shao	actin binding, metal ion binding
gi|40714549	CG12473	Stoned B	neurotransmitter secretion
gi|41058170	CG6827	Neurexin IV	Neurotransmission,cell communication
gi|45550877	CG1732-PA		neurotransmitter transport
gi|45551165	CG2727-PB	Epithelial membrane protein	adehsion, cell adhesion
gi|45553437	CG5670-PG	Sodium pump alpha subunit	transport, sodium:potassium-exchanging ATPase activity
gi|45553439	CG5670-PF	Sodium pump alpha subunit	transport, sodium:potassium-exchanging ATPase activity
gi|45554791	CG1725-PH	Discs large 1	protein binding, establishment or maintenance of epithelial cell apical/basal polarity
gi|45645191	CG18405	Semaphorin-1A	signal transduction (receptor activity)
gi|4574736	CG10382	Wrapper	axogenesis & nervous system development
gi|47271230	CG3665	Fasciclin 2	adhesion, homophilic cell adhesion
gi|4972752	CG18617	Vha100-2	transport, proton transporting V-type ATPase
gi|51951046	CG40452-PA	Synapse protein 25	neurotransmitter secretion
gi|54650560	CG8048	Vacuolar H+ ATPase 44kD C subunit	transport, proton transporting V-type ATPase
gi|557084	CG1651	Ankyrin	signal transduction
gi|60677949	CG1084	Contactin	adehsion, cell adhesion
gi|62471615	CG9261-PF	Nervana 2	transport, potassium ion transport, sodium ion transport
gi|62484222	CG31795-PA	Ia2	protein tyrosine phosphatase activity
gi|62484401	CG2165-PB		transport, calcium-transporting ATPase activity
gi|62484414	CG18069-PD	Calcium/calmodulin-dependent protein kinase II	synaptic transmission, cell-cell signaling
gi|6782318	CG3694	G protein γ30A	signal transduction
gi|7289861	CG17947-PA	alpha Catenin	adehsion, cell adhesion
gi|7290447	CG2934-PA	VhaAC39	transport, proton transporting V-type ATPase
gi|7290947	CG1634-PA	Neuroglian	adhesion, neuron adhesion
gi|7291403	CG3413-PD	Windpipe	unknown
gi|7291663	CG11303-PA	Transmembrane 4 superfamily	unknown
gi|7292118	CG17248-PB	n-synaptobrevin	neurotransmitter secretion
gi|7292157	CG1977-PA	Alpha-spectrin	structural, cell-cell signaling (neuromuscular synaptic transmission), cytoskeleton,
gi|7292470	CG1268-PA		transport, proton transporting V-type ATPase
gi|7292924	CG11111-PB	retinal degeneration B	transport, Ca-transporting ATPase, signaling (phototransduction)
gi|7293146	CG10545-PA	G protein β-subunit 13F	signal transduction
gi|7293150	CG9066-PA	Membrane steroid binding protein	hormone binding, heme binding
gi|7293373	CG5870-PA	Beta-spectrin	structural, cell-cell signaling (neuromuscular synaptic transmission), cytoskeleton,

Table 3.3

Accession no.	CG number	Name	Function
gi|7293756	CG8770-PA	G protein β-subunit 76C	signal transduction
gi|7293861	CG3979-PA	I'm not dead yet	transport, succinate transmembrane transporter, citrate transmembrane transporter
gi|7295158	CG7962-PA	CDP diglyceride synthetase	signal transduction, signaling (phototransduction)
gi|7296533	CG6395-PA	Cysteine string protein 3	neurotransmitter secretion
gi|7296536	CG5837-PA	HEM-protein	protein bindng, axogenesis, CNS development, NMJ development, cytoskeleton organization
gi|7296719	CG1088-PA	Vacuolar H^+-ATPase 26kD E subunit	transport, proton transporting V-type ATPase
gi|7297508	CG3747-PA	Excitatory amino acid transporter 1	transport, glutamate:sodium symporter activity, sodium:dicarboxylate symporter activity
gi|7297994	CG12403-PA	Vha68-1	transport, proton transporting V-type ATPase
gi|7298751	CG1099-PA	Dynamin associated protein 160	neurotransmitter secretion
gi|7298786	CG8663-PB	Nervana 3	transport, potassium ion transport, sodium ion transport
gi|7299191	CG9375-PA	Ras1	GTPase, development & cell growth
gi|7299548	CG3359-PB	Midline fasciclin	adhesion, axogenesis
gi|7299734	CG17907-PA	Acetylcholine esterase	synaptic transmission, cell communication/signaling
gi|7300560	CG4550-PA	Neither inactivation nor afterpotential E	signal transduction
gi|7300672	CG10830-PA		transport, potassium ion transport
gi|7301693	CG9990-PA		transport, metabolite transport (ABC complex)
gi|7302024	CG1744-PA	Chaoptic	adhesion, homophilic cell adhesion
gi|7302508	CG11949-PA	Coracle	establishment or maintenance of cell polarity
gi|7302861	CG6518-PA	Inactivation no afterpotential C	signal transduction
gi|7303046	CG8210-PA	Vacuolar H^+ ATPase 14kD subunit	transport, proton transporting V-type ATPase
gi|7303053	CG8200-PB	Flotillin-1	structural
gi|7303058	CG8186-PA	Vha36	transport, proton transporting V-type ATPase
gi|7303429	CG8604-PA	Amphiphysin	neurotransmitter secretion
gi|7303741	CG2204-PA	G protein oα 47A	signal transduction
gi|7303987	CG8261-PA	G protein γ 1	signal transduction
gi|73920221	CG12369	Lachesin	adhesion, homophilic cell adhesion
gi|73920223	CG10443	Leukocyte-antigen-related-like	adehsion, cell adhesion
gi|73920745	CG10975	Protein tyrosine phosphatase 69D	phosphatase, axonal defasciculation, axon guidance
gi|73920746	CG11516	Protein tyrosine phosphatase 99A	phosphatase, axonal defasciculation
gi|7481	CG3039	Optic ganglion reduced	nervous system development
gi|76803826	CG7875	Transient receptor potential protein	transport, Ca ion transport, Ca-mediated signaling
gi|77403907	CG7050	Neurexin 1	Neurotransmission,cell communication
gi|7767570	CG10181	Multiple drug resistance 65	transport, ATPase
gi|7807	CG4379	cAMP-dependent protein kinase 1	signal transduction
gi|7833	CG18102	Dynamin	endocytosis
gi|78706449	CG6963-PG	Gilgamesh	signal transduction (Wnt signaling pathway)
gi|78706950	CG7100-PI	N-cadherin	adehsion, cell adhesion
gi|81175197	CG12210	Synaptobrevin	neurotransmitter secretion
gi|85725242	CG7535-PD	GluClalpha	neurotransmitter receptor, GABA-A receptor
gi|85857592	CG42314		transport, Ca-transporting ATPase
gi|8810	CG17369	Vacuolar H^+-ATPase 55kD B subunit	transport, proton transporting V-type ATPase
gi|881340	CG9258	Nervous system antigen 1	transport, potassium ion transport, sodium ion transport
gi|8855	CG3533	Unzipped	axogenesis
gi|8896016	CG3504	Inactivation no afterpotential D	signal transduction
gi|90855663	CG2165-RC		transport, Ca-transporting ATPase
gi|92109790	CG9261	Nervana 2	transport, potassium ion transport, sodium ion transport
gi|93141332	CG3762	V-ATPase 69 kDa subunit 2	transport, proton transporting V-type ATPase

Table 3.3

Accession no.	CG number	Name	Function
gi|944924	CG17759	G protein alpha49B	signal transduction
gi|9501917	CG1448	Innexin 3	transport, gap junction channel activity
gi|996081	CG31136	Syntaxin 1A	neurotransmitter secretion

Mansi Khanna

208 Mueller Lab, Penn State University, Univ Park 16802 **Ph**. :(814) 441-9669 **Email**: mrk225@psu.edu

Education

The Pennsylvania State University **Aug 2005 – Aug 2011**
IBIOS Cell and Developmental Biology Ph.D.

The University of Pune, Pune, India **2003-2005**
MS in Microbiology with Distinction.

MES Abasaheb Garware College, Pune, India **2000-2003**
BS in Industrial Microbiology with Distinction.

Research Presentations and Publications

Publications

Tjota, M., Lee, S-K., Wu, J., Williams, J.A., Khanna, M.R. and Thomas, G.H. (2011). Annexin B9 binds to β_{Heavy}-spectrin and is required for multivesicuar body formation and stress resistance of the endosomal system in *Drosophila*. Manuscript in press with Journal of Cell Science.

Khanna, M.R., Stanley, B.A. and Thomas, G.H. (2010). Towards a Membrane Proteome in *Drosophila*: A Method for the Isolation of Plasma Membrane. *BMC Genomics*. **11**: 302

Khanna, M.R., Bhavsar, S.P. and Kapadnis, B.P. (2006). Effect of temperature on growth and chemotactic behaviour of *Campylobacter jejuni*. *Letters in Applied Microbiology*. **43**: 84-90

Posters Presented

βH-Spectrin and Annexin B9 Have Roles in Protein Recycling and Multivesicular Body Function in *Drosophila*
Khanna, M.R., Tjota, M., Lee, S.K., Wu, J., Williams, J.A. and Thomas, G.H.
Presented as poster at the 52nd Annual Drosophila Conference
March 30-April 3, 2011 at San Diego, CA

Purification of *Drosophila* Plasma Membranes: a head membrane sub-proteome
Khanna, M.R., Stanley, B.A. and Thomas, G.H.
Presented as poster at the 51st Annual Drosophila Conference
April 7-11, 2010 at Washington D.C.

Isolation and Purification of *Drosophila* Plasma Membrane.
Khanna, M.R. and Thomas, G.H.
Presented as poster at the 48th Annual Meeting of the American Society for Cell Biology
December 13-17, 2008 at San Francisco, CA

Testing the Role of Spectrin in Plasma Membrane Protein Presentation: A Proteomic Approach
Khanna, M.R., Phillips, M.D., Williams, J.A. and Thomas, G.H.
Presented as poster at the 47th Annual Meeting of the American Society for Cell Biology
December 1-5, 2007 at Washington D.C.

Awards

J. Ben and Helen D. Hill Memorial Fund Award 2010
Awarded to outstanding graduate students in the College of Science to support graduate research in Genetics/Development and Plant Sciences
The Pennsylvania State University, University Park, USA

The Huck Institutes of Life Sciences Fellowship 2005/2006
Awarded by the Huck Institutes of Life Sciences
The Pennsylvania State University, University Park, USA